THE UNIVERSITY OF MICHIGAN

INDUSTRY PROGRAM OF THE COLLEGE OF ENGINEERING

KINETICS OF THE THERMAL DECOMPOSITION OF ETHANE TO ACETYLENE IN NONUNIFORM TEMPERATURE FIELDS

Gordon D. Towell

September 1960

IP-454

Doctoral Committee:

Professor Joseph J. Martin, Chairman
Associate Professor Richard B. Bernstein
Professor Stuart W. Churchill
Professor Guiseppe Parravano
Professor Lawrence H. Van Vlack

ACKNOWLEDGEMENTS

The author wishes to express his appreciation to the members of his committee for their guidance during the course of this work. Special thanks are due to Professor Joseph J. Martin who suggested the topic for this research and served as Chairman, and also to Professor Lawrence H. Van Vlack who served as Acting Chairman during the temporary absence of Professor J. J. Martin.

The author is indebted to the Horace H. Rackham School of Graduate Studies for financial aid through the award of University Fellowships for two years.

Finally, the author would like to thank his wife for her constant encouragement throughout and for typing the first draft of this manuscript. The preparation of the final form of this manuscript by the Industry Program of the College of Engineering is also very much appreciated.

TABLE OF CONTENTS

TABLE OF CONTENTS CONT'D

LIST OF TABLES

LIST OF FIGURES

LIST OF FIGURES CONT'D

LIST OF FIGURES CONT'D

LIST OF APPENDICES

I. INTRODUCTION

A. Scope of Research

The main objective of this research is a kinetic study of the thermal decomposition of ethane to acetylene. The reaction conditions necessary are temperatures of about 1000°C and higher, and residence times of the order of 1/100 of a second. The thermal decomposition of ethane consists mainly of a series of consecutive reactions proceeding through ethylene to acetylene and finally to carbon. A thermodynamic equilibrium limitation in the formation of acetylene from ethylene is the reason for the high temperature. The reactions are very fast at these elevated temperatures so that the residence time must be very short in order to prevent complete decomposition to carbon and hydrogen. A batch kinetic experiment is obviously out of the question for this rapid a reaction. The experimental program was carried out using a steady state flow system consisting essentially of an electrically heated tubular reactor through which the gas passed at high velocity. The gas temperature distribution was measured with movable thermocouples.

In a conventional kinetic study the experiments are carried out isothermally. The reaction conditions necessary in this study made it impossible to even approach an isothermal experiment because of the heat transfer rate limitation. Therefore, the apparatus used in this work was designed to measure an accurate gas temperature distribution. A mathematical technique was developed for analyzing the non-isothermal kinetic data for the order of reaction and the rate constants. A digital computer was required to obtain solutions to the equations developed since the large amount of computation required would cause hand calculation to be prohibitively slow. This method of kinetic analysis of data obtained with an arbitrary temperature distribution is applicable to all kinetic studies and particularly to the case of fast high temperature thermal reactions. Previous workers in the literature have been faced with the problem of a non-uniform temperature distribution and the usual solution has been to estimate some average constant temperature for an arbitrary fraction of the reactor. This kind of approximation results in considerable scattering of the data.

Experiments carried out such that the whole series of consecutive reactions are occurring together are very difficult to analyze for the individual rate constants. Therefore, the thermal decompositions of pure ethane, ethylene and acetylene were investigated independently. In each of these independent studies the main reaction and the products of any significant side reactions were established and the order of reaction and the rate constants at various temperatures were determined. The results on the individual steps of the reaction were then combined and an overall kinetic correlation was developed for the complete set of reactions. The overall kinetic correlation can now be used to predict the product distribution for any reaction conditions. Some experiments were carried out under conditions where all of the steps occurred to significant amounts to check out the predictions of the correlation. The correlation was also used to show the variation of product distribution throughout the course of the overall reaction. Some calculations were also made to investigate the effect of various reaction conditions, outside the experimental range of this work, on the product distributions.

Some effort was devoted to the consideration of possible mechanisms for the reactions, although this was not a primary objective of this work. Previous workers have shown that high temperature thermal decomposition of hydrocarbons occurs at least in part by free radical mechanisms. Therefore, a few experiments were carried out in which a free radical inhibitor was added in various amounts. These data together with the rest of the data were considered from the viewpoint of reaction mechanism and possible mechanisms are discussed in a speculative manner.

B. Review of Literature

The pertinent literature can be divided into a number of sections, the first and largest of which is concerned with the kinetic data for the thermal decomposition of ethane at relatively low temperatures (500°C to 800°C). The next and much smaller section deals with the same reaction in the temperature range 800°C to 1100°C. There has also been considerable work devoted to the determination of the mechanism of the thermal decomposition reaction of ethane from a free radical point of view. The last two sections are quite small and deal with the thermal reactions of ethylene and acetylene, mostly at lower temperatures (800°C) where polymerization predominates. These sections of the literature are reviewed briefly below and any literature data that can be compared directly with this work are discussed in greater detail in the section on experimental results.

The kinetic data on the decomposition of ethane at lower temperatures (500°C to 800°C) are contained in the papers of Pease,[33] Frey and Smith,[20] Paul and Marek,[32] Sachsse[37] and Steacie and Shane.[43]

The work of these authors was reviewed by Steacie[44] and Brooks et al.[10] The agreement between the various workers is good and the data are presented as first order rate constants for the disappearance of ethane. The reaction was found to be homogeneous and the main products were ethylene and hydrogen (no acetylene can be produced at these temperatures because of an equilibrium limitation).

The kinetics of ethane decomposition in the temperature range 750°C to 1000°C have been investigated by Eastwood and Potas,[16] Hepp et al.[24] and Kinney and Crowley.[26] Schutt[38] reviewed these papers and compared the data with some commercial scale measurements. This higher temperature work agrees reasonably well with the lower temperature data but with much more scatter evident which is probably due to the uncertainty of the temperature. The kinetic correlations were confined to first order rate constants for the disappearance of ethane. Some experiments were made by Tropsch and Egloff[47] at temperatures up to 1400°C but only product distributions were obtained. There is some literature concerning commercial and pilot plant processes for the high temperature pyrolysis of ethane and other saturated hydrocarbons to ethylene and acetylene. The significant authors in this field are Farnesworth et al.,[19] Bogart et al.,[7] Sittig,[40] Bixler and Coberly,[6] Hasche,[23] and Akin et al.[1] These papers do not contain any kinetic data but only process descriptions and product distributions.

There is a considerable literature on the study of the mechanism of the thermal decomposition of ethane. Rice and Dooley[36] detected free radicals by the lead mirror technique and Eltenton[17,18] detected free radicals with a mass spectrometer. Rice and Herzfeld[35] have suggested a free radical mechanism and this work has been the basis for many further studies which are reviewed very well by Benson.[5] The literature on the mechanisms will be discussed in more detail in section VA of this work. It is pointed out that even after many years of study the free radical mechanism is still not well enough understood to make quantitative calculations of great accuracy. In a recent piece of work by Snow et al.[41] the most up to date free radical mechanisms and their appropriate rate constants were used to try and predict the existing literature experimental results on ethane pyrolysis to ethylene and hydrogen at low to moderate temperatures. In order to obtain agreement the radical mechanism rate constants had to be changed by a trial and error procedure.

The kinetics of the thermal reactions of ethylene have mostly been studied at relatively low temperatures where polymerization predominates over decomposition. This work is contained in the papers of Burk et al.,[11] Dahlgren and Douglas,[13] and Molera and Stubbs.[31] They found the polymerization reaction to be homogeneous and second order. Tropsch et al.[47] obtained some product distribution data at temperatures up to 1400°C. The thermal decomposition of acetylene at high temperatures is often an explosive reaction as shown in the early work of Bone and Coward.[9,10] Pease,[34] Zelinski,[49] and Taylor and van Hook[46] studied the kinetics of the polymerization of acetylene at moderate temperatures and found it to be homogeneous and second order.

A small amount of kinetic data on the thermal decomposition of hydrocarbons has been reported recently by workers using shock tubes as a means of obtaining high temperatures. Greene et al.[21] and Miller[30] have obtained some shock tube kinetic data on ethane and ethylene pyrolysis and Aten and Greene[4] on acetylene pyrolysis.

II. THEORY

A. Introduction

When ethane is subjected to thermal decomposition at elevated temperatures the major products are ethylene, acetylene, carbon and hydrogen. The work in the literature indicates that the reaction proceeds through a series of consecutive steps as outlined below.

$$\text{Ethane} \rightarrow \text{Ethylene} \rightarrow \text{Acetylene} \rightarrow \text{Carbon}$$

Hydrogen is formed at each step and there are also some small amounts of side reactions. In this kinetic study each step in the series was investigated separately as this approach will yield much more information than attempting to interpret data resulting from experiments in which all of the reactions were occurring. In fact, data resulting from all of the reactions occurring together would be almost impossible to interpret so as to obtain individual rate constants.

A kinetic study was carried out on each of the steps and the conversions were kept low so that the primary reactions of any particular step could be studied. The product distributions were determined for each step at various amounts of conversion. These data were useful in determining which were the primary reactions and which were the secondary reactions. The determination of the order of a particular reaction and the method of obtaining the kinetic rate parameters from the data will be discussed later in this section.

B. Reaction Equilibria

$$C_2H_6 \rightleftharpoons C_2H_4 + H_2 \qquad (1)$$

$$C_2H_4 \rightleftharpoons C_2H_2 + H_2 \qquad (2)$$

$$C_2H_2 \rightleftharpoons 2C + H_2 \qquad (3)$$

The equilibrium constants for the three reactions shown above are plotted against reciprocal temperatures in Figure 1. We can determine from this figure the temperatures at which the equilibrium yield of the products become appreciable. The equilibrium yield of ethylene becomes significant in reaction (1) at about 785°C (the equilibrium constant is 1 at this temperature). In reaction (2) the equilibrium yield of acetylene reaches a significant value at about 1115°C. The equilibrium position for reaction (3) is almost completely on the product side over the whole temperature range. The equilibrium yield of the products can be increased somewhat by a reduction in pressure (by inert dilution or by reducing the total pressure) since the forward reactions result in an increase in volume. Therefore, the products could be made at somewhat lower temperatures than previously indicated. However, generally speaking, it can be said that temperatures of 1000°C and upwards will be necessary to produce high acetylene yields. Equilibrium considerations only place certain limits on the product distributions. The actual product distributions will, of course, depend upon the actual rates of the various reactions, the investigation of which is the purpose of this work.

C. Temperature Distribution

The thermodynamics of the system indicate that temperatures in the range 800°C to 1000°C and higher are necessary to carry out these

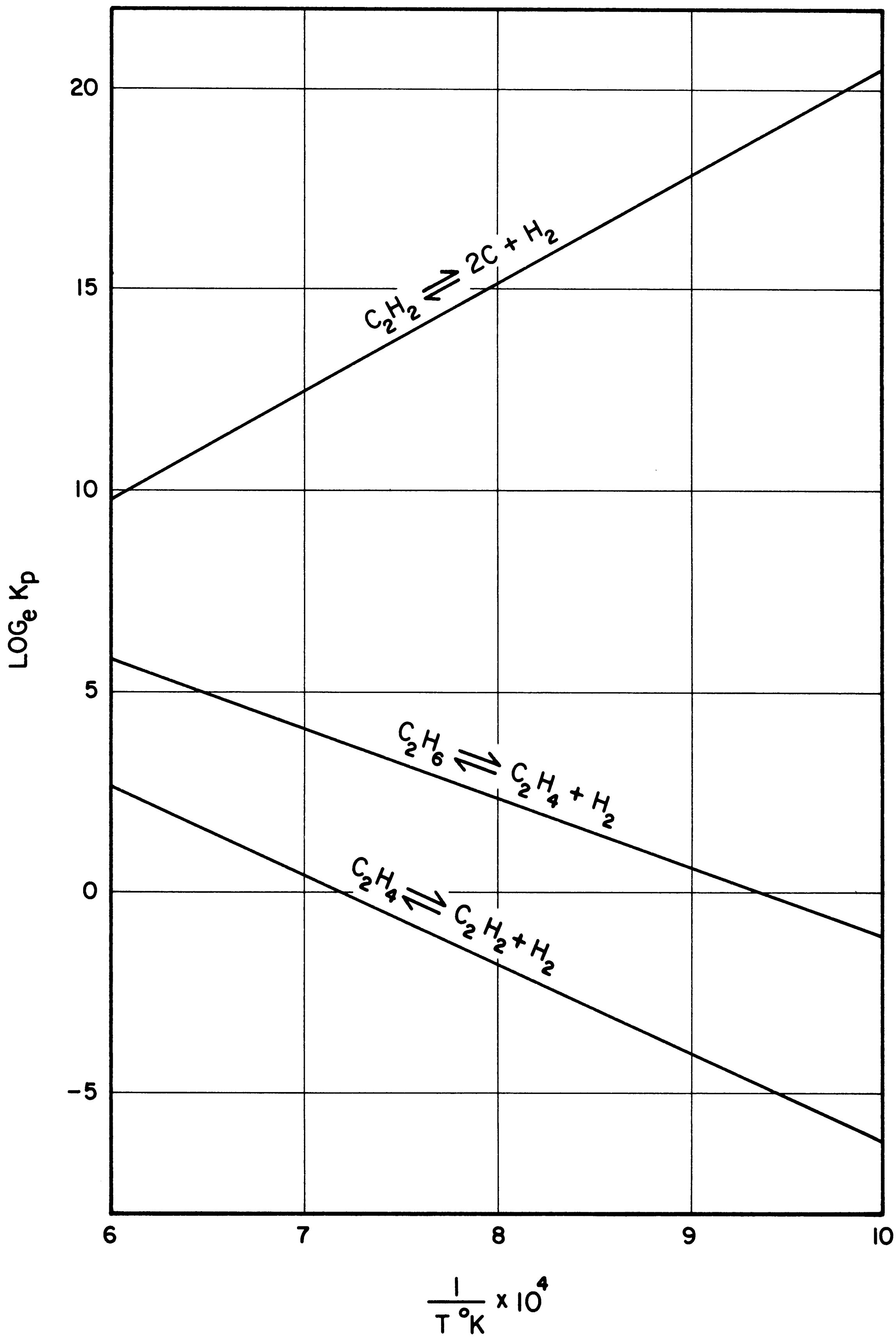

Figure 1. Equilibrium Constants in Atm.
(Free Energy Data Ref. (2)).

reactions. The rates of these reactions are quite high at these elevated temperatures so that the products will be mostly carbon and hydrogen unless the residence time is kept very small (residence times are of the order of 1/100 of a second). Obviously, a batch kinetic experiment is out of the question at this small a residence time, so steady state flow kinetic experiments were carried out.

When a kinetic study is carried out it is extremely useful to have an isothermal experiment, i.e. temperature profile 1 in Figure 2. A set of isothermal experiments at different temperature levels allows relatively simple processing of the data to obtain the kinetic rate parameters [a log (rate constant) versus reciprocal temperature plot can be used]. The short residence time required for the reactions under study

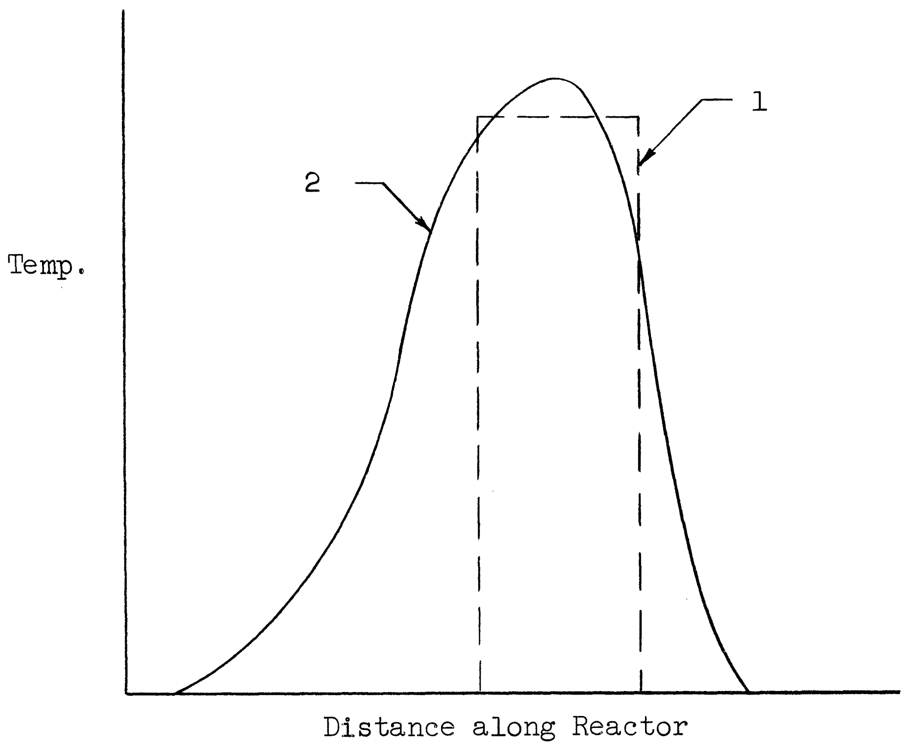

Figure 2. Schematic Temperature Profiles.

here gives rise to a temperature profile like number 2 in Figure 2. The shape of curve 2 is due to the fact that the heat can only be transferred to the gas at a finite rate. The main point of this discussion is that a square profile like curve 1 cannot be obtained or even approached. This fact is true for all high temperature fast reactions. Many workers in the literature have been faced with this problem and the usual solution adopted is to estimate a mean temperature that is applied over an arbitrary fraction of the heated section of the apparatus. These approximations result in considerable scatter of the data especially since the shape of the temperature profile is dependent very closely on the flow rate (which determines the heat transfer rate) which is changed considerably from run to run during a kinetic study.

In this work no attempt was made to try and approach a square temperature profile (i.e. an isothermal experiment). The temperature profile was allowed to take whatever shape it wanted to and then the actual temperature distribution was measured carefully. The use of this experimental data to determine rate constants is now quite difficult since the rate constants themselves are functions of temperature. The equations and their method of solution to obtain these rate constants are developed in the next few sections.

D. Determination of the Order of Reaction with an Arbitrary Temperature Distribution

The data taken to study the order of reaction require a simple mathematical treatment to deal with the arbitrary temperature profile. In an isothermal kinetic study the order of reaction can be found from a set of data at constant temperature in which the rate is measured at various concentrations of the reactant. The concentration of the reactant can be altered by changing the total pressure or by diluting with an inert gas. The amount of reaction is kept very low so that the concentration of the reactant is essentially unchanged and the rate measured can be considered as a differential rate. A plot of log (reactant concentration) versus log (rate) will result in a straight line the slope of which is the order of the reaction. The same technique can be used with an arbitrary temperature profile provided that the profile remains constant for the set of runs. This will be demonstrated by the following derivation.

Suppose an irreversible reaction of the form

$$A \longrightarrow \text{Products}$$

for which the rate equation in a flow reactor is

$$-\frac{dN_A}{dV_R} = k(C_A)^n \qquad (1)$$

where N_A is the flow rate of reactant A in gm moles/sec., V_R is the reactor volume in liters, n is the order of reaction, k is the rate constant in liter $^{n-1}$/gm. mole $^{n-1}$ sec., C_A the concentration of reactant in gm. moles/liter.

The rate constant can be expressed by the Arrhenius equation as

$$k = A e^{-E/RT} \qquad (2)$$

where A is the pre-exponential factor with the units of k, E is the activation energy in cal/gm. mole, T is the temperature in °K and R is the gas constant in cal/gm. mole.

Substituting in Equation (1)

$$-\frac{dN_A}{dV_R} = A e^{-E/RT} (C_A)^m \tag{3}$$

The concentration is related to the mole fraction by the following expression:

$$C_A = \frac{N_A}{N_T}\frac{P}{RT} = \frac{M_A P}{RT} \tag{4}$$

where N_T is the total flow rate in gm moles/sec., P is the pressure in atmospheres and M_A is the mole fraction of A.

Also

$$V_R = a\,\ell \tag{5}$$

where a is the cross-sectional area of the reactor in cm^2 and ℓ is length along the reactor in cm.

Substituting expression (4) and (5) in Equation (3)

$$-\frac{dN_A}{a\,d\ell} = A e^{-E/RT}\left[\frac{M_A P}{RT}\right]^m \tag{6}$$

Assuming that the conversion is small so that M_A stays essentially constant, that the pressure is constant and that there is a negligible radial temperature gradient, we can integrate Equation (6) along the length of the reactor to obtain the following expression:

$$-\int_0^{\Delta N_A} N_A = (M_A)^m\, a\, A\left(\frac{P}{R}\right)^m \int_0^L \frac{e^{-E/RT(\ell)}}{T(\ell)^m}\, d\ell \tag{7}$$

where $T(\ell)$ is the temperature distribution function with respect to reactor length, ΔN_A is the small decrease in moles/sec. of A, and L is the total reactor length in cms.

This reduces to

$$\Delta N_A = M_A^m \left[a A \left(\frac{P}{R}\right)^m \int_0^L \frac{e^{-E/RT(\ell)}}{T(\ell)^m} \right] d\ell \qquad (8)$$

The value of the expression inside the square brackets in Equation (8) will be a constant provided that the temperature distribution $T(\ell)$ is constant. Taking logarithms of Equation (8), Equation (9) results.

$$\text{Log}(\Delta N_A) = m \,\text{Log}(M_A) + \text{Log}(\text{CONSTANT}) \qquad (9)$$

We can see that a plot of log (ΔN_A) against log (M_A) will result in a straight line the slope of which will be the order of reaction n, if the temperature distribution for the set of runs is kept constant. A similar derivation to this has been presented by Lee and Oliver.[28]

E. Derivation of the Kinetic Equations for an Arbitrary Temperature Distribution

We will assume an irreversible homogeneous reaction of the type

$$A \longrightarrow B + C$$

It also is assumed that plug flow is obtained and that there are negligible radial temperature variations. There is, of course, a large variation in longitudinal temperature distribution $T(\ell)$ the form of which is only known as a set of measured temperatures at known positions.

The rate equation for this reaction is

$$-\frac{dN_A}{dV_R} = k\, C_A^m \qquad (10)$$

Let the feed rate of A be F gm. moles/sec, the fractional conversion of A be x, and the feed rate of inert gas N_D gm. moles/sec.

Then

$$N_A = F(1-x) \tag{11}$$

and

$$dN_A = -F\,dx \tag{12}$$

Also

$$C_A = \frac{M_A P}{RT} = \frac{F(1-x)}{[F(1+x)+N_D]}\frac{P}{RT} \tag{13}$$

and

$$dV_R = a\,d\ell \tag{14}$$

Where the symbols are as defined in Section IID and the nomenclature.

Substituting (12), (13), (14), (2) in (10) we obtain

$$\frac{F}{a}\frac{dx}{d\ell} = A e^{-E/RT}\left[\frac{(1-x)}{(1+x+N_D/F)}\frac{P}{RT}\right]^m \tag{15}$$

Rearranging Equation (15)

$$\frac{F}{a}\frac{dx}{\left[\dfrac{1-x}{1+x+N_D/F}\right]^m} = A\left(\frac{P}{R}\right)^m\frac{e^{-E/RT}}{T^m} \tag{16}$$

and integrating (16) along the length of the reactor from 0 to L, over the temperature distribution $T(\ell)$, and from the inlet conversion x_i to the outlet conversion x_o we obtain

$$\frac{F}{a}\int_{x_i}^{x_o}\frac{dx}{\left[\dfrac{1-x}{1+x+N_D/F}\right]^m} = A\left(\frac{P}{R}\right)^m\int_0^L\frac{e^{-E/RT(\ell)}}{T(\ell)}\,d\ell \tag{17}$$

The values of a,L are known dimensions of the reactor. The experimental data from a run will be values of F, N_D, P, x_o, x_i and $T(\ell)$. The temperature distribution will only be known as a set of temperature measurements at known distances along the reactor axis.

F. Solution of the Equations for the Kinetic Parameters

The rate constant k cannot be solved for directly from the data obtained in this work since it is temperature dependent and the data is obtained in a non-isothermal system. However, the more basic kinetic parameters, pre-exponential factor A and the activation energy E can be solved for. The mathematical problem is to solve Equation (17) for A and E. The order of reaction n is determined experimentally from a separate set of data by the method developed in Section IID so that n will have a numerical value.

Rearranging Equation (17) we obtain

$$A = \frac{\frac{F}{a}\left(\frac{R}{P}\right)^m \int_{x_i}^{x_o}\left[\frac{1+x+N_D/F}{1-x}\right]^m dx}{\int_0^L \frac{e^{-E/RT(\ell)}}{T(\ell)^m}\,d\ell} \tag{18}$$

Since the temperature distribution $T(\ell)$ is only known graphically, the integral containing it will have to be evaluated numerically. The numerical integrations are carried out using Simpson's rule. The data obtained from one experiment are insufficient to solve Equation (18) since an infinite number of values of the two parameters A and E would satisfy the equation. Unique values of A and E can only be obtained from Equation (18) by taking the data from two separate experiments (with different experimental conditions) and solving simultaneously.

Let the data from the two different experiments be denoted by subscripts 1 and 2 respectively. Then substituting each of the sets of data into Equation (18) we obtain the following two equations

$$A = \frac{\frac{F_1}{a}\left(\frac{R}{P_1}\right)^m \int_{x_{i,1}}^{x_{o,1}} \left[\frac{1+x+N_{D,1}/F_1}{1-x}\right]^m dx}{\int_0^L \frac{e^{-E/RT(\ell)_1}}{T(\ell)_1^m}\, d\ell} \tag{19}$$

$$A = \frac{\frac{F_2}{a}\left(\frac{R}{P_2}\right)^m \int_{x_{i,2}}^{x_{o,2}} \left[\frac{1+x+N_{D,2}/F_2}{1-x}\right]^m dx}{\int_0^L \frac{e^{-E/RT(\ell)_2}}{T(\ell)_2^m}\, d\ell} \tag{20}$$

We can now set about solving Equations (19) and (20) simultaneously to obtain values of E and A.

The method of solution used is to assume values of E and calculate values of A from Equations (19) and (20) the integrals being evaluated numerically. The solution is obtained when for a chosen value of E the values of A computed from (19) and (20) are identical. These calculations represent considerable computational labor which would result in the method being prohibitively time consuming if carried out by hand. The calculations were however, readily handled with the aid of a digital computer so they were programed for an IBM 704 digital computer. The flow diagram for the calculation upon which the program is based is contained in Appendix VII. The input for the computer program is the experimental data for a pair of runs and a set of values of E that brackets the solution. The output from the computer is two sets of A values corresponding to the set of E values chosen. If these E and A values are plotted it would look like Figure 3 below:

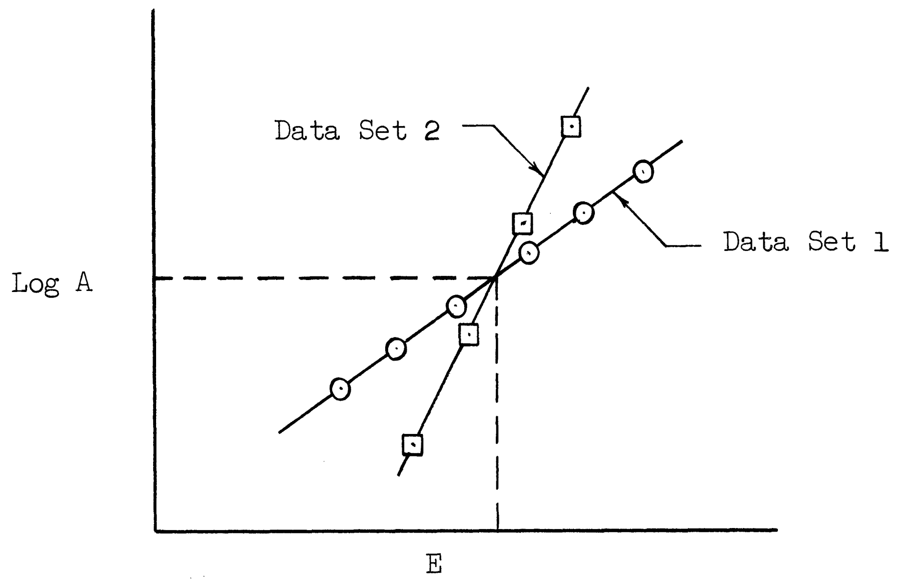

Figure 3. Solution for Kinetic Parameters.

The intersection of the two lines represents the solution for E and A. It is found that the logarithm of A is practically a linear function of E so that linear interpolation from the four points bracketing the intersection is quite accurate.

A sample calculation using actual experimental data is contained in Appendix IV. The technique developed here enables one to calculate E and A values from any pair of experiments. This method of calculation is quite sensitive to the accuracy of the data so that fairly small experimental errors product large variations in the E and A values. The next section will develop a method of smoothing the data and will show why the method of calculation is so sensitive.

G. Calculation of Rate Constants and Smoothing of the Data

Now that we have computed the E and A values from the data from a pair of experiments, we can go back and calculate rate constants from the Arrhenius expression

$$k = A\, e^{-E/RT} \tag{21}$$

The temperatures that are used in Equation (21) are the maximum temperatures of the temperature profiles for the pair of experiments. No error at all is introduced or assumption made here in selecting the maximum temperature to use in Equation (21) since the rate constant calculated is then plotted against this temperature.

If a number of experiments are carried out at different temperatures, we can obtain solutions for each pair of experiments. In this way we can build up the usual log (rate constant) versus reciprocal temperature plot (see Figure 4). It is important to note that this plot has been obtained without the requisite of an isothermal experiment. The sensitivity of the calculation of E and A to experimental error is illustrated in Figure 4. The E values (the slopes) and the A values (the intercepts) can be seen to differ quite markedly depending on which pair of points are selected for the solution. However, the dotted line is a

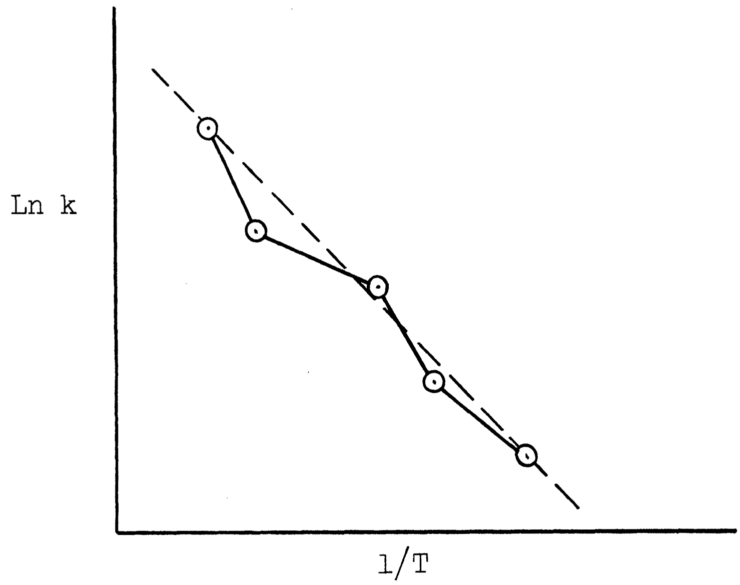

Figure 4. Data Smoothing (Fictitious Points).

fair representation of the data so that the ln k versus 1/T plot is seen to be a convenient way of smoothing the data.

III. APPARATUS AND EXPERIMENTAL TECHNIQUE

A. Description of Apparatus

A diagram of the apparatus is shown in Figure 5. The gases used in this study were obtained in cylinders from the Matheson Company, Inc. The ethylene and acetylene were 99.5 mol % purity, the ethane 97.0 mol % purity and the nitrogen 99.996% purity (8 p pm oxygen). More detailed analyses of the feed gases are contained in Table II. The gases were supplied from the cylinders at a steady pressure of 10 to 20 p.s.i. by Matheson No. 1 single stage regulators. The gas flowed throughout the system in 1/4 or 3/8 in. copper tubing with brass compression fittings. The flow rates of the various gases used were controlled manually with 1/8 in. needle valves and were measured with various sizes of rotameters (Matheson Universal Flowmeters). The gases then passed into the ceramic reactor which was contained inside the furnace. Temperatures were measured with Chromel P-Alumel thermocouples and pressures were measured with mercury or water filled manometers. A sample of the gas stream was taken as it left the reactor. A vacuum pump was connected to the sample system to facilitate air removal from the sample bulbs. The gas then passed through a wet test meter which measured the volumetric rate and then out through a vent.

The details of the furnace are shown in Figure 6. The alundum muffle was obtained from the Norton Company and was 1-1/2 in. bore with 1/4 in. walls of type RA 139 material. The platinum wire for the winding was obtained from the Baker Platinum Division of Engelhard Industries, Inc. and was 0.020 in. in diameter and 50 ft. long. The furnace was

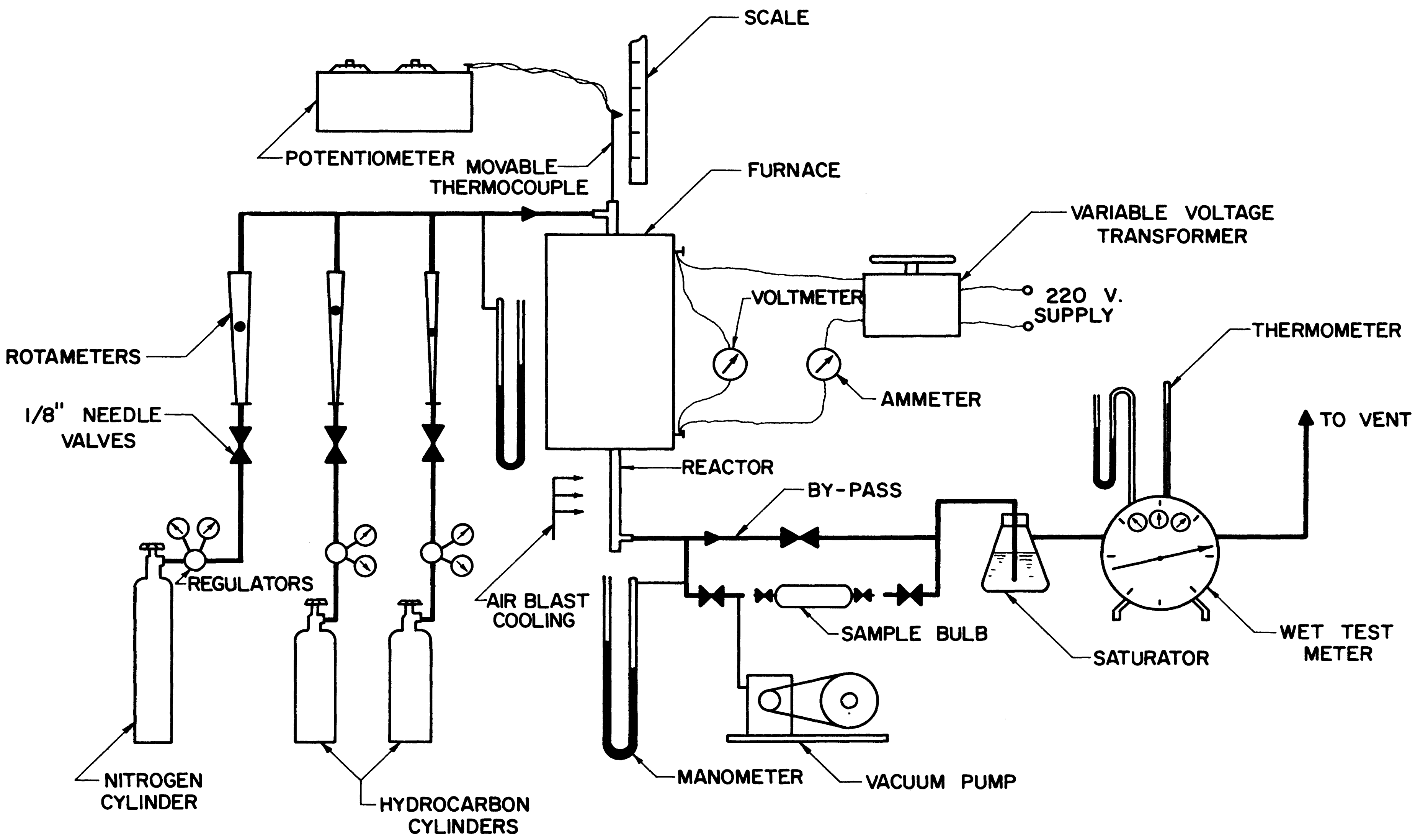

Figure 5. Diagram of Apparatus.

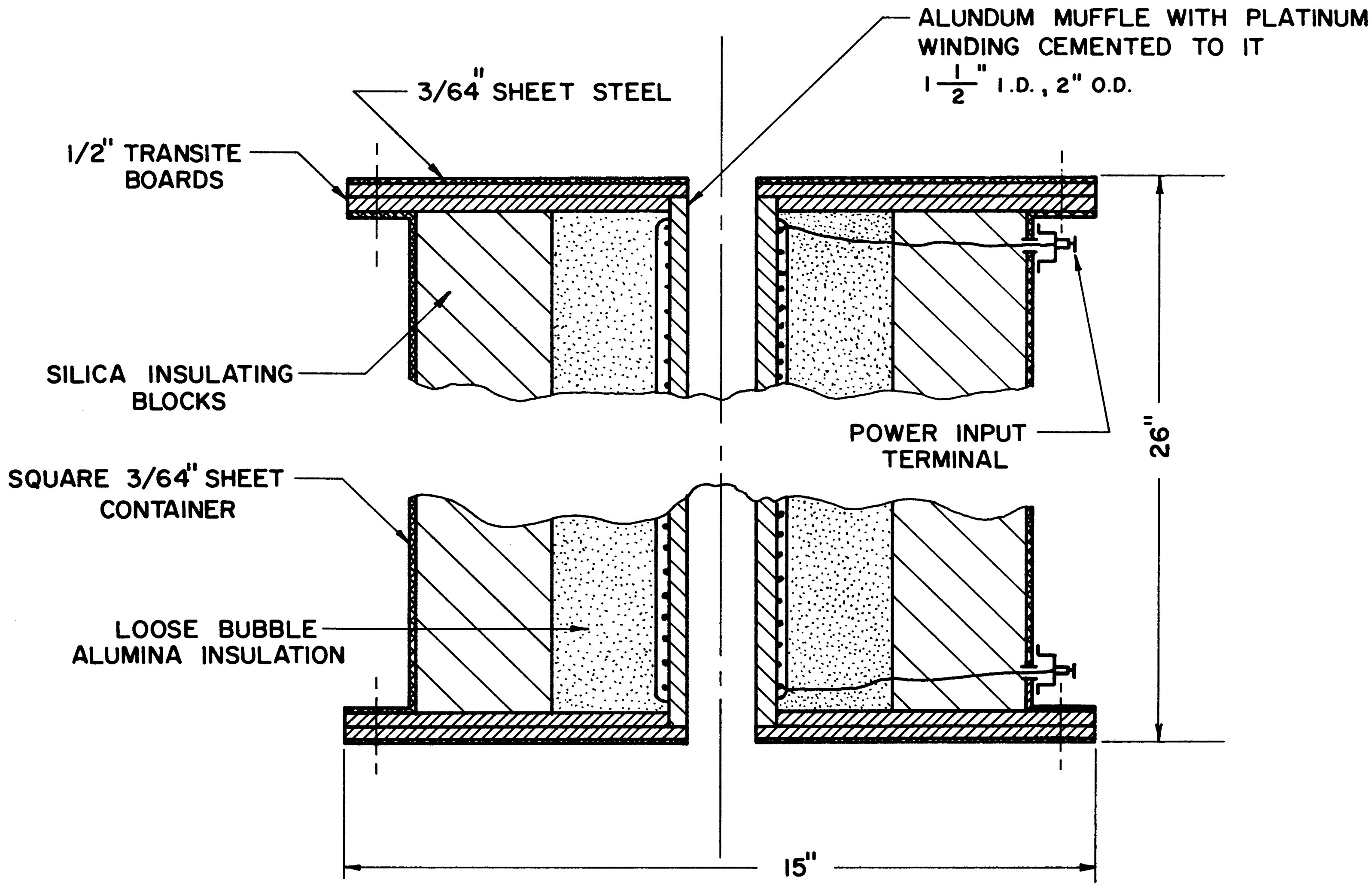

Figure 6. Furnace Details.

designed to operate up to 1600°C and the watt density on the winding at 1500 watts power input was 40 watts/sq.cm. The winding was all in one piece and the turns were placed closer together at the ends to compensate for the large end heat losses. The actual spacings were (starting from one end) 1 in. at 8 turns/in., 1 in. at 6 turns/in., 4 in. at 4 turns/in., 10 in. at 3 turns/in., 4 in. at 4 turns/in., 1 in. at 6 turns/in., 1 in. at 8 turns/in. Double lead in wires for the power supply were used to prevent overheating in the passage through the insulation. The platinum winding was cemented to the muffle with Norton RA 1139 cement. Norton Bubble Type alumina was used as the high temperature insulation close to the muffle, and was poured in loosely. Johns Manville Superex (a silica type insulation) blocks were used for the lower temperature insulation. The whole furnace was contained in a light sheet steel rectangular box. Transite boards (1/2 in. thick) were bolted onto both ends of the sheet steel container to center and support the muffle and to contain the loose insulation.

Three different reactors were used in the course of the experiments. The first of these reactors is illustrated in Figure 7 and was a 3/4 in. I.D. packed reactor. The other two reactors were concentric tube type reactors as shown in Figure 8. The packed reactor was the initial design and the purpose of the packing was to prevent radiation from the reactor wall affecting the center thermocouple reading. This ensures that the center thermocouple is reading the true gas temperature at that point. A second thermocouple sheath was placed between the reactor and the muffle. However, this design of reactor was found to be limited in its use since its pressure drop became too high as the

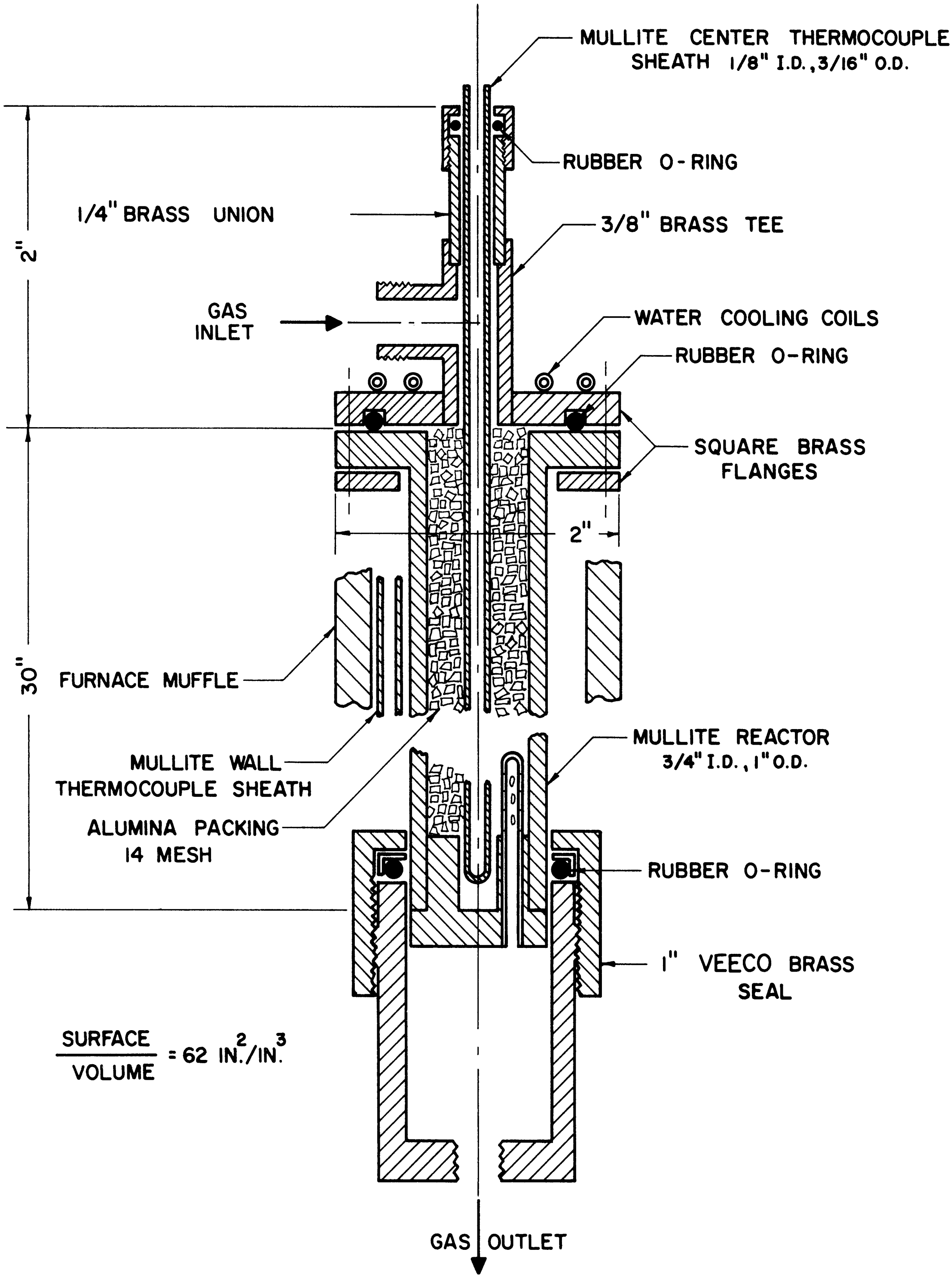

Figure 7. Constructional Details of the Packed Reactor (No. 1).

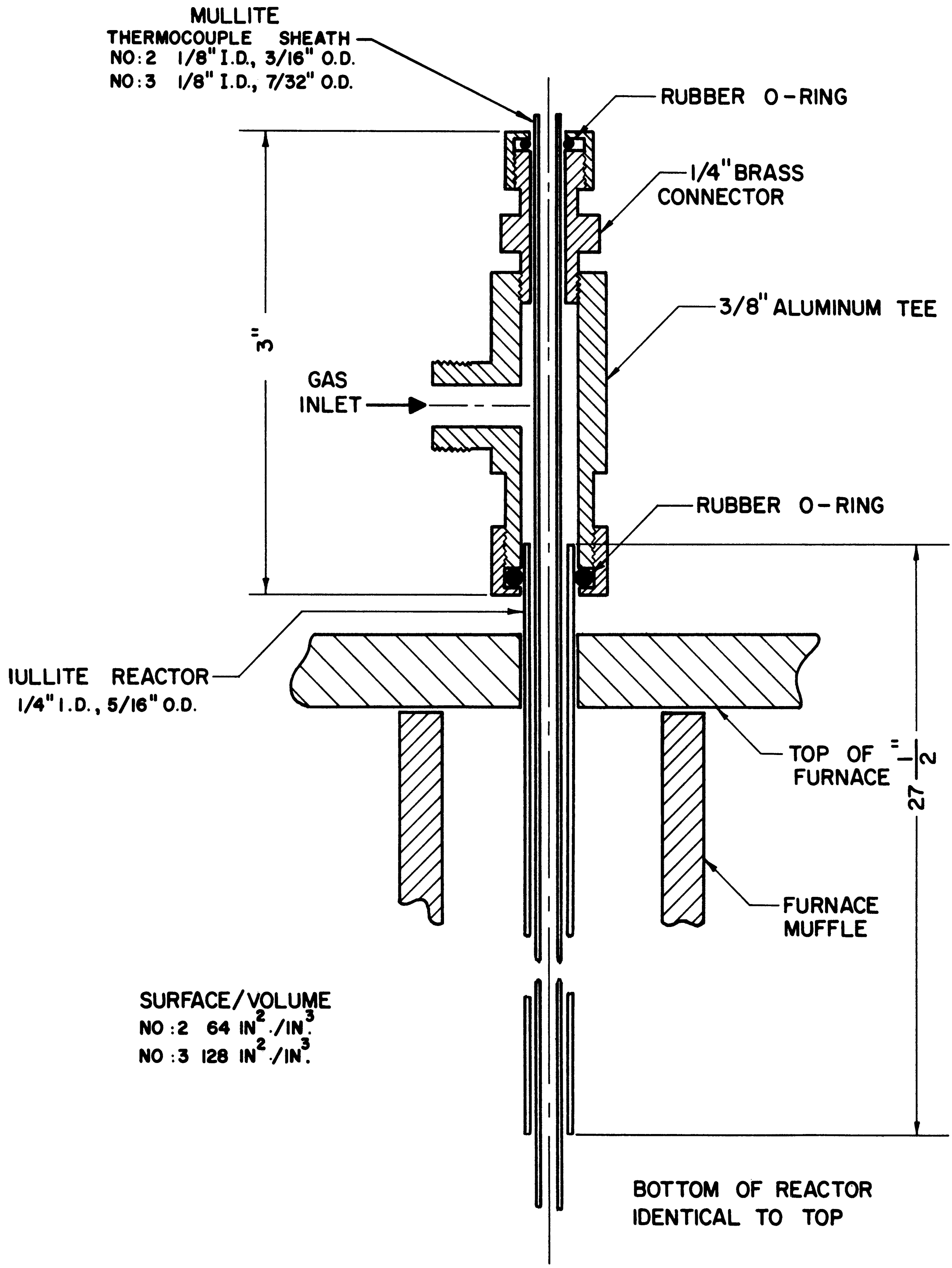

Figure 8. Constructional Details of the Annular Reactors (Nos. 2 and 3).

flow rate increased, so that the concentric tube type reactor was constructed. The great gas velocity through the narrow annulus in this reactor ensured that the center thermocouple read the true gas temperature (this is discussed further in Section IVA(iv)). The reactors and thermocouple sheaths were made from Vitreous Refractory Mullite (type MV 30) obtained from the McDanel Refractory Porcelain Company. The seals were made on each end with rubber O-rings. The top seal on the packed reactor was water cooled and the bottom seals were cooled by an air blast. The cooling of the seals was to lessen the heat deterioration of the rubber O-rings. The thermocouples were made from 26 gauge Chromel P-Alumel wires and could be moved up and down inside the thermocouple sheath (see Figure 9). A scale was mounted vertically so that the position of the thermocouple in the sheath could be determined precisely.

B. Experimental Technique

About 5 or 6 hours were required to heat the furnace up to operating temperature as heating rate was limited to 5°C per minute to prevent thermal shock damage to the alundum muffle. The feed rates of the various gases were observed with the rotameters and were controlled manually with the needle valves. The temperature was controlled manually with the variable voltage transformer. A sample bulb was inserted in the exit line and the air pumped out of it with the vacuum pump. When the system had reached steady state a gas sample was obtained by diverting the exit gas stream into the sample bulb by closing the bypass line. At that time a temperature profile was obtained as quickly as possible

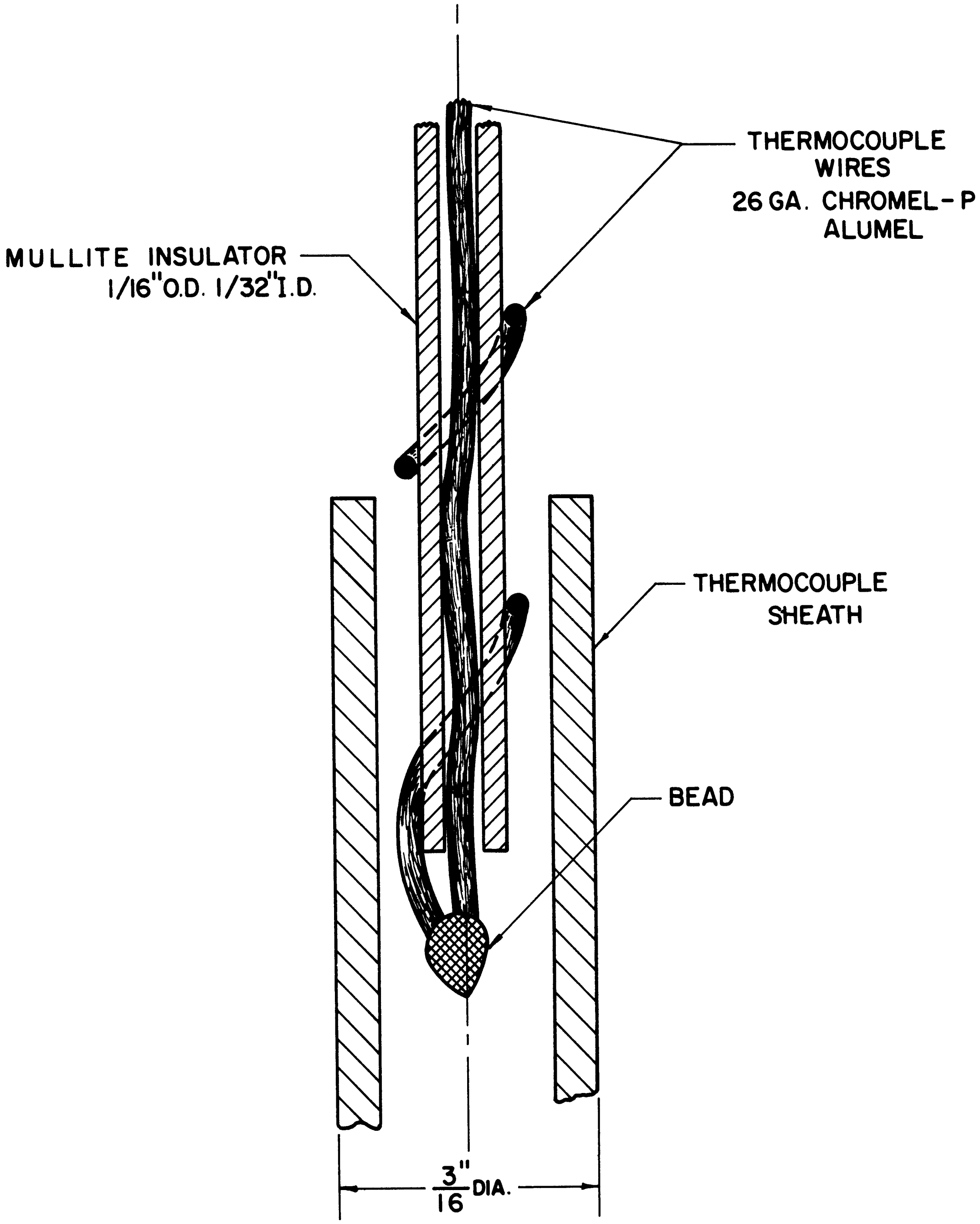

Figure 9. Thermocouple Details.

along the length of the reactor. The inlet and exit manometers were read and the volume of gas passing out through the wet test meter was recorded for a measured time. The temperature and pressure in the wet test meter were noted and the atmospheric pressure was read and recorded. The experimental conditions were then changed to the next set of desired values and the system was allowed to come to steady state again (which would take from 1/2 hour to 1-1/2 hours). Air was passed through the hot reactor after each series of runs to burn off any carbon deposited during the reaction.

C. Chemical Analysis

The analyses of the gas samples were carried out on a mass spectrometer (Consolidated Engineering Corporation Type 21-103B). The carbon analysis was obtained by material balance. The mass spectrometer is a comparative instrument in that a quantitative analysis of a mixture can only be obtained by comparing the sample cracking pattern with those for the pure components in the mixture. The cracking pattern is the relative amounts of ion fragments at each mass to charge ratio resulting from electron bombardment of the sample. If a pure sample of a compound in the mixture is not available, then a comparison can be made with published cracking patterns[3], although this is less accurate because patterns change slightly from machine to machine. In this work pure samples were available for most of the components (C_2H_6, C_2H_4, C_2H_2, CH_4, H_2, N_2, C_3H_6, C_3H_8, C_6H_6, 1-3 C_4H_6) of the mixtures so that reference was only made to the literature patterns in the case of some minor components (C_3H_4, C_4H_4, C_4H_2, C_5H_6).

A difficulty arises when a component has a number of possible structures for the same chemical formula because the cracking patterns are quite similar. If considerable amounts of one of these components are present in a mixture, it can usually be identified but if it is only present in small quantities, identification of the structure is practically impossible. The difficulty is increased if the compound is also one for which a pure sample is not available. Most of the components of the mixtures analyzed in this work only have one possible structure. The major product C_4H_6 has three possible structures 1-3, 1-2 butadiene and butadiyne but was present in large enough amounts to allow positive identification with the mass spectrometer as 1-3 butadiene. The other components with alternative structures were, C_3H_4 methylacetylene or allene, C_4H_4 vinylacetylene or butatriene, and C_5H_6 cyclopentadiene or a penten-yne. These possibilities are discussed further in the sections on product distributions.

D. Experimental Program

The overall reaction was broken down into three steps for the purposes of experimentation, namely the thermal decompositions of ethane, ethylene and acetylene. Sets of runs were carried out for each of the compounds to determine the product distribution, the orders of the reactions and the kinetic rate constants.

The product distributions were determined at various conversions with the temperature profile held constant. The purpose of these runs was to show the origin and order of appearance of the various products formed. The orders of reaction were studied by a series of runs in which the concentration of the reacting component was varied by nitrogen dilution whilst keeping the temperature profile constant. The kinetic rate constants were investigated with a series of runs at spaced temperature intervals with the flow adjusted to give the desired conversion. In all of the runs the amount of reaction was kept reasonably low so that the initial reactions in each case would predominate over the secondary reactions of the products. The conversions were not usually much below 10% since the accuracy of the chemical analysis would be lessened at this conversion. The conversions were as high as 60% - 70% in some of the higher temperature runs since the limitations of the equipment would not permit a high enough flow rate to reduce the residence time sufficiently.

Some data were also obtained at high conversions using ethane feed and producing ethylene, acetylene and carbon as well as other side products. These runs were used to check out the overall correlation resulting from the combination of the data on the individual steps. Some data were also obtained on the effect of addition of propylene which acts as a free radical chain inhibitor.

IV. EXPERIMENTAL RESULTS AND DISCUSSION

A. Thermal Decomposition of Ethane

(i) Product Distribution

A set of runs (Nos. 80, 81, 83, 84) was carried out at approximately the same temperature in which the product distributions were measured at various levels of conversion. The amount of conversion was varied by changing the flow rate which alters the residence time. The temperature need not be controlled or measured precisely for these runs since the product distribution is not affected very much by moderate variations in temperature. Table II contains the raw data and Table VI the conversions and product distributions (expressed as moles formed per 100 moles of ethane reacted) computed from the raw data. The product distributions are plotted against the conversion in Figure 10 and this plot is studied to determine the primary stable molecular species that result from the thermal decomposition. The primary products are those products that appear in significant amounts at low conversions and the secondary products are those that appear only after considerable conversion has taken place.

It can be seen from Figure 10 that ethylene and hydrogen together with lesser amounts of methane and a small quantity of propane are primary molecular products. The only secondary product to occur is 1-3 butadiene (C_4H_6) which appears only in small amounts at the highest conversion. The propylene shown in the analysis is not a reaction product but is an impurity present in the ethane feed. Previous workers[12, 24,48] in the literature have found the same products as were detected in this work.

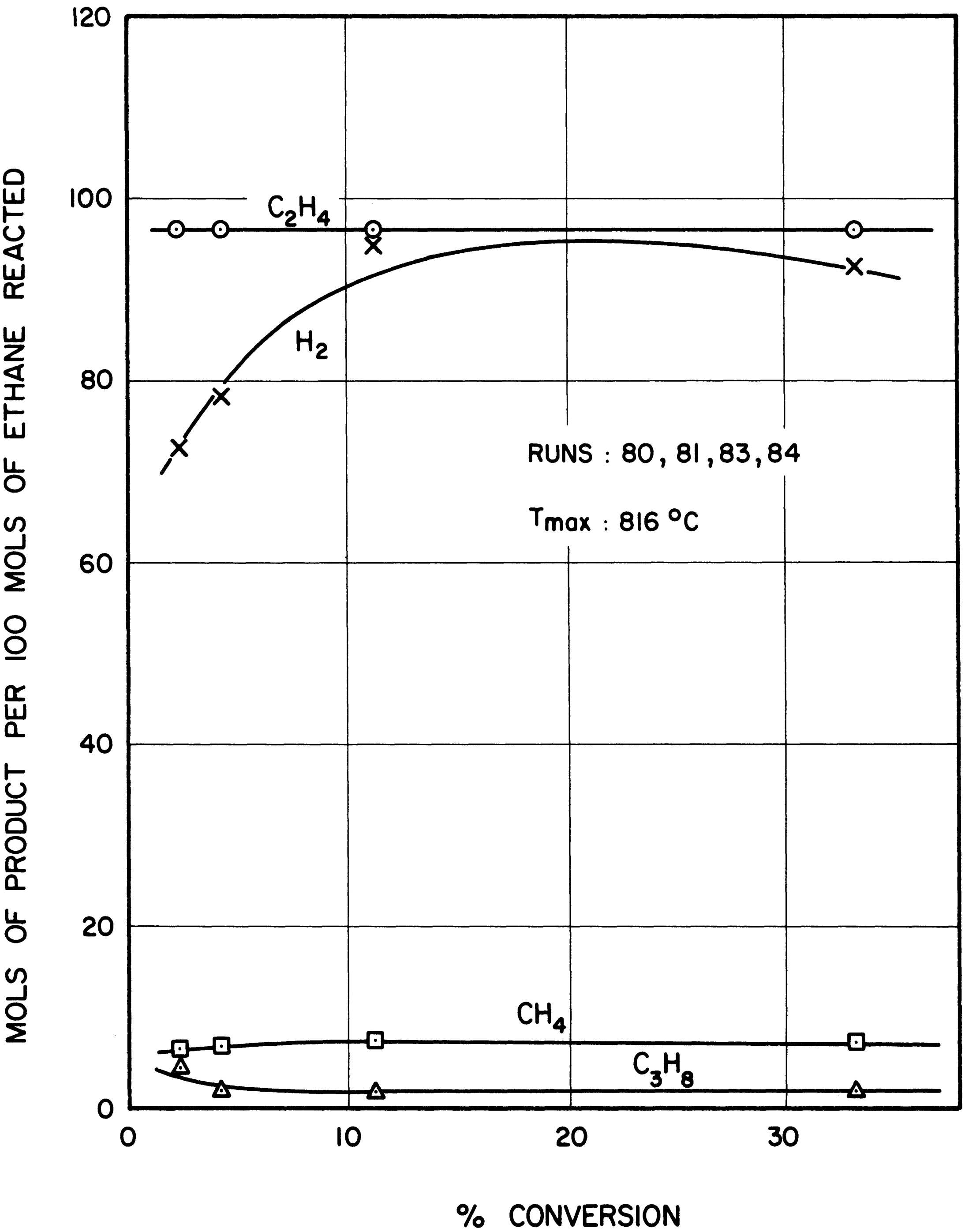

Figure 10. Product Distribution in Ethane Decomposition.

(ii) Order of Reaction

This set of runs (Nos. 49 - 53) was undertaken to determine the order of reaction for the formation of the primary molecular products with respect to the ethane concentration. The experiments were conducted at constant temperature profile and the mole fraction of ethane was varied with nitrogen dilution. The total flow rate was kept constant for all of the runs so that the temperature profile would not be disturbed. The conversions were kept to a low value so that a differential rate measurement was obtained and also so that the mole fraction of ethane was not changed significantly. The raw data are contained in Table III and the calculated rates and mole fractions are to be found in Table VII. The logarithm of the rate is plotted against the logarithm of the mole fraction (arithmetic mean of inlet and outlet values) of ethane in Figure 11 the slope of which represents the order of reaction (the validity of this is shown in Section IID).

The disappearance of ethane and the formation of ethylene and methane are seen to be first order in ethane concentration. This is in agreement with the previous work of Pease[33] and Frey and Smith[20] at 600 °C and Calderbank and Hovnanian[12] at 800 °C who showed that the disappearance of ethane was first order. The last named authors also showed that the formation of methane was first order in ethane concentration.

(iii) Rate Constants

Now that we have established that the significant primary molecular products are ethylene and methane (together with the attendant hydrogen in quantities that fulfill the material balance) and that the

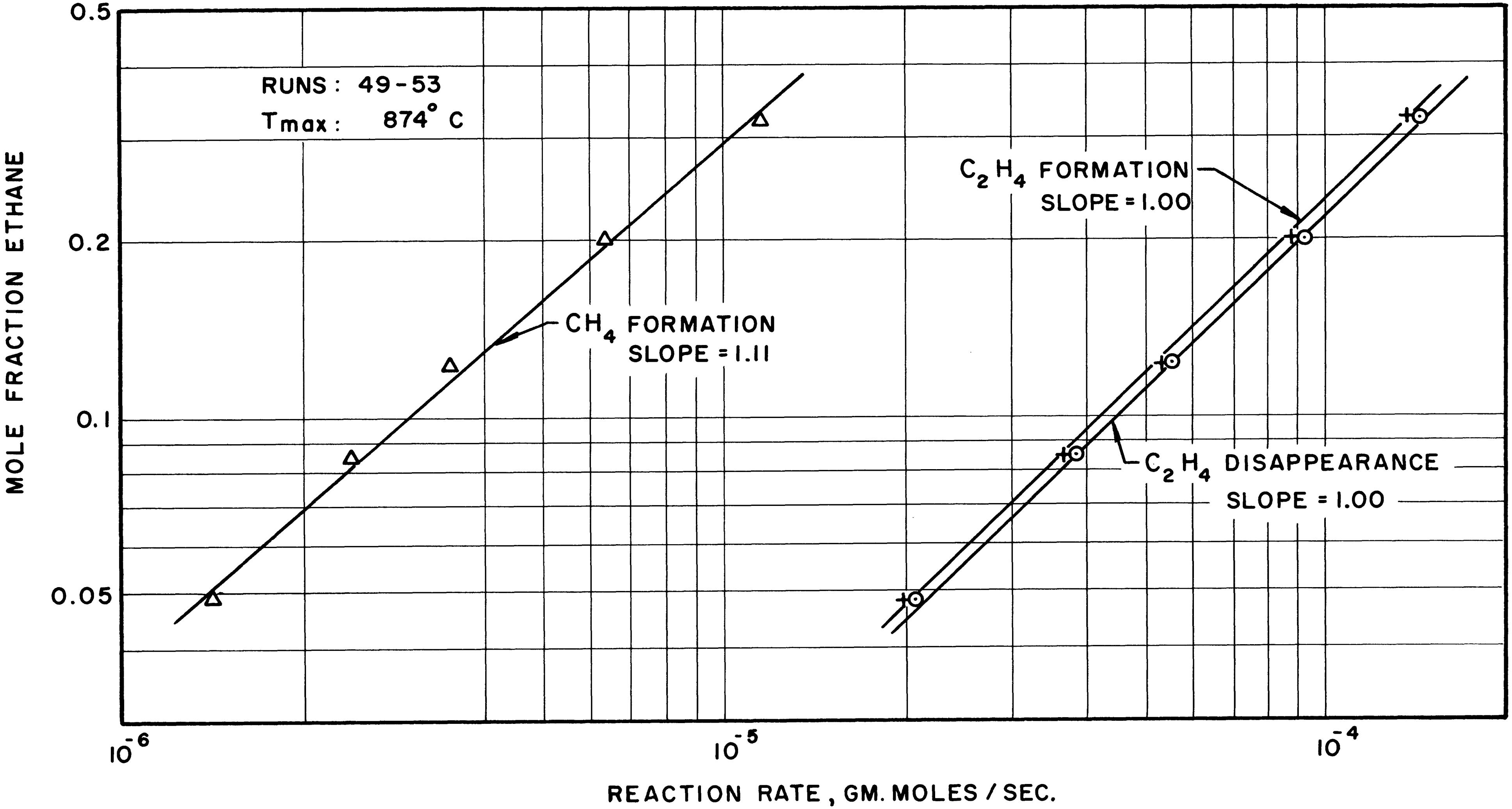

Figure 11. Ethane Decomposition Orders of Reaction.

reactions are first order in ethane concentration, we can set about determining the rate constants. A number of experiments (Nos. 18, 19, 21, 22, 41 - 46, 128, 129) were carried out each with a different temperature profile in order to obtain the rate constants. A typical temperature profile is shown in Figure 12. The conversions were kept fairly low so that the primary reactions would predominate and this was achieved by reducing the residence time (by increasing the flow rate) as the temperature was raised. Nitrogen dilution was used to reduce the effect of reverse reaction (some calculations showing the reverse reaction to be negligible are in Appendix VI) and to lower the conversion. The raw data for these runs are presented in Table IV. The method of calculation of the rate constants from these data obtained with a nonuniform temperature distribution has been developed in Section II of this work. A sample calculation showing all of the numerical details is contained in Appendix IV. It is recalled that values of the activation energy and the pre-exponential factor of the Arrhenius rate equation are computed from pairs of data points. These kinetic constants are then used with the maximum temperature for a run to compute a value of the rate constant at that temperature. The assumptions used in the derivation were irreversible homogeneous reaction, negligible radial temperature gradient and plug flow. Table VIII contains the first order rate constants for the disappearance of ethane and these are plotted versus reciprocal temperature in Figure 13.

The rate constants were determined from pairs of runs (indicated in Table VIII) which were adjacent in temperature. It is apparent that very many pairs of points could be selected from a set of runs (Nos.

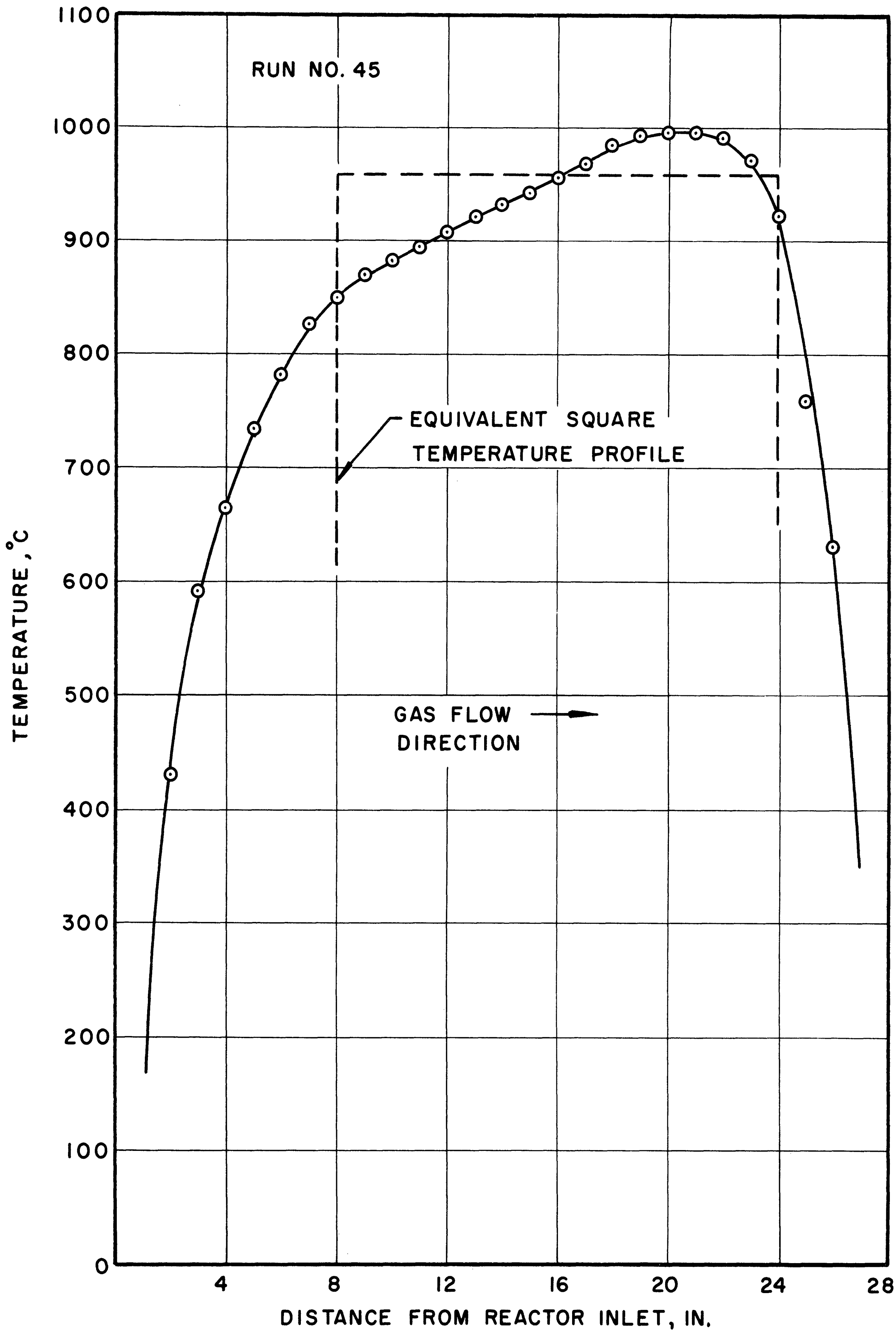

Figure 12. Typical Experimental Temperature Profile.

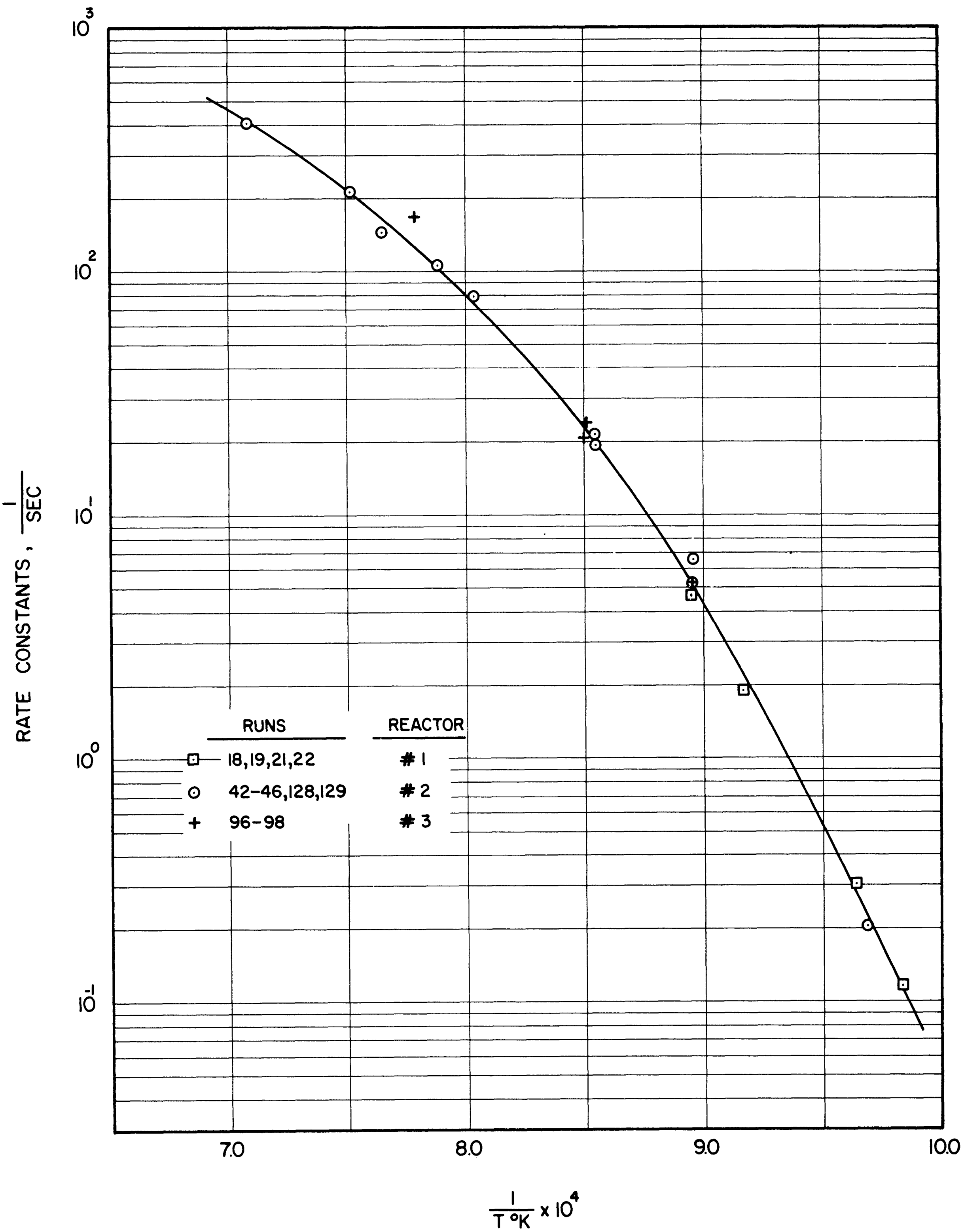

Figure 13. First Order Rate Constants for the Disappearance of Ethane.

18, 19, 21, 22) and the values of the rate constants compared. The results are contained in Table VIII and are plotted in Figure 14 which shows that there is very close agreement between the different solutions. Therefore, in the rest of this study only adjacent pairs of points are used to calculate the rate constants.

The presentation of the rate data as first order rate constants for the disappearance of ethane is a simplification as we have seen that there are two parallel reactions forming ethylene and methane. The calculation method has to be modified a little to enable the rate constants for the two reactions to be evaluated. These modifications are explained in detail in Appendix V. The rate constants for the first order formation of ethylene and methane are contained in Table VIII and are plotted against reciprocal temperature in Figure 15.

The majority of the literature data is presented as first order rate constants for the disappearance of ethane. The results of a number of workers (including some shock tube work) are plotted in Figure 16 and are found to compare well with the results of this work. The data of this work show less scatter than the literature data especially at higher temperatures and this is attributed to the careful measurement of the temperature profile and its proper consideration in the calculations. A definite downward curvature of the rate constants plot is exhibited by the results of this work. The literature data do not disagree with this curvature although the curvature is not apparent from the literature data alone because of the large amount of scatter. The curvature apparently indicates a decreasing activation energy but this is found not to be the explanation. In a later section of this work the curvature is shown to

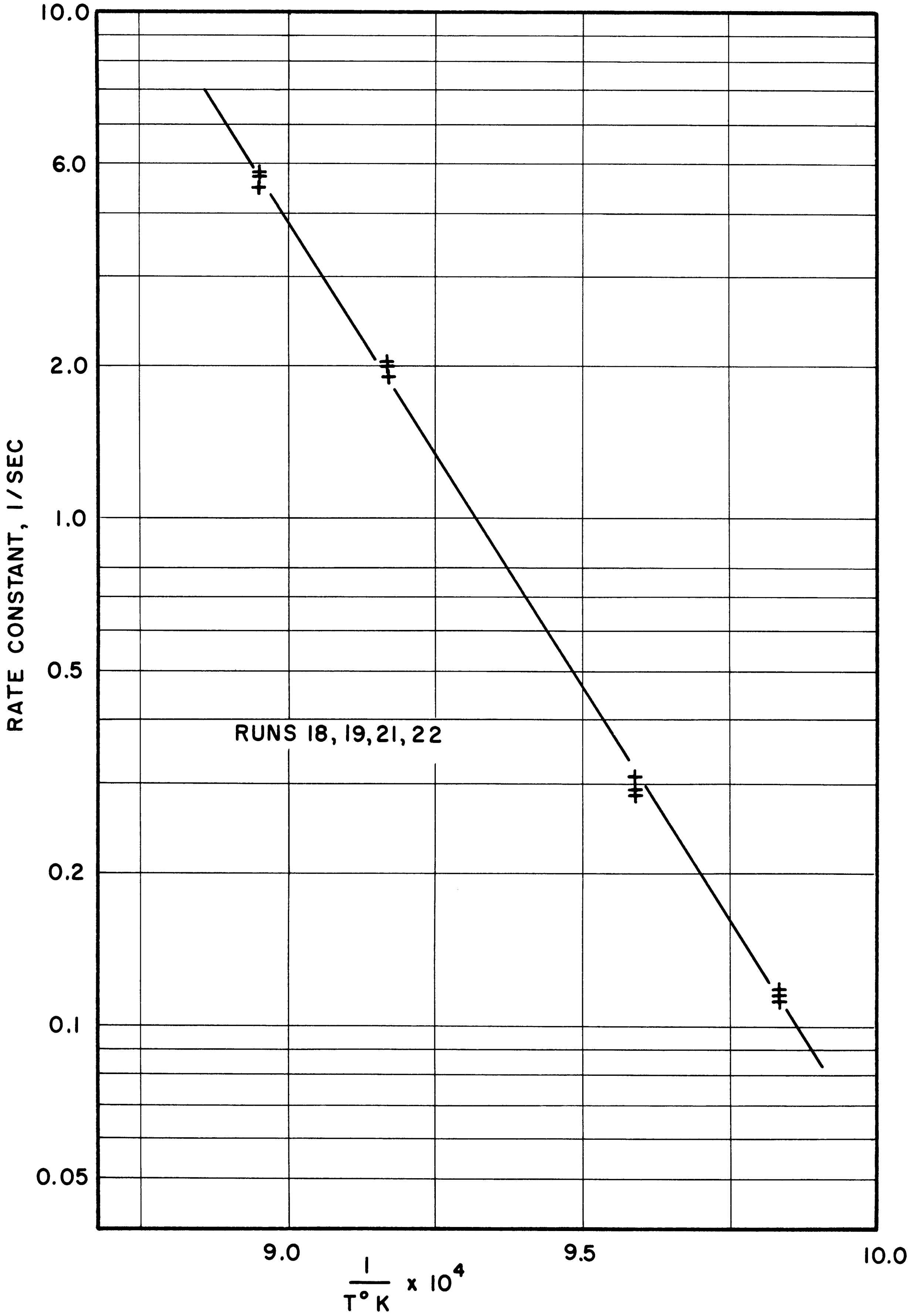

Figure 14. Solutions for All Possible Pairs from Four Points (First Order Rate Contents for Disappearance of Ethane).

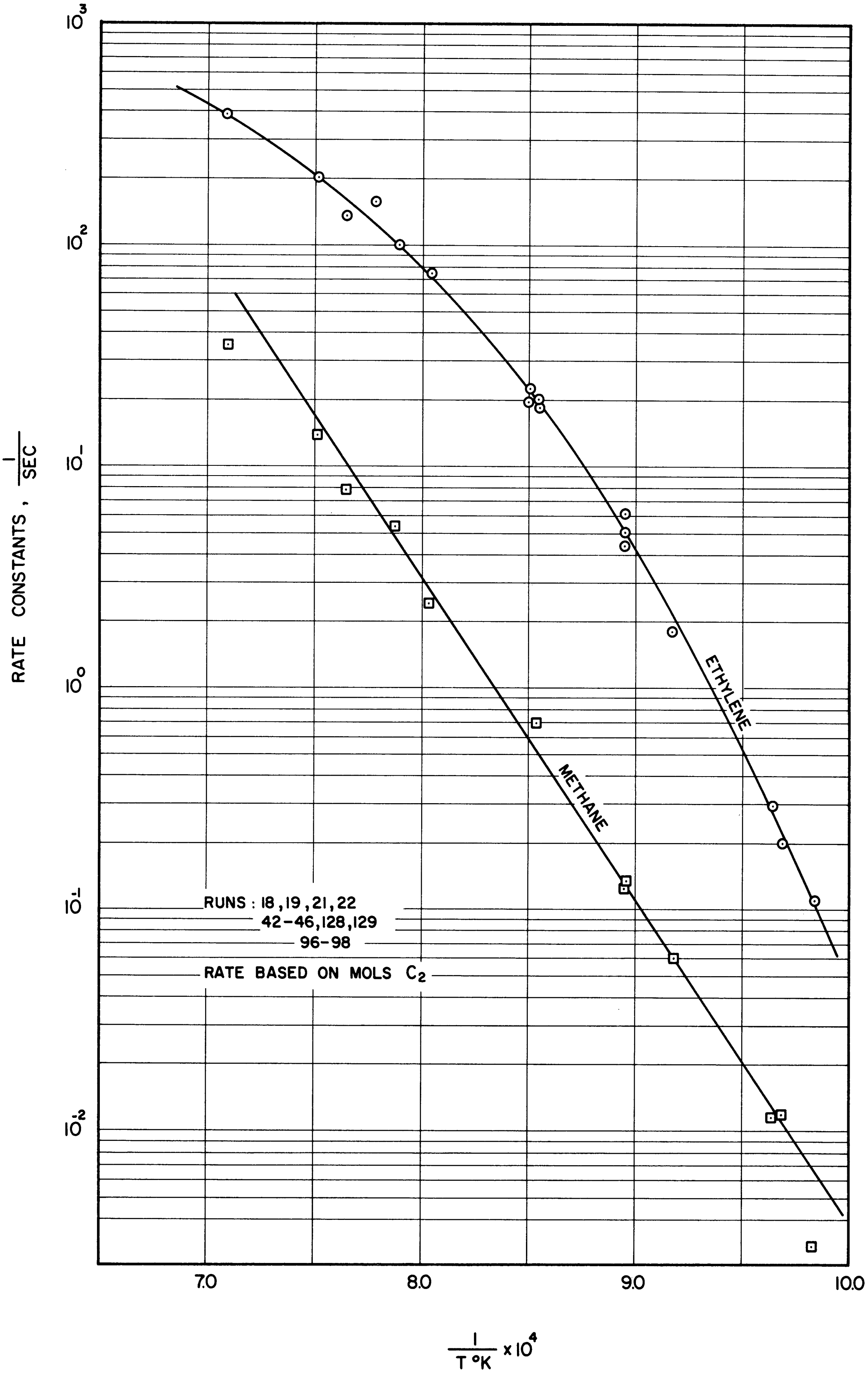

Figure 15. First Order Rate Constants for Formation of Ethylene and Methane from Ethane.

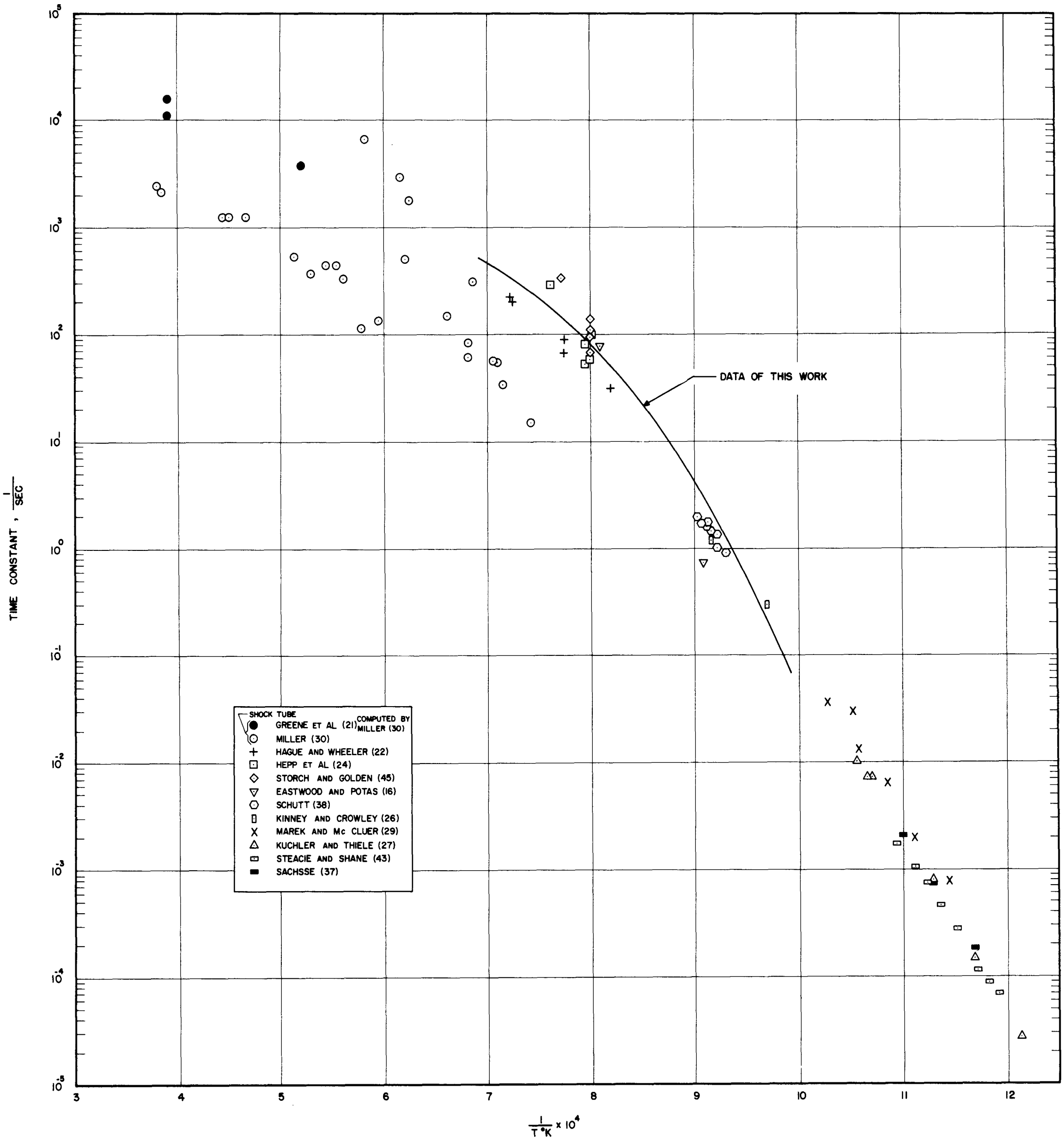

Figure 16. First Order Rate Constants for Ethane Disappearance, a Comparison with Literature Data.

be a result of inhibition of the rate by secondary products of the reaction which are formed at higher temperatures. One previous piece of work by Calderbank and Hovnanain[12] contained some rate constant values for the first order formation of methane which agree well with this work.

In the temperature range 730°C to 900°C for this work the first order rate constants for ethane disappearance (and ethylene formation) show an activation energy of 82.4 k cals/gm. mole. Above 900°C the reaction becomes inhibited by reaction products (the empirical representation of the data in this region is developed further in Section VIA). This value of the activation energy is a little higher than that found by the previous workers whose values lie between 66 and 75 k cals/gm. mole. Over the whole temperature range studied in this work (730°C to 1160°C) the first order rate constants for methane formation show an activation energy of 66.9 k cals/gm. mole which agrees quite well with the value of 64.4 k cals/gm, mole reported by Calderbank.[12]

Various workers have shown that the reaction is homogeneous,[33,43] however, this was checked with a few runs carried out in a reactor (No. 3) which had a different surface to volume ratio. These points are plotted on Figure 13 and are seen to be coincident with the data in No. 2 reactor, which indicates that the reaction is homogeneous.

(iv) Temperature Distribution

The problems that will be considered here are firstly, do the thermocouples in the various reactors read the true gas temperature and secondly, can the radial temperature gradients be considered negligible. Figure 17 contains radial sections through the various reactors used

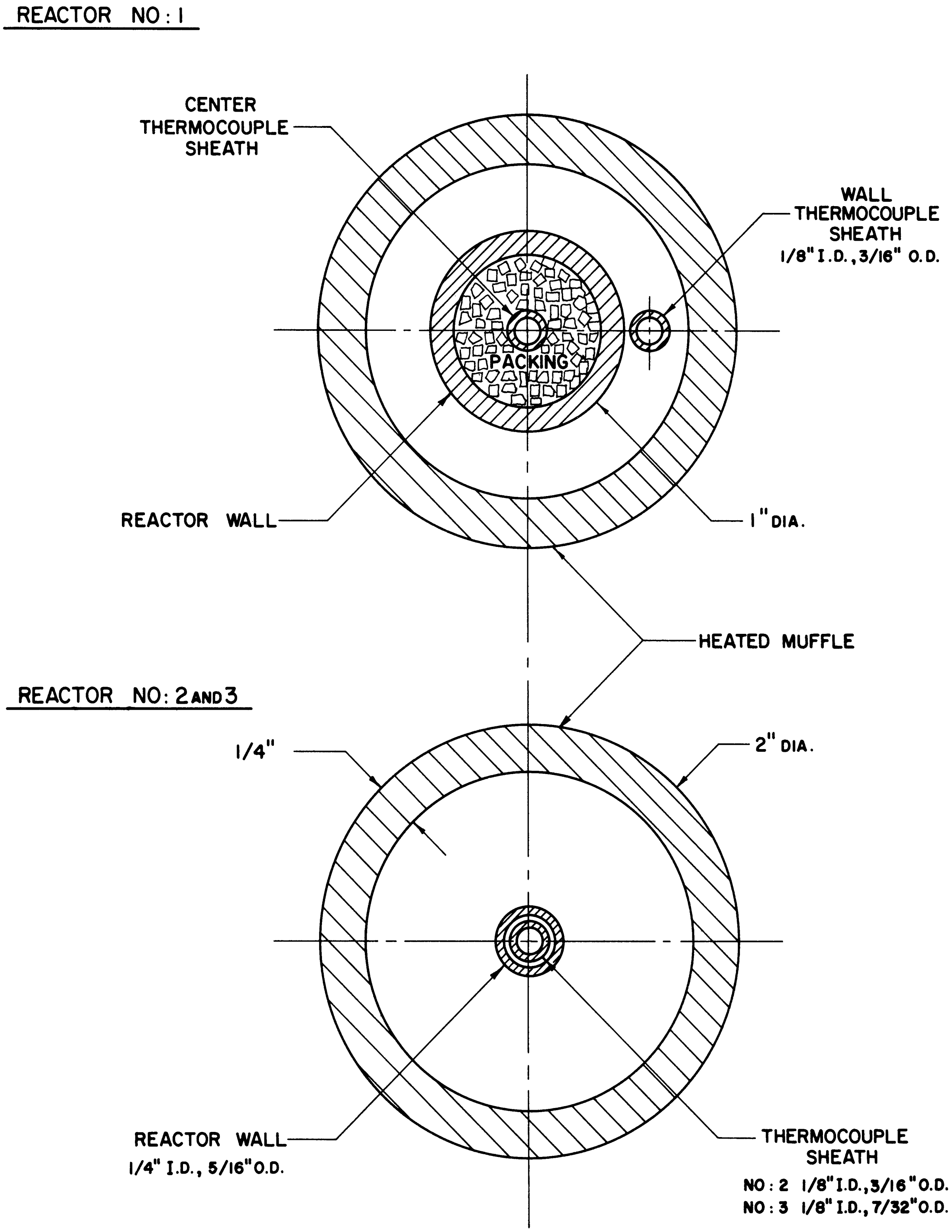

Figure 17. Radial Section Through Reactors Showing Location of Thermocouples.

showing the location of the thermocouples. The first reactor used in the experimental work was No. 1 and it was designed to contain refractory packing which would shield the center thermocouple from radiation from the hot reactor wall. The gas velocity through the packing in reactor No. 1 is quite high so that the packing and the gas will be close to thermal equilibrium. The center thermocouple in reactor No. 1 is considered then to measure the true gas temperature at the center of the reactor. A second thermocouple was placed alongside the reactor wall in the annulus between the reactor and the furnace muffle. The purpose of this thermocouple was to measure the wall temperature of the reactor, however, it can be seen that this thermocouple will read a temperature greater than the desired wall temperature because of the radiation from the hot furnace muffle (there is no radiation shield for this thermocouple or gas flow to reduce the radiation error). Runs 18, 19, 21 and 22 were carried out in reactor No. 1 and both the center temperature (Tc) and the wall temperature (Tw) profiles were measured (see Table IV). Then the rate constants were calculated using in one case the center temperature and in the other case the radial distribution. A linear radial distribution is assumed between Tw and Tc and some calculations contained in Appendix III show that the correct mean temperature to use in the calculations is Tc + 0.75 (Tw - Tc). The values of the rate constants for the two cases are contained in Table VIII and are plotted versus reciprocal temperature in Figure 18. It is seen that the difference in the rate constants is quite small and it is pointed out that this difference is greater than the maximum possible error since it is known that the wall thermocouple will be reading greater than the true wall

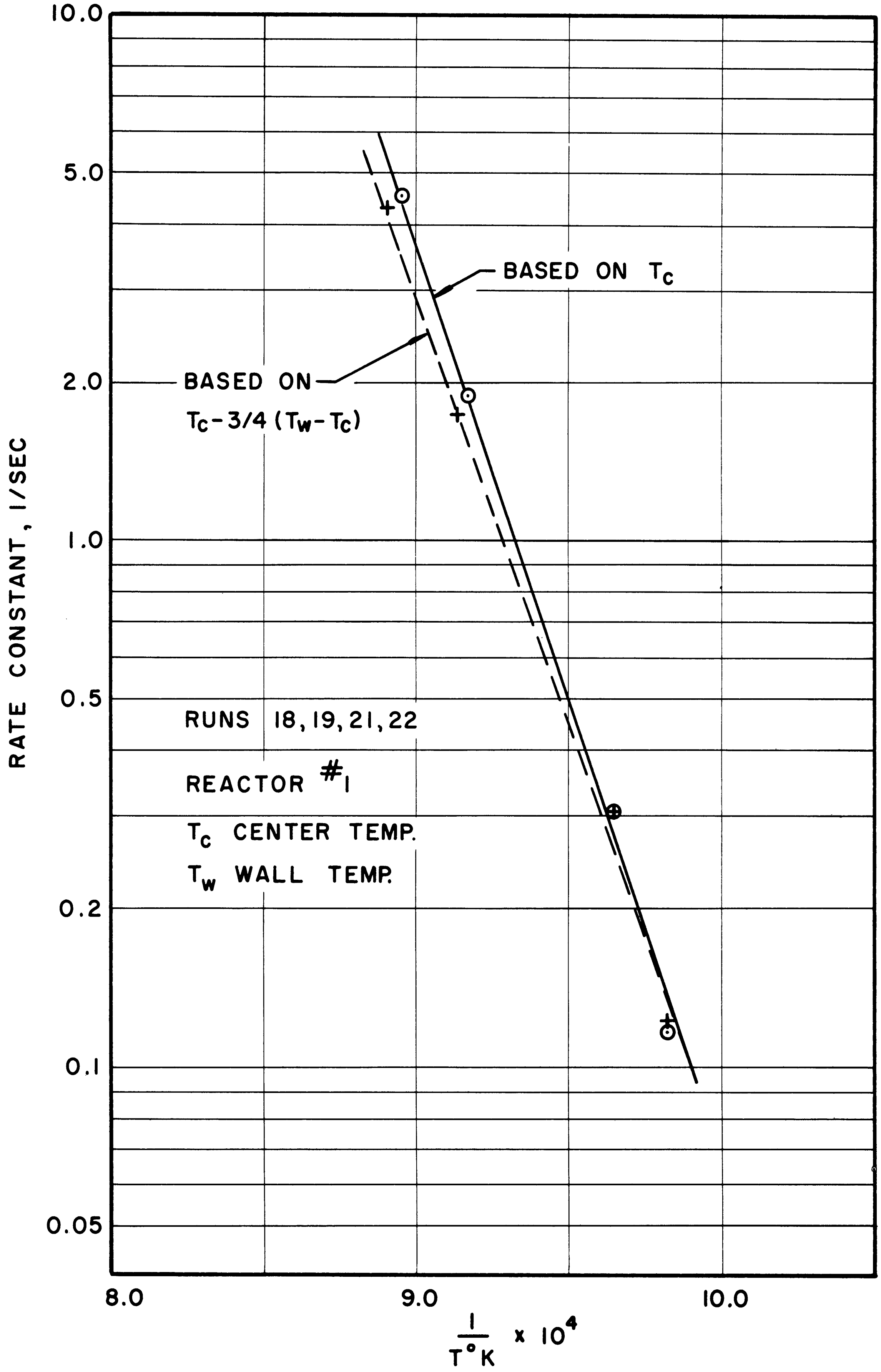

Figure 18. Effect of Radial Temperature Distribution.

temperature, and the assumption of linear temperature distribution is an unfavorable one. It is concluded then that the radial temperature distribution is negligible in reactor No. 1 so that the center temperature can be used in the calculations of rate constants.

Reactor No. 1 was found to be unsuitable for the higher temperature experiments since a pressure drop limitation would not allow high enough flow rates to give the low residence times required. Therefore, reactors No. 2 and No. 3 were built and used for the higher temperature experiments. These two reactors are similar in design and are just simple annular spaces between two tubes with the center tube acting as the single thermocouple sheath. These annular reactors are of much smaller diameter than the packed reactor so that they have a higher gas velocity and a lower mass flow rate. These last two factors both will reduce the radial temperature gradients below that experienced in the packed reactor so that we can safely say that the radial temperature gradient is negligible with respect to its effect on the computed values of the rate constants. These annular reactors do not have any radiation shielding between the reactor wall and the center thermocouple sheath so that the question arises of whether the center thermocouple is reading the true gas temperature. The gas velocity through the annulus is very high (of the order hundreds of feet per second) and this will reduce the radiation error. Some experiments were carried out in the annular reactor within the same temperature range as the previous experiments in the packed reactor and the values of the rate constants were coincident (see Figure 13). Since we have already established that in the packed reactor the true gas temperature is measured, we can conclude that the center thermocouple measures the true gas temperature in the annular reactors.

B. Thermal Decomposition of Ethylene

(i) Product Distribution

The product distribution runs (Nos. 86 - 89, 126) were carried out in a similar fashion to those for ethane. The raw data is contained in Table II, the results in Table VI and the product distribution is plotted against conversion in Figure 19. Figure 19 shows the major primary molecular products to be acetylene, hydrogen and 1-3 butadiene and the major secondary products to be C_4H_4, benzene, methane and carbon. Propane, propylene, ethane, C_4H_2, C_3H_4 and C_5H_6 are also formed in small amounts. The C_4H_4 is thought to be vinylacetylene as a structure containing three double bonds seems unlikely, and the C_4H_2 can only be diacetylene. The C_3H_4 could be either propadiene or methyl acetylene and the structure of the C_5H_6 is not known.

Previous workers have studied the product distribution in this reaction although mostly at lower temperatures where polymerization predominates. Burk et al.[11] found the primary products to be butene (C_4H_8), acetylene and hydrogen at 625°C. Dahlgren and Douglas[13] found propylene, butene, butadiene and ethane as primary products at 480°C to 580°C. The results of this work agree with the literature results except for the product butene which was not detected at all in this work. In the kinetic study carried out in this work the primary products are considered to be acetylene, hydrogen and 1-3 butadiene.

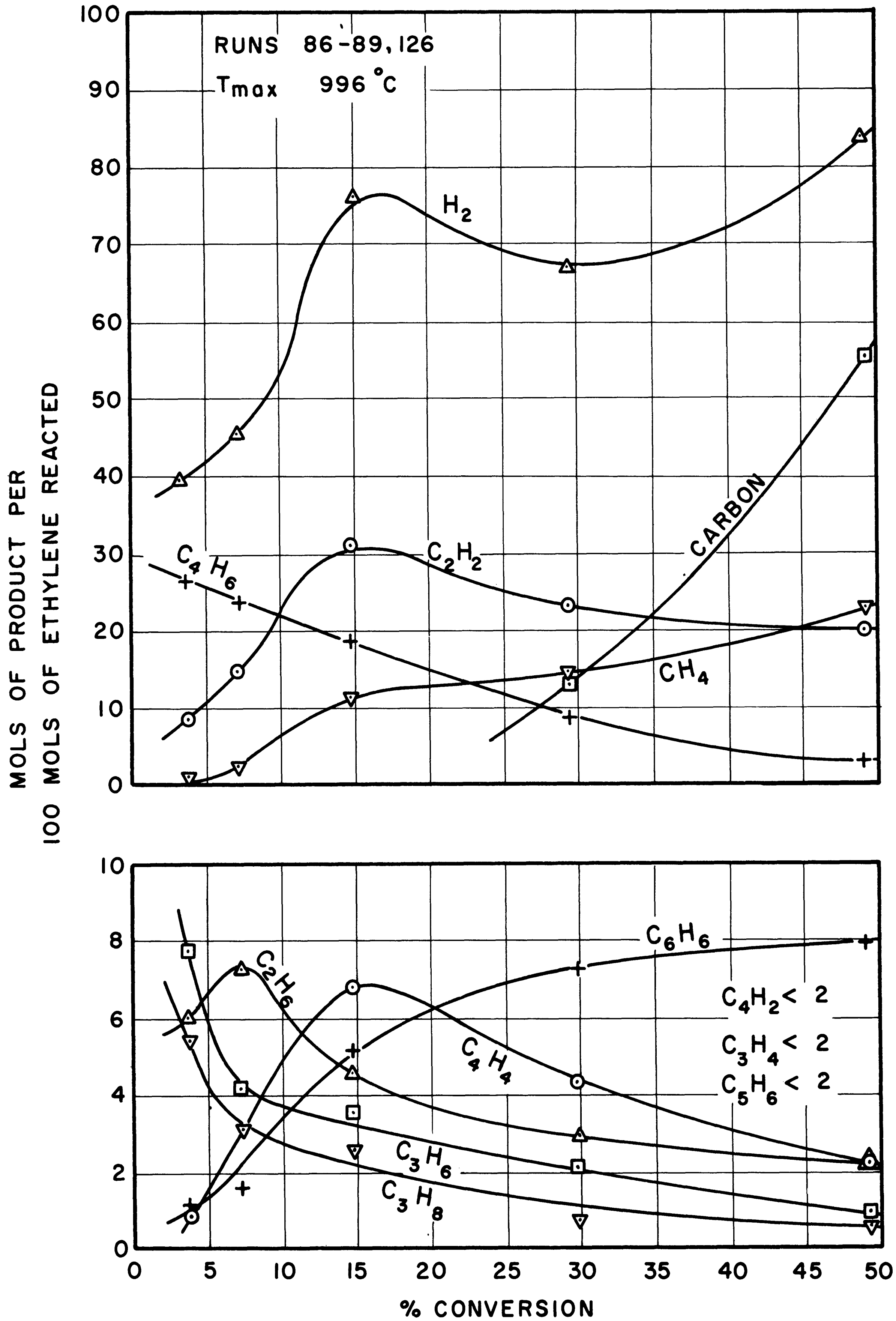

Figure 19. Product Distribution in Ethylene Decomposition.

(ii) Order of Reaction

The orders of reaction for the formation of the primary products from ethylene decomposition were determined in the same way as for ethane. The raw data (Runs 54 - 58) are found in Table III, the computed results in Table VII and the rates are plotted versus mole fraction in Figure 20. The polymerization products included C_4H_6, C_4H_4, C_5H_6 and C_6H_6. The acetylene formation is seen to be first order and the polymerization rate second order with respect to ethylene concentration. The literature data are mostly at lower temperatures where polymerization predominates and a homogeneous second order reaction is reported.[13,31]

(iii) Rate Constants

The raw data are contained in Table IV (Runs 24, 67, 68, 47, 48, 99 - 101) and the results in Table VIII. Figure 21 shows a plot of the first order rate constants for ethylene disappearance, however, this is a simplification of the reaction since there are actually two reactions occurring in parallel. Some data were obtained on reactor No. 3 which has a different surface to volume ratio and these also are plotted on Figure 21. The data from the two reactors are coincident so that this agrees with already reported fact[13] that the reaction is homogeneous. Using a modification (see Appendix V) to the calculation method developed in Section II, the rate constants for the first order decomposition and the second order polymerization are calculated, listed in Table VIII, and plotted versus reciprocal temperature in Figures 22 and 23. There is very little literature kinetic data in the temperature range of this work

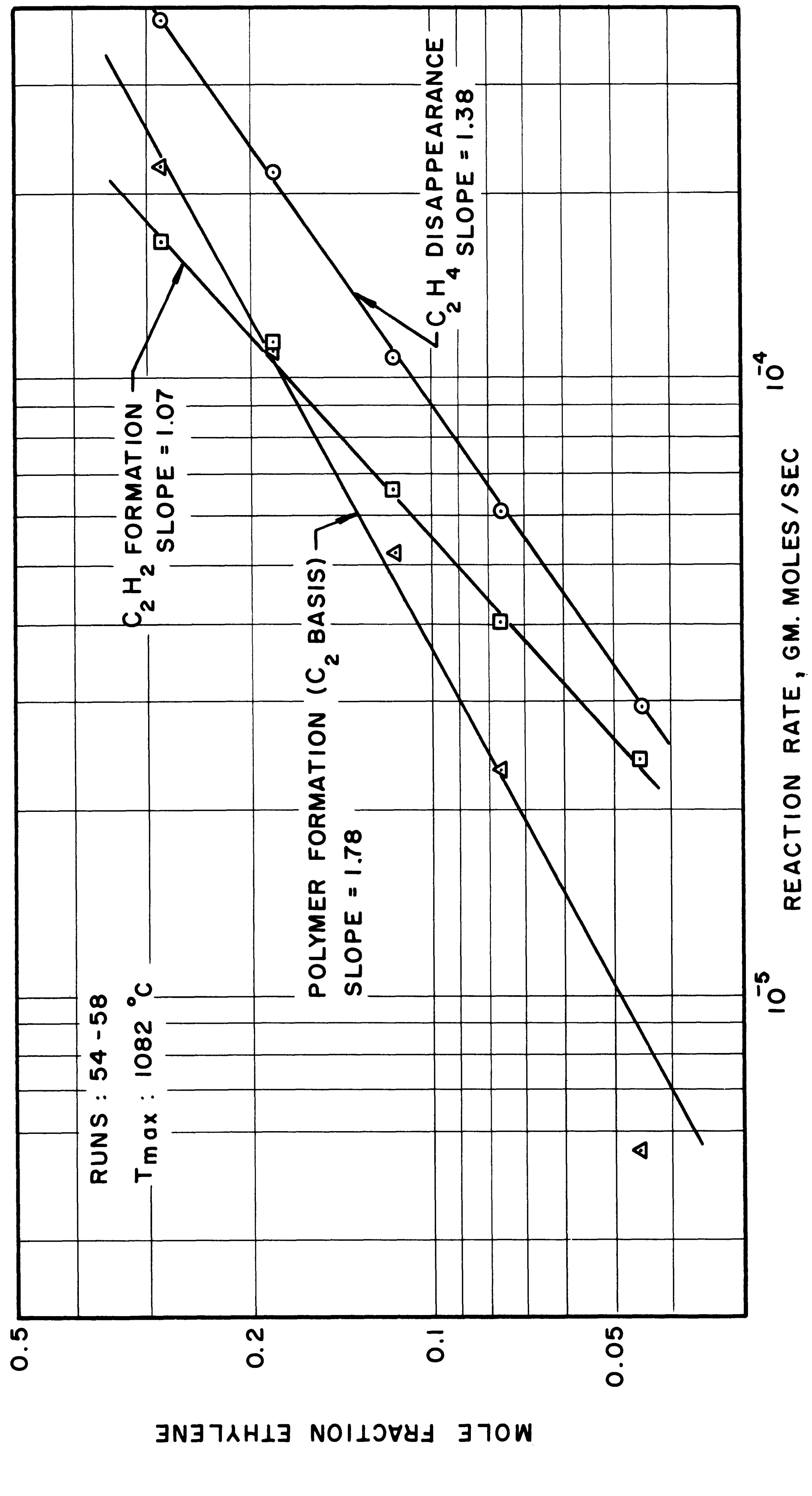

Figure 20. Ethylene Decomposition Order of Reaction.

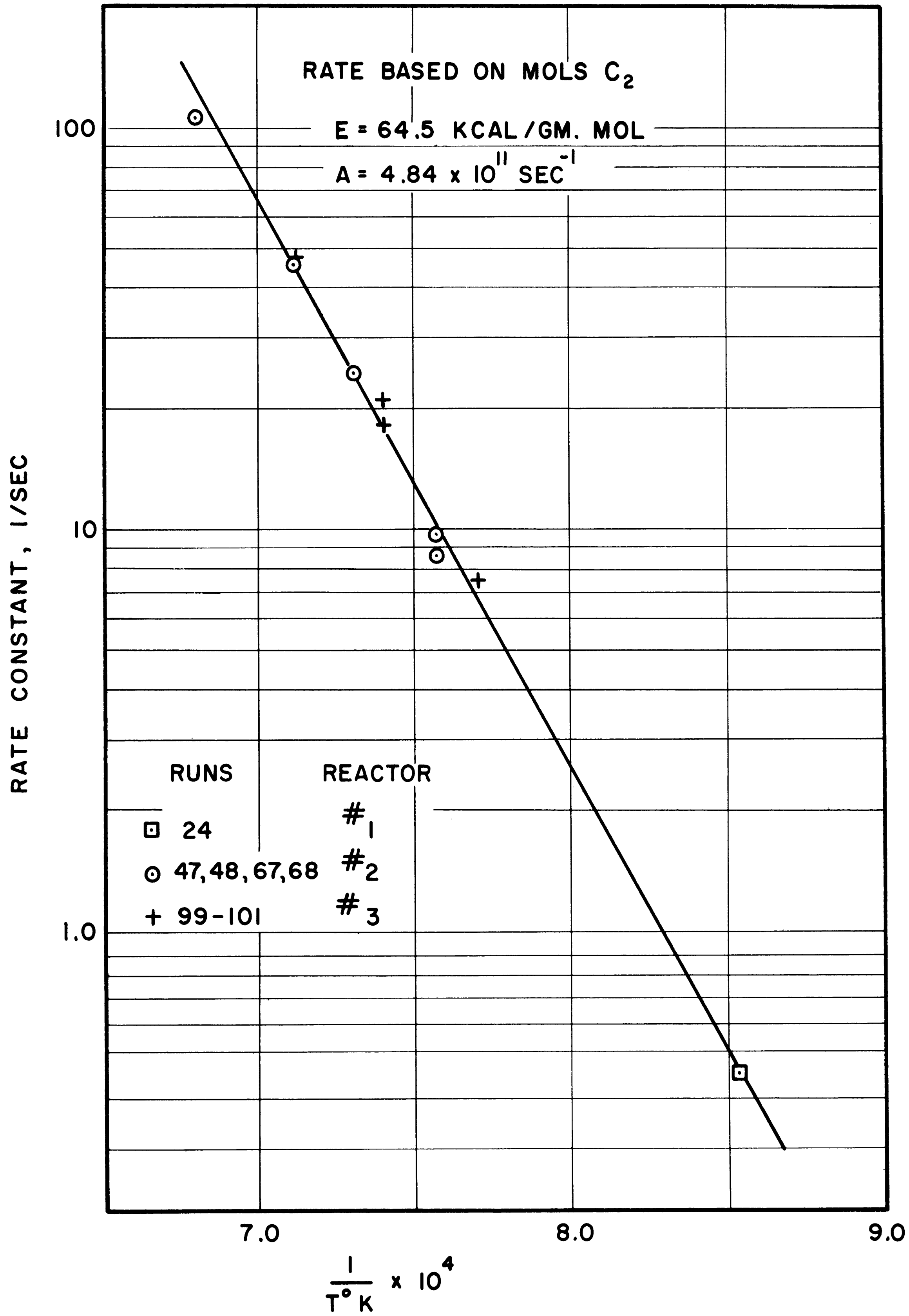

Figure 21. Ethylene Disappearance First Order Rate Constants.

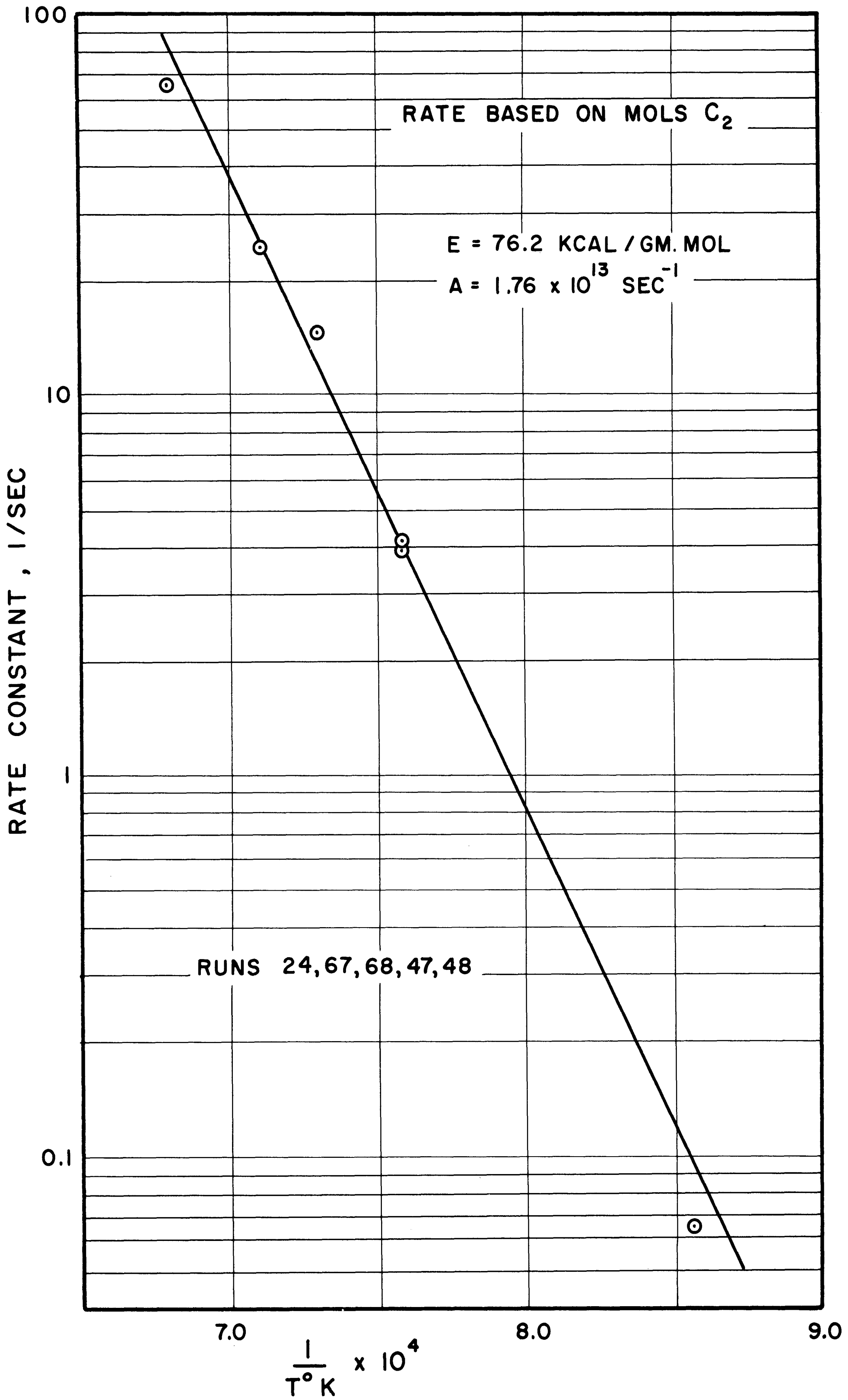

Figure 22. Acetylene Formation from Ethylene First Order Rate Constants.

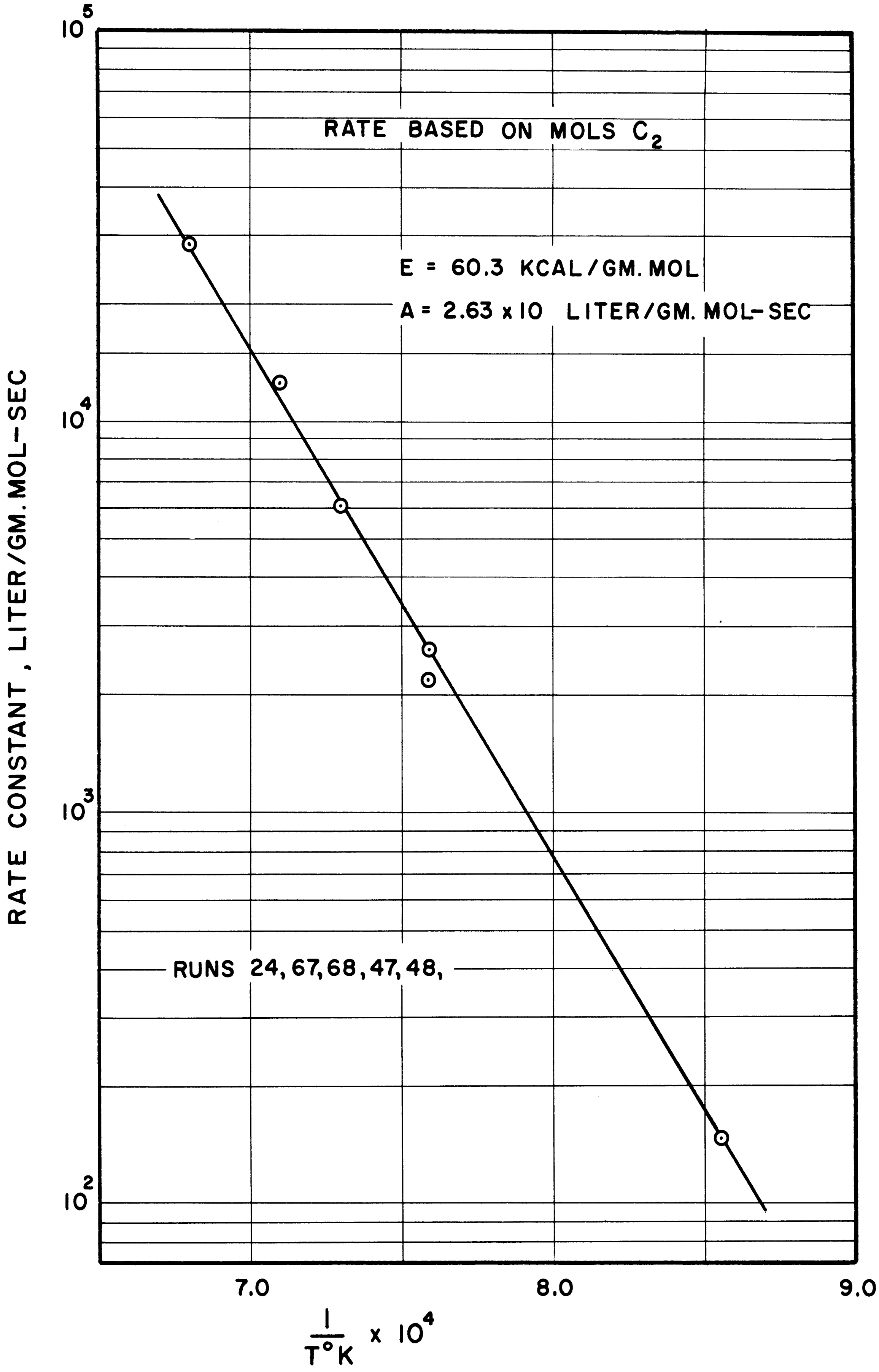

Figure 23. Polymerization of Ethylene Second Order Rate Constants.

with which to compare the data. Miller[30] and Greene[21] have some shock tube data which is based on a first order decomposition and their data are compared with this work in Figure 24 and the shock tube data is seen to have a lower activation energy although the rate constant values agree around 1160°C.

In the temperature range 875°C to 1200°C the activation energy for first order acetylene formation from ethylene is found to be 76.2 kcal/gm. mole and for second order polymerization of ethylene 60.3 kcal/gm. mole. Molera and Stubbs[31] around 700°C reported 75 kcal/gm. mole for the first order decomposition and 35 kcal/gm. mole for the polymerization. Other work is reported in Steacie[44] at lower temperatures (600°C - 700°C) and the activation energy values for second order polymerization are around 40 kcal/gm. mole.

C. Thermal Decomposition of Acetylene

(i) Product Distribution

The raw data is contained in Table II (Runs 115, 78, 127) the results in Table VI and the product distribution is plotted versus conversion in Figure 25. The primary molecular products are seen to be carbon, hydrogen and C_4H_4 together with benzene as the only secondary product of any magnitude. Small amounts of methane ethylene, diacetylene (C_4H_2) and C_3H_4 were also detected. The C_4H_4 is thought to be vinylacetylene and the C_3H_4 methylacetylene since the starting material was acetylene.

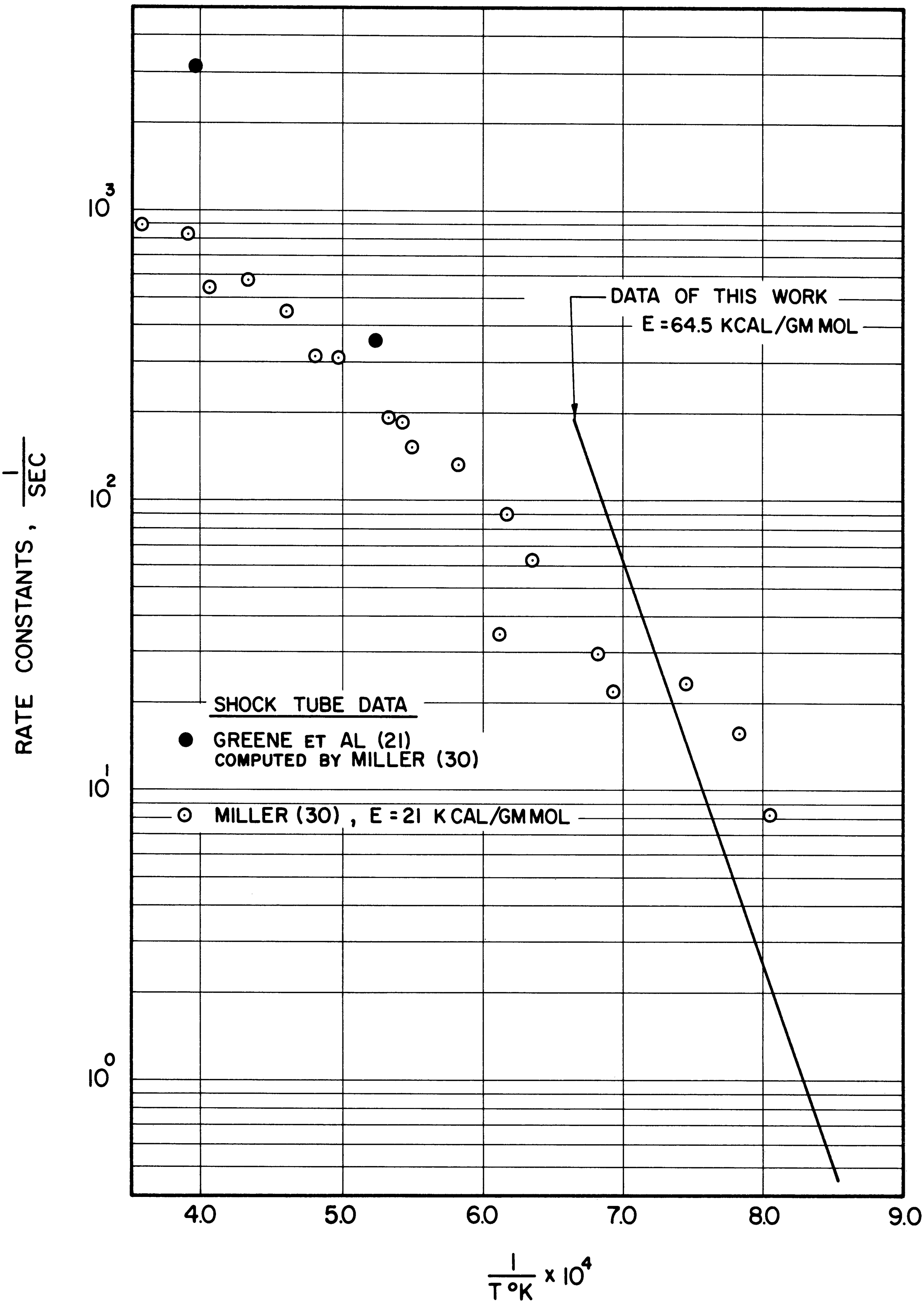

Figure 24. Ethylene Disappearance First Order Rate Constants, a Comparison with Literature Data.

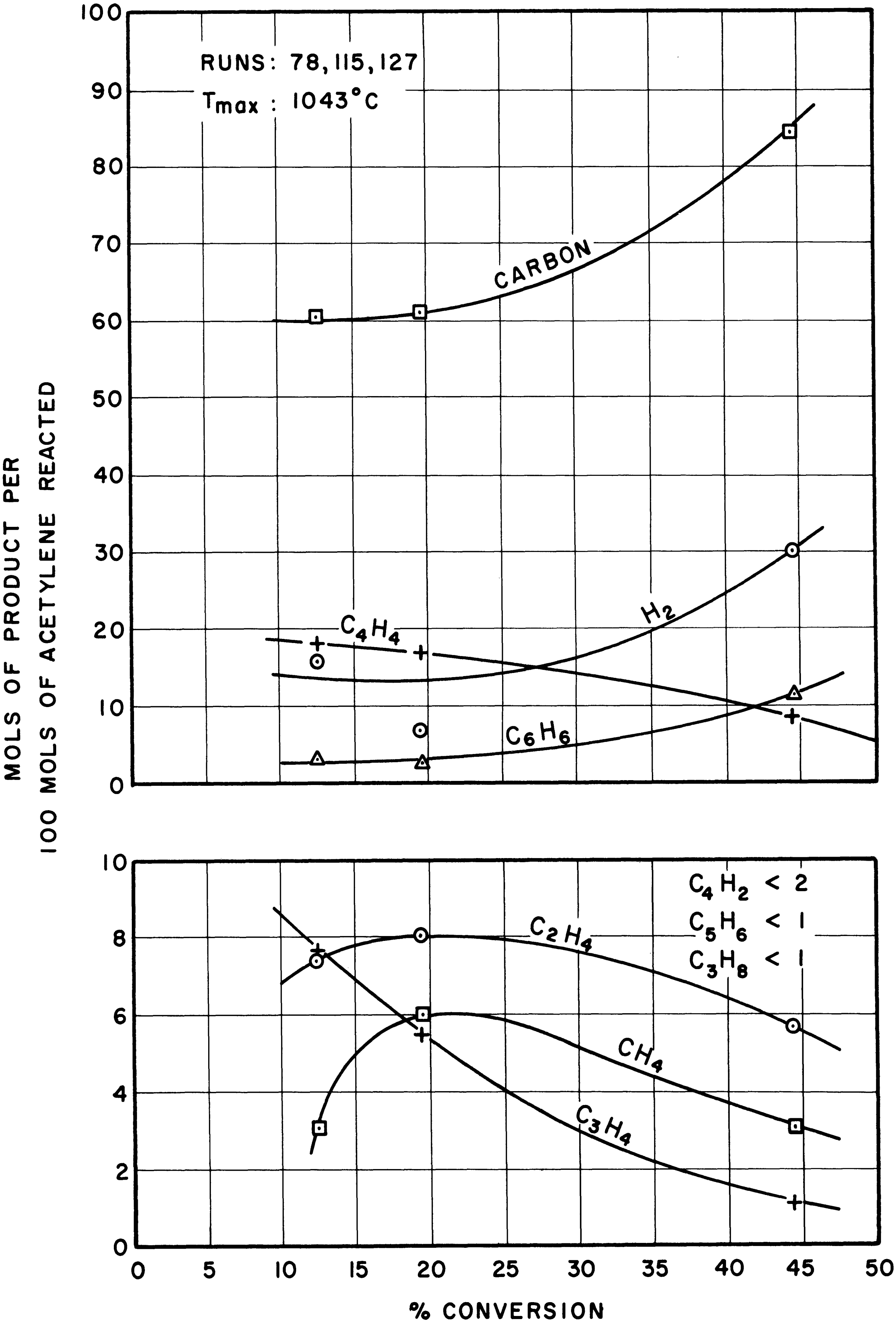

Figure 25. Product Distributions in Acetylene Decomposition.

(ii) Order of Reaction

These data (Runs 112 - 115) are contained in Table V, the results in Table VII and the rates of reaction are plotted against acetylene concentration in Figure 26. The amount of carbon formed was calculated by material balance. The carbon formation is found to be first order and the polymerization second order (actually, slope is 1.5 but second order is assumed) with respect to the acetylene. Considerable nitrogen dilution was used to prevent detonation of the acetylene. The polymerization products include C_4H_4, C_6H_6, and C_4H_2. Steacie[44] reported on the small amount of literature data on acetylene decomposition and the order is usually found to be two, although the data reported is at much lower temperatures than this work so that polymerization predominates.

(iii) Rate Constants

The raw data (Runs 110 - 112, 116, 117 and 102 - 104) are contained in Table IV, the results in Table VIII, and the first order rate constants for the disappearance of acetylene are plotted in Figure 27. These data are seen to scatter a little more and this is probably due to the fact that the carbon formed has to be determined indirectly by material balance. Data from reactors 2 and 3 (different s/v ratios) are shown in Figure 27 to be coincident (within the experimental error) which shows the reaction to be homogeneous as already reported by Zelinski.[49] The rate constants for the formation of carbon and polymer

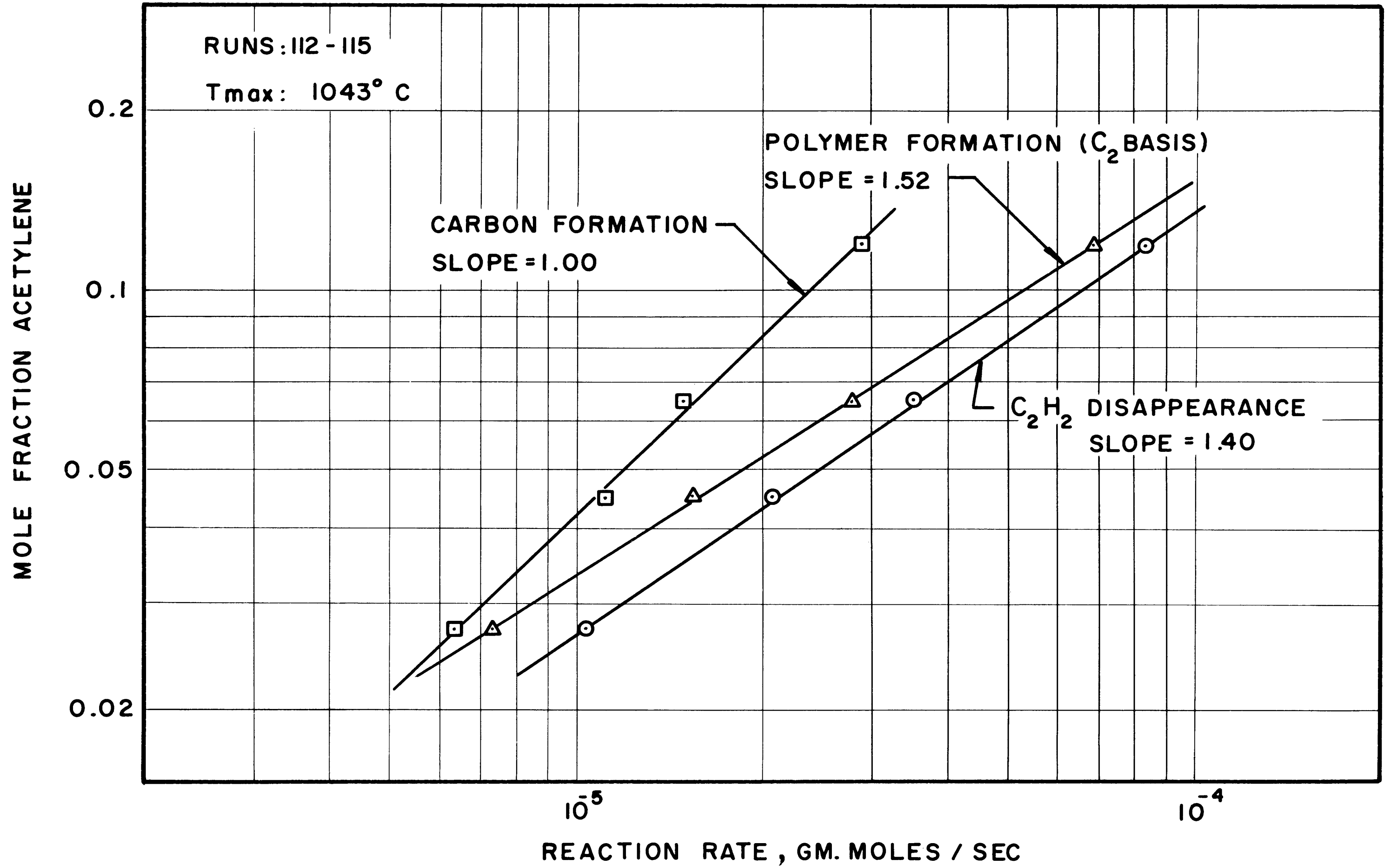

Figure 26. Acetylene Decomposition Orders of Reaction.

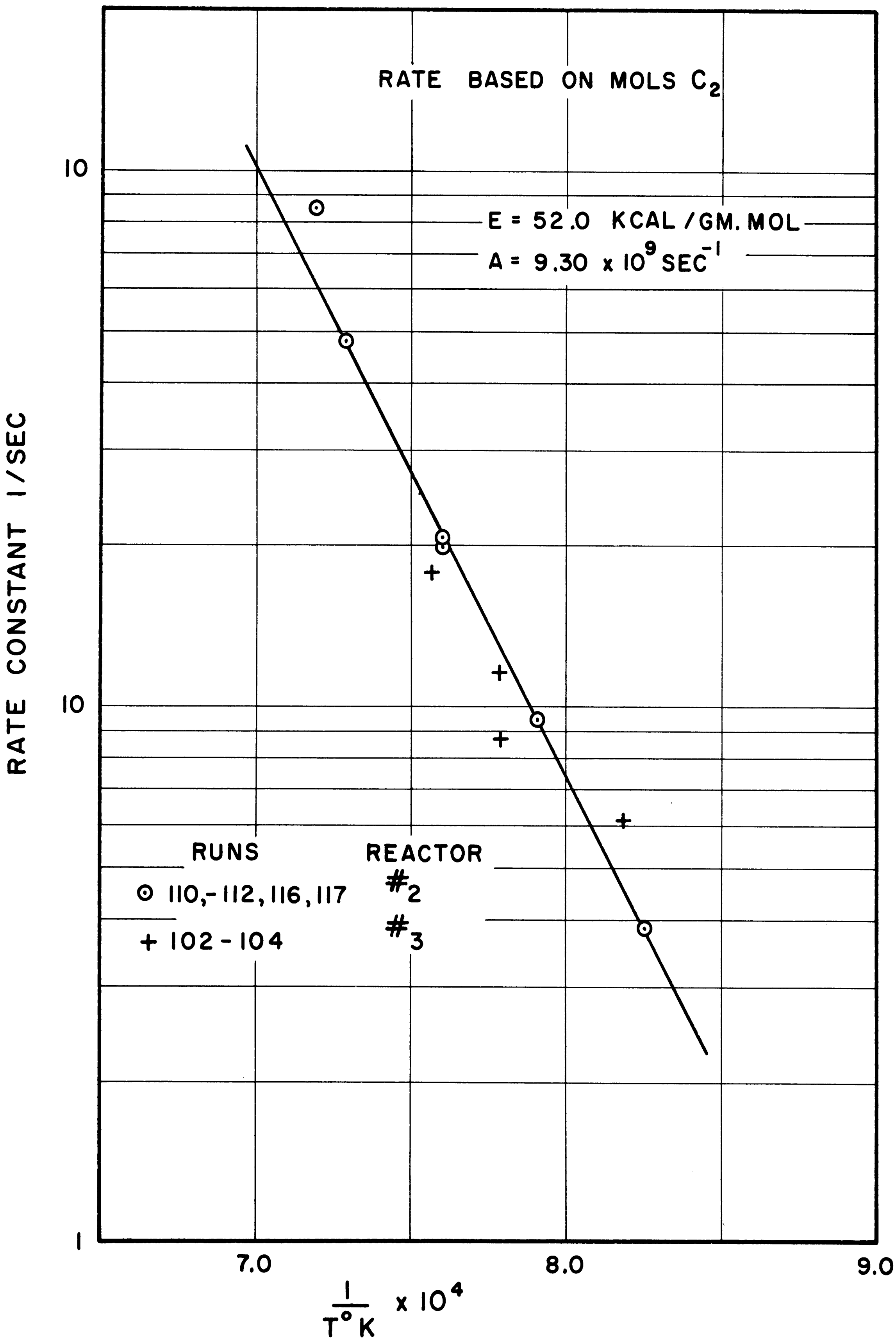

Figure 27. Acetylene Disappearance First Order Rate Constants.

are contained in Table VIII and are plotted in Figures 28 and 29. In the temperature range 900°C to 1150°C the activation energy for first order formation of carbon from acetylene is 61.9 kcal/gm. mol and for second order polymerization of acetylene is 44.6 kcal/gm. mol. The literature rate data[44] on the decomposition of acetylene are rather sparse, are mostly at lower temperatures and are correlated with a second order model for which activation energies between 30 and 40 kcal/gm. mol are reported. Aten and Greene[4] for their shock tube work reported a second order decomposition with an activation energy of 29 kcal/gm. mol.

D. Inhibition of Thermal Decomposition

(i) Propylene Inhibition

Previous workers[36,17,18] have shown that the thermal decomposition of ethane occurs at least in part by a free radical process. Propylene and nitric oxide are compounds that react readily with free radical species[44] and have been used in various studies[42,25] to study the reaction mechanism.

A set of experiments (Runs 70 - 74) was carried out at a constant temperature profile with varying additions of propylene. The conversions were kept low so that a differential rate could be measured. The raw data are contained in Table V and the rates of formation of the products calculated from the raw data are presented in Table IX. The rates are plotted against the fraction of propylene present in the feed in Figure 30. It is seen that the rate of ethylene formation is markedly reduced by small quantities of propylene which is indicative of a chain reaction. It is noted that the methane and propane rates are unaffected

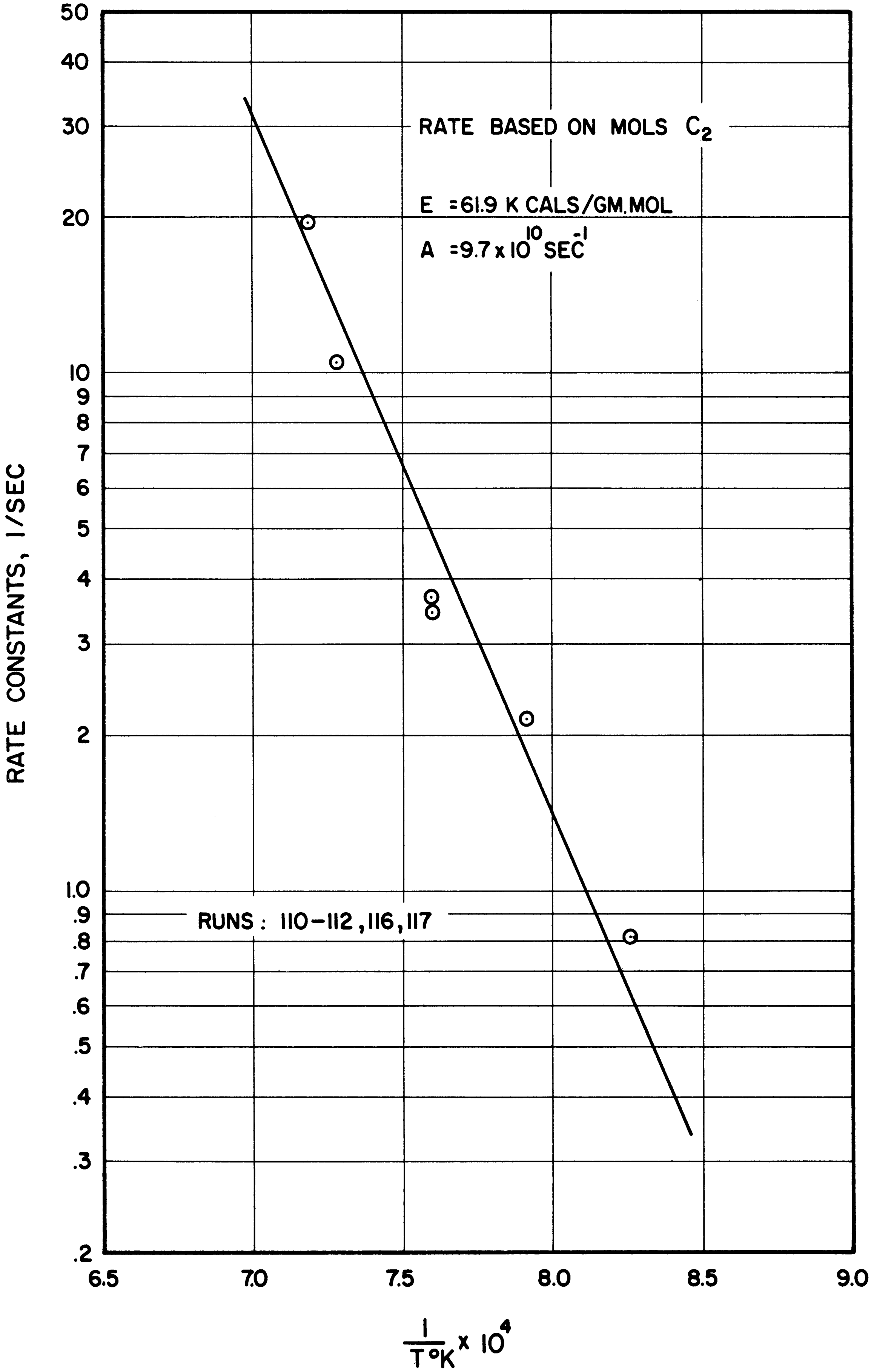

Figure 28. Carbon Formation from Acetylene First Order Rate Constants.

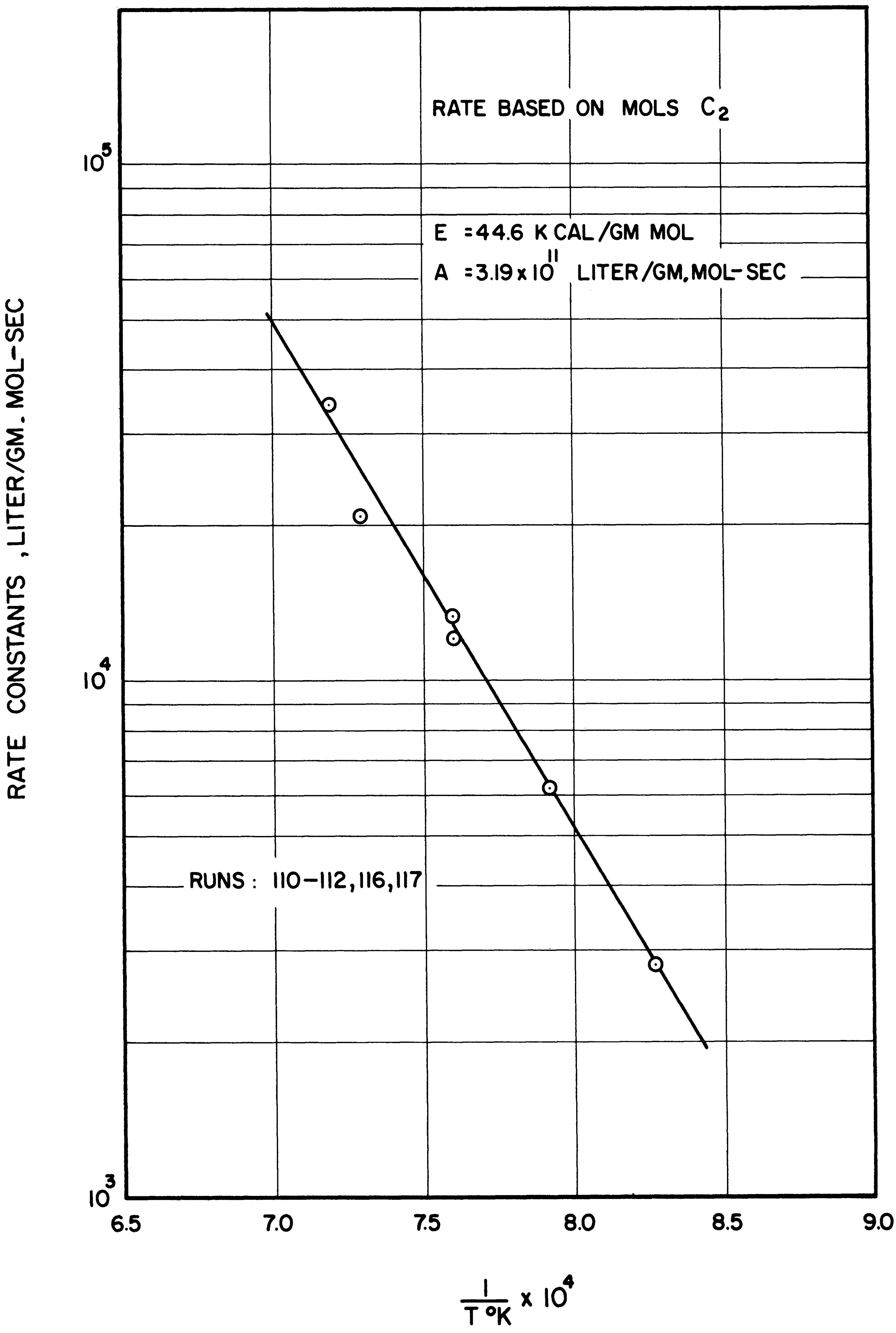

Figure 29. Acetylene Polymerization Second Order Rate Constants.

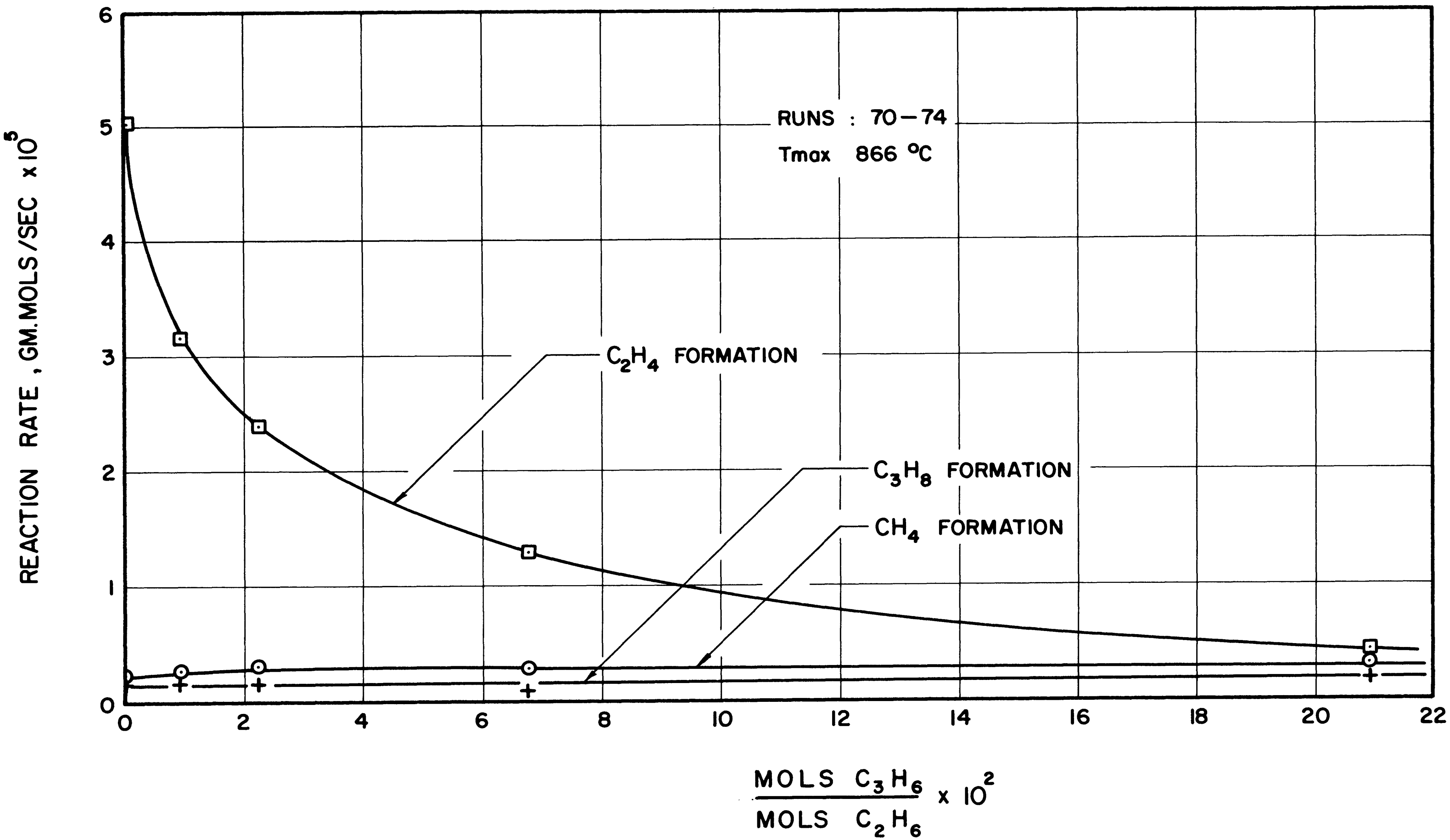

Figure 30. Inhibition of Ethane Decomposition with Propylene.

by the propylene addition. A possible explanation can be advanced now as to why the rate constants for ethylene formation (Figure 15) and ethane disappearance (Figure 13) fall off at high temperatures and is that the reaction products at higher temperatures inhibit the reaction rate. The product distribution data for ethylene shows that a small amount of propylene is formed as the ethylene decomposes so that this will cause some inhibition of the rate. The reaction products from ethane obtained at the higher temperatures of this work were then tested to determine their inhibition effect on the rate (these experiments are described in Section IVD(ii)).

The effect of propylene addition was also investigated for the thermal decomposition of ethylene, the results of which are contained in Tables V and IX (Runs 90 - 94). The rates of reaction are plotted against propylene fraction in Figure 31. There does not seem to be much inhibition effect but the data is somewhat inconclusive due to the fact that the propylene itself decomposes at the temperature of these experiments (see Run No. 95).

(ii) Inhibition of Ethane Decomposition by Reaction Products

The various reaction products were added in turn to ethane to see if they could inhibit the reaction rate. The data are contained in Tables V and IX (Runs 119 - 125), and they show that butadiene (C_4H_6) is quite a strong inhibitor whereas ethylene, acetylene, hydrogen do not inhibit the reaction at all. The effect of butadiene as an inhibitor is shown in Figure 32 and is noted that the methane and propane rates are not affected as was the case with propylene addition. It is concluded

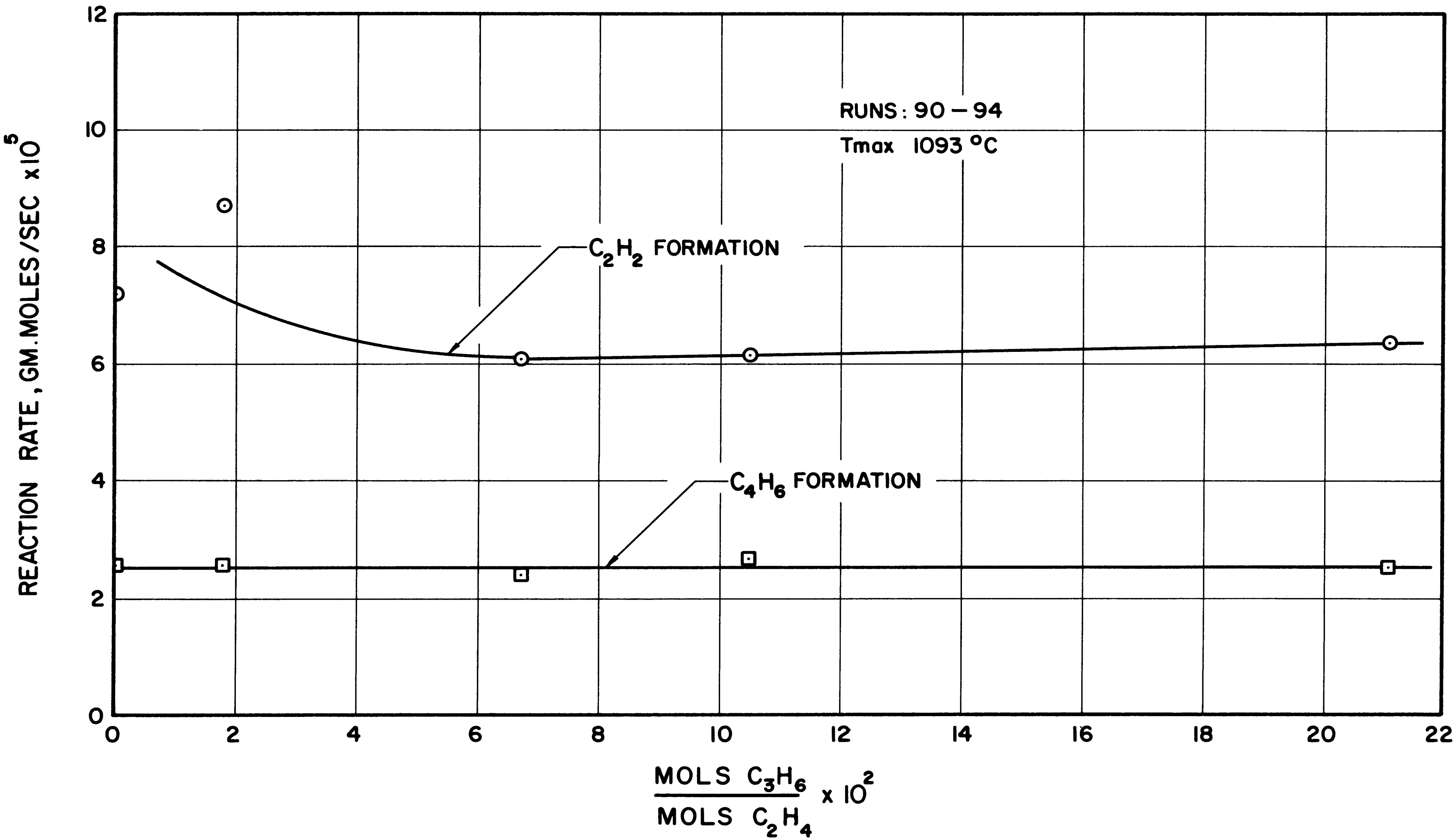

Figure 31. Inhibition of Ethylene Decomposition with Propylene.

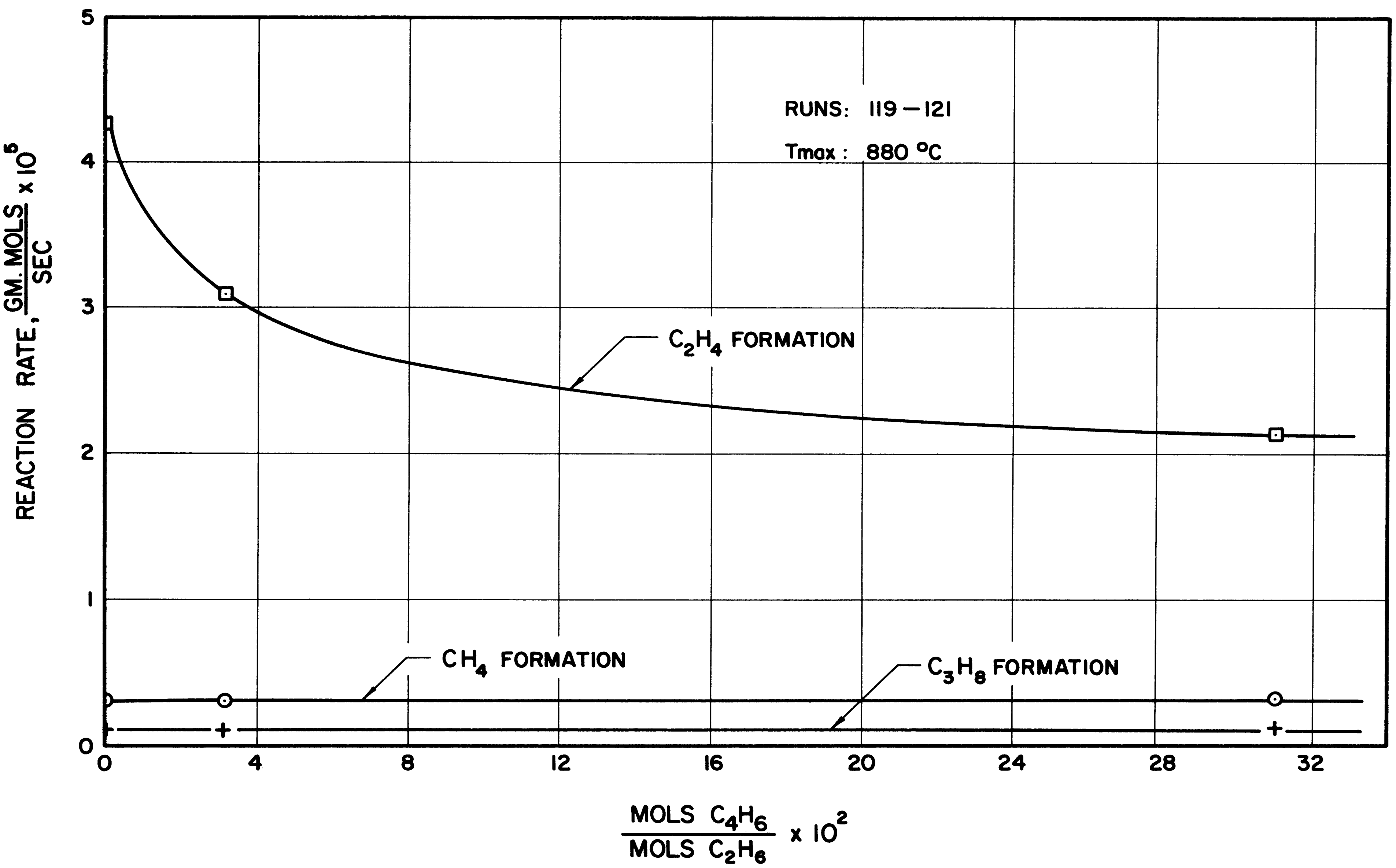

Figure 32. Inhibition of Ethane Decomposition with Butadiene.

then that the curvatures of the plots in Figures 13 and 15 are due to inhibition by the reaction products butadiene and propylene. These inhibition experiments are discussed further in the next section on reaction mechanism.

V. REACTION MECHANISMS

A. Review of Literature on Reaction Mechanisms

There has been a tremendous amount of work carried out to determine the reaction mechanism of the thermal decomposition of saturated hydrocarbons, especially ethane, and this literature has been very well reviewed in four recent books by Steacie, 1954,[44] Brooks et al., 1955,[10] Semenov, 1959,[39] and Benson, 1960,[5] and the following discussion is based upon these works. The following brief review is almost exclusively limited to the thermal decomposition of ethane. A number of early workers were able to show the existence of free radicals in the decomposition of ethane. Rice and Herzfeld[35] proposed a free radical chain mechanism in 1934 and this type of mechanism has been widely accepted and used as a basis for a large amount of later work.

A simplified form of the Rice-Herzfeld mechanism for ethane decomposition will be presented and discussed now. The ethane molecule splits at the weakest link (the carbon bond) to form two CH_3 readicals. These radicals then attack the ethane to form the C_2H_5 radicals. A free radical chain is set up which produces the bulk of the products and this chain reaction is terminated by some reaction which removes radicals. The following set of equations gives a qualitative picture of the mechanisms.

$$C_2H_6 \longrightarrow 2\ CH_3$$

$$CH_3 + C_2H_6 \longrightarrow C_2H_5 + CH_4$$

Radical initiation

$$C_2H_5 \longrightarrow C_2H_4 + H$$
$$C_2H_6 + H \longrightarrow C_2H_5 + H_2 \qquad \text{Chain reaction}$$

$$C_2H_5 + H \longrightarrow C_2H_6$$
$$CH_3 + C_2H_5 \longrightarrow C_3H_8 \qquad \text{Chain termination}$$

Using the steady state assumption for the free radicals, the rate of disappearance of ethane can be solved for in terms of the rate constants for the individual reactions and the concentration of ethane and is found to be approximately first order in ethane, which agrees with experiment. The activation energy for the overall reaction is shown to be less than the value for the primary split into radicals which is also in agreement with experiment. The difference, however, is fairly small since the overall activation energy is dominated by the primary radical split because the reactions between a radical and a molecule have a very small activation energy and radical radical reactions have almost zero activation energy. The rate of reaction, however, can be quite high if the chain length is long. (The chain length is defined as the rate of chain reaction divided by the rate of radical initiation). The very powerful inhibition effects exhibited by nitric oxide and propylene are explained by removal of the chain carrying radicals which reduces the chain length (i.e. the reaction rate). The actual mechanism of radical removal by these two inhibitors is not very well understood. Addition of large amounts of inhibitor does not reduce the rate to zero and there has been much controversy over whether the residual mechanism is free radical or molecular in nature. Some recent work using isotopic mixing has established that the residual reaction is free radical in nature. This type of mechanism can explain in a qualitative manner all of the observed experimental facts but the prediction of quantitative rates of reaction from data on the individual steps of the mechanism is not yet possible. A recent piece of work by Snow et al.[41] tried to predict the literature experimental data using a more complex form of the Rice Herzfeld mechanisms and the latest experimental data on the individual mechanism steps. Quantitative agreement could only be obtained by empirically changing some of the rate constants for the individual radical steps.

In spite of the disappointing quantitative results from the Rice-Herzfeld type mechanisms, there is no doubt that these mechanisms are correct in principle and that the discrepancies probably arise because of a lack of good data on the individual radical reactions and oversimplification of the reaction mechanism scheme.

The nature of reaction mechanisms in the decomposition of ethylene and acetylene have not been studied very well and the little work that has been done is reviewed by Steacie.[44] The mechanisms proposed are quite speculative and there is considerable doubt as to whether the mechanism is free radical or molecular in nature.

B. Ethane Decomposition Reaction Mechanism

The purpose of this discussion is to qualitatively show that the experimental facts in this work are consistent with the current free radical mechanisms proposed in the literature rather than to try and deduce any new facts concerning the mechanism on the basis of these experiments. This approach is taken here since it is not the objective of this study to investigate mechanisms nor is the experimental technique suitable to do so. Nevertheless, this discussion proves illuminating especially with regard to the inhibition experiments.

The primary stable molecular products are found to be ethylene, hydrogen, methane and propane. The ethylene and hydrogen are, of course, the obvious products, but the methane and propane are not. A Rice-Herzfeld type mechanism, as outlined in the previous section, shows that methane can be formed by the **attack of a** methyl radical on an ethane molecule, and that propane can result from a chain termination reaction between two radicals. The activation energy for the decomposition 70 kcal/gm. mole; this is the true value discussed later on in this section and not the apparent value that is used in the kinetic correlation) is seen to be fairly close to but less than the bond dissociation energy (see Table X for approximate values) for the splitting of ethane into two methyl radicals. This fact is also consistent with the predictions of the Rice-Herzfeld mechanisms. The Rice-Herzfeld mechanisms can be shown to lead to first order kinetics (an experimental fact) by making certain assumptions about the radical termination reactions.

The experiments carried out with propylene inhibition are significant as the marked reduction in reaction rate by small additions of propylene is indicative of a chain reaction. The rates of formation of the products are plotted against propylene fraction in the feed in Figure 30. It is noted that the ethylene rate is very rapidly reduced whereas the methane rate is unaffected. The ethylene rate is seen to approach a limiting rate as the propylene concentration increases which is almost the same as the constant methane rate. The propylene inhibition can be explained if the propylene reacts with the chain carrying radicals (H and C_2H_5). The methane rate remains unaffected so that this means that the radical initiation steps (which produce the methane) are unaffected by the propylene. The residual rate at full inhibition is then probably due to the radical initiation reactions. The chain length of the reaction is defined as the rate due to chain reaction divided by the rate of radical initiation and we can see that this is equivalent to the rate of ethylene formation divided by the rate of methane formation. The chain length is then computed on this basis and plotted against the propylene fraction in the ethane feed (Figure 33). The chain length is seen to vary from 24 down to 1.5 as the propylene amount is increased with the most rapid decrease occurring at low fractions of propylene. The upper limit of 24 is due to the normal chain termination reactions of the uninhibited reaction. The inhibition of ethane decomposition by nitric oxide has been investigated by Staveley[42] and Hinshelwood and Hobbs[25] and they found chain lengths ranging from 4 to 21. Dinstes et al.[15] showed that propylene inhibited ethane decomposition but no chain lengths were reported. A weakness of the Rice-Herzfeld mechanisms is that they predict a very much greater chain length than is found experimentally.

The curvature of the rate constants plot for ethane disappearance and ethylene formation can now be explained on the basis of varying chain length. The chain length is simply represented by the ratio of the ethylene formation rate constant to the methane formation rate constant and the values of the chain length are shown in Figure 34. The chain lengths are never as high as 24 since there is a small impurity of

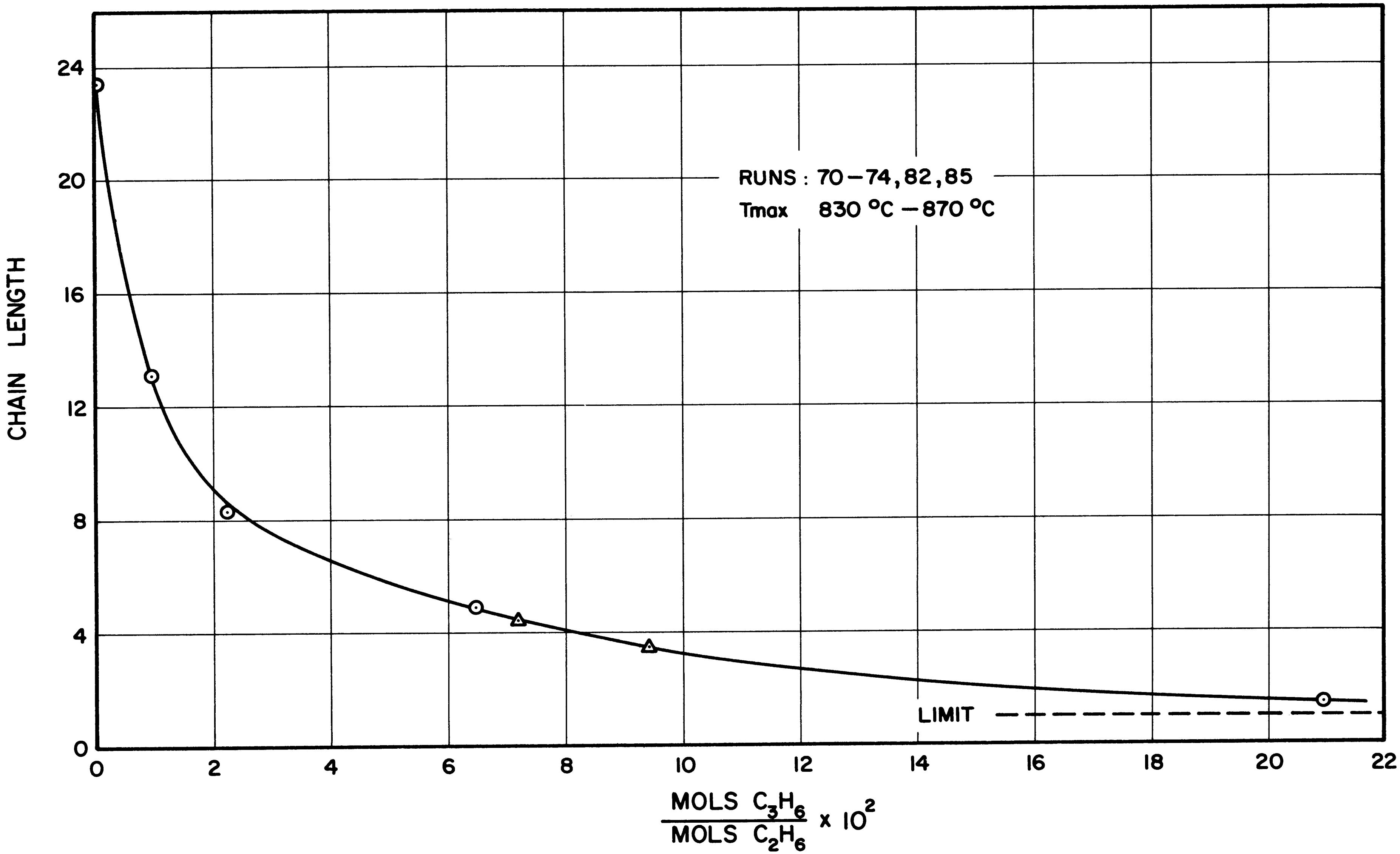

Figure 33. Chain Lengths for Ethane Decomposition with Propylene Inhibition.

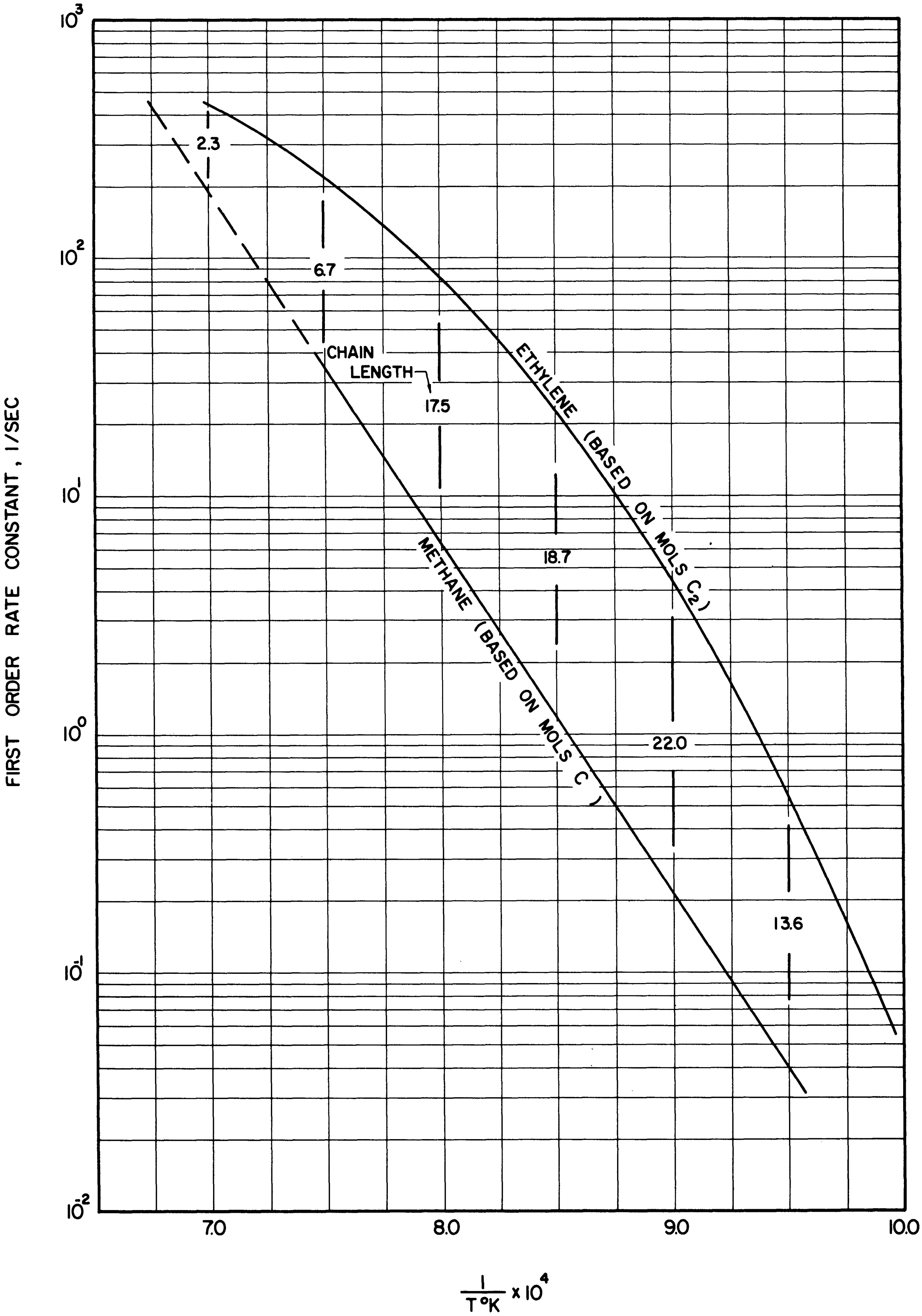

Figure 34. Chain Lengths for Ethane Decomposition.

propylene in the ethane feed used which limits the maximum possible chain length to about 13 which is the value at the lower temperatures in Figure 34. As the temperature is raised the chain length increases at first and then drops rapidly. The rapid drop is explained by the fact that at these higher temperatures considerable amounts of the secondary product butadiene are formed which was found to be an inhibitor (see Section IVD). The small increase in chain length at lower temperatures cannot be explained very well except for the suggestion that the amount of inhibition resulting from the propylene impurity in the feed may change with temperature.

The curvature of the rate constant plot for ethylene formation has been explained on the basis of varying chain length rather than saying that the activation energy is decreasing. It will be of interest to determine whether the activation energy of the inhibited reaction does in fact remain almost the same, which it will if the effect of the inhibitor is on the chain length rather than on the primary split (the dominating reaction with regard to activation energy) into methyl radicals. Some experiments (Runs 82 and 85) were carried out with quite large additions of propylene inhibitor to determine the activation energy. The results are compared with the essentially uninhibited reaction results in Figure 35 and it is seen that the activation energies are about the same. This substantiates the conclusion that inhibition of ethane decomposition by reaction products is due to shortening of the chain length rather than decrease in the activation energy. Previous workers who studied nitric oxide inhibition found the activation energy for the inhibited reaction to be the same (Kuchler and Theile[27]) or a little higher (Steacie and Shane[43]) than for the uninhibited reaction.

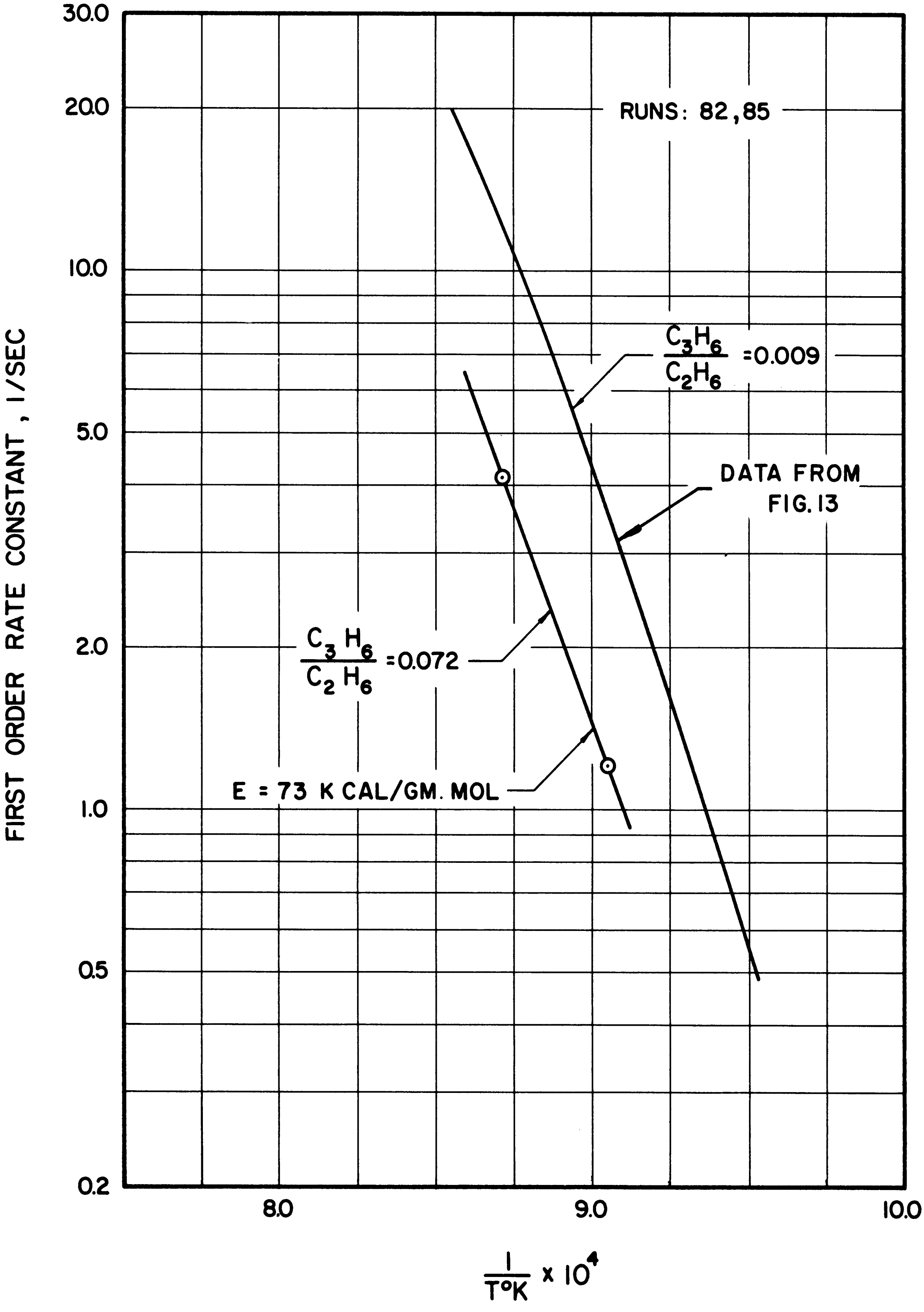

Figure 35. Ethane Decomposition Activation Energy for Reaction Inhibited with Propylene.

C. Ethylene and Acetylene Decomposition Reaction Mechanisms

The Rice-Herzfeld mechanisms only apply to the decomposition of saturated hydrocarbons so are of no use for ethylene and acetylene decomposition. There are no firm ideas in the literature about the mechanism of decomposition of ethylene and acetylene and the little work that does exist is discussed by Steacie[44] who only concludes that the reactions contain in part at least some free radical processes.

A consideration of the bond energies in ethylene and acetylene (see Table X) shows that the carbon hydrogen bonds are weaker than the double and triple carbon carbon bonds so that the inference is made that the decomposition occurs by hydrogen removal. The energy requirements for hydrogen removal are quite high (around 100 kcal/gm. mole) and this would indicate lower reaction rates for acetylene and ethylene decomposition than for ethane decomposition as is found experimentally. The activation energies for acetylene and ethylene dehydrogenation are found experimentally to be 76 and 62 kcal/gm. mole respectively which are inconsistent with the high bond energies.

Some experiments were carried out with propylene addition in ethylene decomposition. The results are plotted in Figure 31 but are rather inconclusive because it is found that the propylene is decomposing at the temperatures used to form ethylene, acetylene and methane. If we consider the points at low propylene fraction (where the effects of propylene decomposition will be small), it is seen that the acetylene formation data scatter too much to a meaningful. The only conclusion that can be drawn from the data is that the polymerization to butadiene is not inhibited by propylene.

The product distribution experiments can be studied to obtain the sequence of formation of the various products which can be the basis of speculation into possible mechanisms. In the case of ethylene decomposition (see Figure 19) the butadiene appears to be formed from polymerization of ethylene rather than the reaction of acetylene with ethylene. The carbon appears to result from the decomposition of acetylene since none is formed until the acetylene quantity has become appreciable. The vinylacetylene (C_4H_4) can result either from dehydrogenation of butadiene or the polymerization of acetylene. The benzene can result from the reaction between vinylacetylene and acetylene. The experiments on acetylene decomposition (see Figure 25) show that the carbon can result by direct dehydrogenation of the acetylene and the vinylacetylene from the polymerization of two acetylenes. The benzene can result from the reaction of vinylacetylene with acetylene. It is emphasized that these last comments based on the product distributions are purely speculative since they pre-suppose a molecular process for which there is no evidence for or against in this work.

VI. KINETIC CORRELATION FOR THE COMPLETE SERIES OF REACTIONS IN THE FORMATION OF ACETYLENE FROM ETHANE

A. Overall Kinetic Correlation

The rate data on the individual reaction steps are now combined to give an overall kinetic correlation. Kinetic correlations have been developed for the individual thermal decompositions of ethane, ethylene and acetylene in Section IV. These are now combined to give the following overall scheme:

First order	$C_2H_6 \rightleftharpoons C_2H_4 + H_2$	(1)
First order	$C_2H_6 = 2CH_4 - H_2$	(2)
First order	$C_2H_4 \rightleftharpoons C_2H_2 + H_2$	(3)
Second order	$C_2H_4 = 1/2(C_4 \text{ polymer}) + H_2$	(4)
First order	$C_2H_2 \rightleftharpoons 2C + H_2$	(5)
Second order	$C_2H_2 = 1/2(C_4 \text{ polymer})$	(6)

These reactions represent the best correlation of the rate data and are not intended to demonstrate the reaction mechanism. The negative hydrogen in reaction (2) is necessary to maintain material balance. The C_4 polymer in reactions (4) and (6) includes all the C_4, C_5 and C_6 products and also the small amounts of C_3 products formed. The C_4 polymer is assumed to have the approximate formula C_4H_4 for material balance purposes. The assumption is made that all of the methane formed results from the decomposition of ethane. It is pointed out that the experimental conditions in this work were such that the reverse reactions (1 and 3) were negligible (See Appendix VI). The rate constants for the six reactions are summarized in Figure 36 and the values of the activation energies and pre-exponential factors are indicated on this figure. The ethylene decomposition data are represented empirically by three straight line sections with different apparent activation energies. This overall kinetic model can be used to calculate the product distribution at all points in any reactor under any reaction conditions. Some additional experiments (Runs 128 - 131) were carried out with ethane feed at reaction conditions such that all of the reactions were occurring (i.e. very high conversions) to provide a check on the correlation. The correlation was also checked out against some of the experiments that were carried out in the measurement of the rate constants for the individual reactions.

The rate equations based upon the six reactions already discussed are:

$$\frac{dN_{C_2H_6}}{dV_R} = -k_1\left[C_{C_2H_6} - \frac{C_{C_2H_4}C_{H_2}}{K_{C,1}}\right] - k_2 C_{C_2H_6} \tag{22}$$

$$\frac{dN_{C_2H_4}}{dV_R} = k_1\left[C_{C_2H_6} - \frac{C_{C_2H_4}C_{H_2}}{K_{C,1}}\right] - k_3\left[C_{C_2H_4} - \frac{C_{C_2H_2}C_{H_2}}{K_{C,3}}\right] - k_4\left[C_{C_2H_4}\right]^2 \tag{23}$$

$$\frac{dN_{C_2H_2}}{dV_R} = k_3\left[C_{C_2H_4} - \frac{C_{C_2H_2}C_{H_2}}{K_{C,3}}\right] - k_5 C_{C_2H_2} - k_6\left[C_{C_2H_2}\right]^2 \tag{24}$$

$$\frac{dN_{CH_4}}{dV_R} = 2k_2 C_{C_2H_6} \tag{25}$$

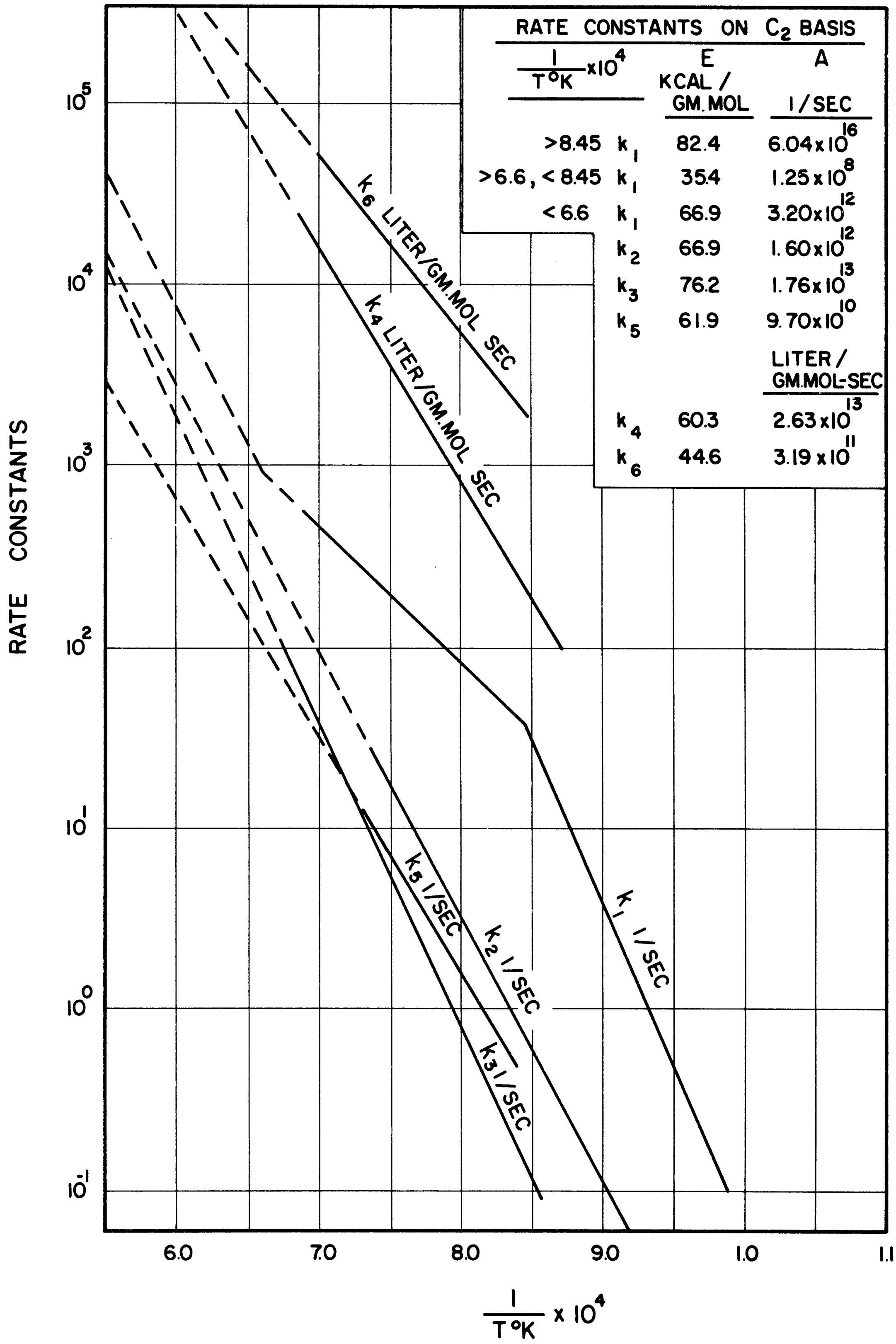

Figure 36. Rate Constants for the Six Major Reactions.

(1) $C_2H_6 \rightleftarrows C_2H_4 + H_2$ 1st order

(2) $C_2H_6 = 2CH_4 - H_2$ 1st order

(3) $C_2H_4 \rightleftarrows C_2H_2 + H_2$ 1st order

(4) $C_2H_4 = 1/2\ (C_4 \text{ poly.}) + H_2$ 2nd order

(5) $C_2H_2 \rightleftarrows 2C + H_2$ 1st order

(6) $C_2H_2 = 1/2\ (C_4 \text{ poly.})$ 2nd order

$$\frac{d\,N_{C_4}}{d\,V_R} = \frac{1}{2} k_4 \left[C_{C_2H_4}\right]^2 + \frac{1}{2} k_6 \left[C_{C_2H_2}\right]^2 \qquad (26)$$

$$\frac{d\,N_{C}}{d\,V_R} = 2\,k_5\,C_{C_2H_2} \qquad (27)$$

$$\frac{d\,N_{H_2}}{d\,V_R} = k_1 \left[C_{C_2H_6} - \frac{C_{C_2H_4} C_{H_2}}{K_{C,1}}\right] - k_2 C_{C_2H_6} + k_5 C_{C_2H_2}$$
$$+ k_3 \left[C_{C_2H_4} - \frac{C_{C_2H_2} C_{H_2}}{K_{C,3}}\right] + k_4 \left[C_{C_2H_4}\right]^2 \qquad (28)$$

where N is the rate in gm. moles/sec., C is the concentration in gm. moles/liter, and K_c the equilibrium constant in concentration units. The rate constants (k) are represented as temperature functions by the familiar Arrhenius equation

$$k = A\,e^{-E/RT} \qquad (21)$$

The equilibrium constants are also represented by an exponential temperature function of the same form as the Arrenhius equation. These equations were solved for the product distributions with the particular flow rates and temperature distributions by Euler's finite difference technique. This calculation is quite tedious so it was programmed for machine calculation. The flow diagram for the computer program is contained in Appendix VII.

The computed product distributions are compared with the experimental distributions for a number of runs in Table I (Calc. 1). Runs Nos. 43 - 46 and 128 - 131 are all for ethane feed and good agreement is observed for the ethane, ethylene, methane and hydrogen quantities. The predicted carbon quantity seems to be somewhat high although the run

TABLE 1. Comparison of Correlation with Experiment

Run No.		Mole % C_2H_6	C_2H_4	C_2H_2	CH_4	C_4	H_2	C	N_2
	Exp.	-	0.086	12.5	-	1.05	0.424	1.29	85.8
116	Calc. 1	-	0.005	12.1	-	1.22	0.836	1.68	84.2
	Calc. 2	-	0.005	12.1	-	1.22	0.836	1.68	84.2
	Exp.	0.167	10.2	4.48	0.686	1.17	6.73	0.895	76.6
48	Calc. 1	0.014	10.0	4.12	0.007	1.39	8.18	1.30	75.0
	Calc. 2	0.014	9.99	4.13	0.007	1.39	8.19	1.30	75.0
	Exp.	7.83	8.76	0.136	0.723	0.08	8.39	-	74.0
43	Calc. 1	7.91	9.25	0.016	0.435	0.01	8.74	-	73.6
	Calc. 2	7.91	9.09	0.086	0.435	0.05	8.89	-	73.5
	Exp.	5.23	10.45	0.344	0.725	0.151	10.6	-	72.4
44	Calc. 1	4.49	11.76	0.064	0.628	0.029	11.3	-	71.7
	Calc. 2	4.48	11.24	0.316	0.625	0.138	11.8	-	71.4
	Exp.	5.83	7.33	0.246	0.691	0.078	7.27	-	78.5
45	Calc. 1	5.89	7.80	0.036	0.539	0.009	7.35	-	78.4
	Calc. 2	5.88	7.48	0.236	0.538	0.057	7.62	-	78.2
	Exp.	2.95	8.96	0.799	1.17	0.118	10.2	-	75.7
46	Calc. 1	2.93	10.10	0.175	1.09	0.044	9.80	-	75.8
	Calc. 2	2.92	9.07	0.813	1.08	0.185	10.6	-	75.2
	Exp.	4.68	7.74	0.484	0.970	0.233	8.13	-	77.6
128	Calc. 1	4.28	9.07	0.093	0.917	0.023	8.60	-	77.0
	Calc. 2	4.26	8.37	0.533	0.911	0.122	9.19	-	76.6
	Exp.	0.985	8.25	1.96	1.94	0.547	12.4	-	73.9
129	Calc. 1	0.547	10.14	1.01	2.41	0.211	11.7	0.10	73.9
	Calc. 2	0.554	7.75	2.52	2.36	0.450	13.7	0.35	72.3
	Exp.	0.128	5.65	4.22	2.47	0.732	15.4	-	73.2
130	Calc. 1	0.018	6.02	3.44	3.08	0.652	15.9	1.46	69.4
	Calc. 2	0.016	4.15	4.08	3.01	0.836	17.7	2.48	67.7
	Exp.	Reactor plugged during run							
131	Calc. 1	-	0.09	0.91	2.49	0.974	20.3	10.7	64.5
	Calc. 2	-	0.07	0.78	2.49	0.997	20.5	10.8	64.4

(No. 131) when the reactor plugged with carbon coincides with a marked increase in computed carbon quantity. The quantity of acetylene and C_4 polymer computed is considerably less than the experimental value at low concentrations of acetylene although the agreement is quite good when appreciable amounts of acetylene are formed. The ratios of the predicted to the experimental acetylene quantity are plotted against the ethane to ethylene ratio in Figure 37, and it is seen that there is a definite trend. This high initial rate of acetylene formation is attributed to the attack of methyl radicals from the ethane on the ethylene to product acetylene and C_4 polymer. The rate of acetylene formation and C_4 polymer then is multiplied by α x ethane/ethylene ratio where α is an empirical constant (found to be 5.5 by selection of the best fit to the data). Runs 116 and 48 were experiments on acetylene and ethylene decomposition respectively and the calculated and experimental results are seen to agree fairly well. The product distributions were recalculated including the empirical correction discussed above and the results are compared with experiments in Table I (Calc. 2) to show that the agreement is satisfactory. The correlation allows the prediction of the product distribution throughout the reactor and this was done for Run No. 129, the results of which are plotted in Figure 38.

B. Use of the Correlation to Predict Product Distributions over a Wide Range of Reaction Conditions

The correlation can be used to predict the product distributions for a wide range of reaction conditions. The correlation is based on data taken in the temperature range 730°C to 1330°C at a total pressure of 1 atmosphere with nitrogen dilution from 60% to 90%. Some example

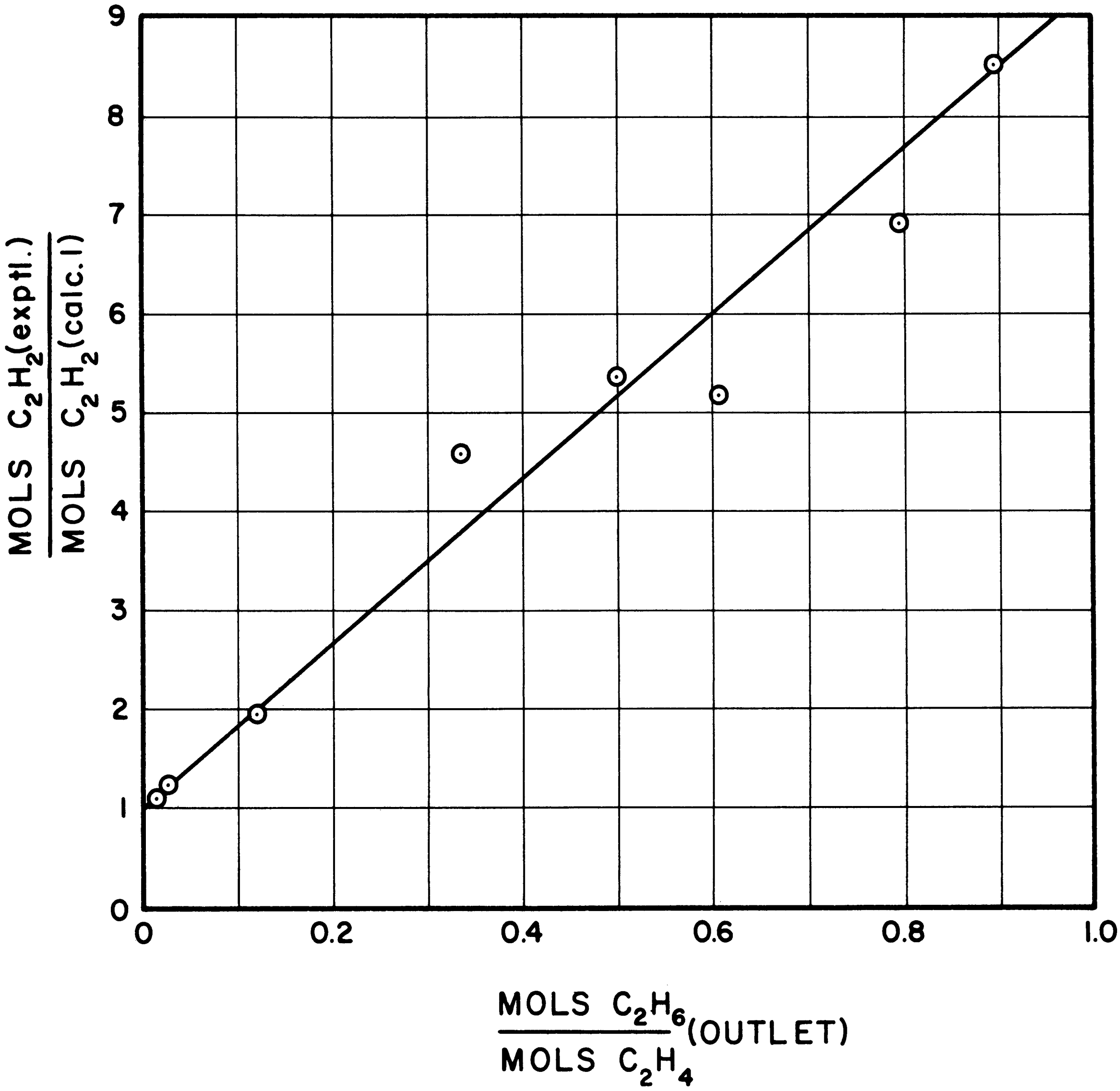

Figure 37. Effect of Ethane on Formation of Acetylene from Ethylene.

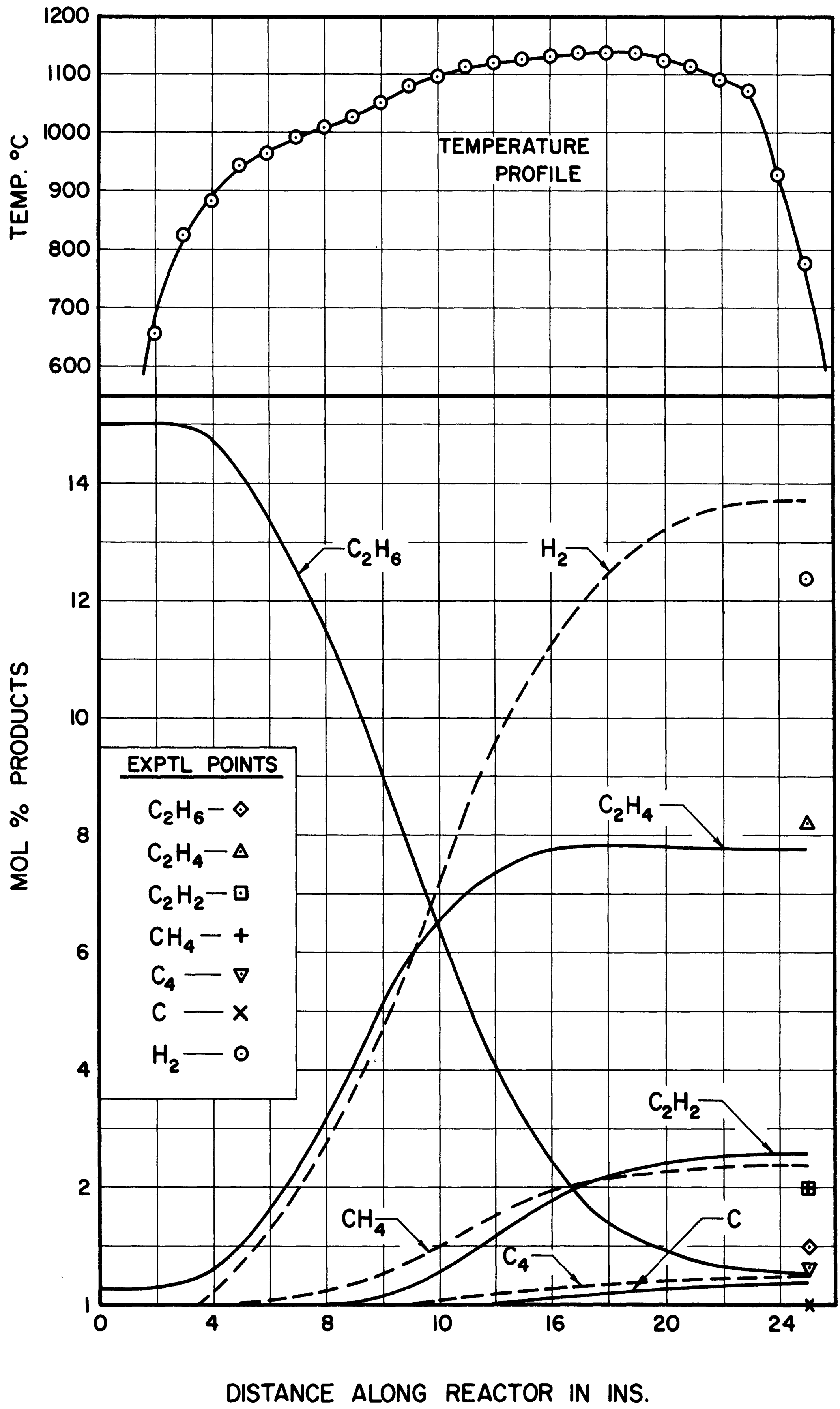

Figure 38. Calculated Product Distribution Throughout the Reactor for Run 129.

calculations were carried out which represent an extrapolation of this data since the reaction conditions considered were total pressures of 0.25 atm. (with no diluent) and 1 atm. (with no diluent and 75% diluent) at temperatures of 1000°C, 1200°C, 1400°C and 1600°C.

These calculations were carried on a digital computer using Euler's method to solve the differential rate Equations (Nos. 22 to 28). The calculations by this finite difference technique are made very much more convenient if the temperature of the gas is allowed to rise at a finite rate at the entrance of the reactor rather than as a step function to the maximum temperature. Incidentally, this sort of temperature profile is much more realistic from a practical point of view. Therefore, the temperature in the first reactor increment was assumed to be 500°C and rose by 100°C in each successive increment until the desired maximum temperature was reached. In these example calculations no consideration was given to the heat transfer limitations that would have to be considered in a reactor design as detailed design such as this was not an objective of this work. The results of these calculations are shown graphically in Figures 39 to 44 in which the yields of products (expressed on the basis of 100 moles of ethane feed) are plotted against reactor increment. The residence time scale is shown beneath the reactor increment scale as this is a much more general parameter. The residence time scale is noted to be nonlinear with respect to equal reactor increments and this is due to changing temperature and extent of reaction at each point. The temperature distribution, pressure conditions and amount of diluent are shown on each graph. The acetylene yield increased with increase in temperature and decrease in pressure. The residence times were very small especially at the highest temperatures.

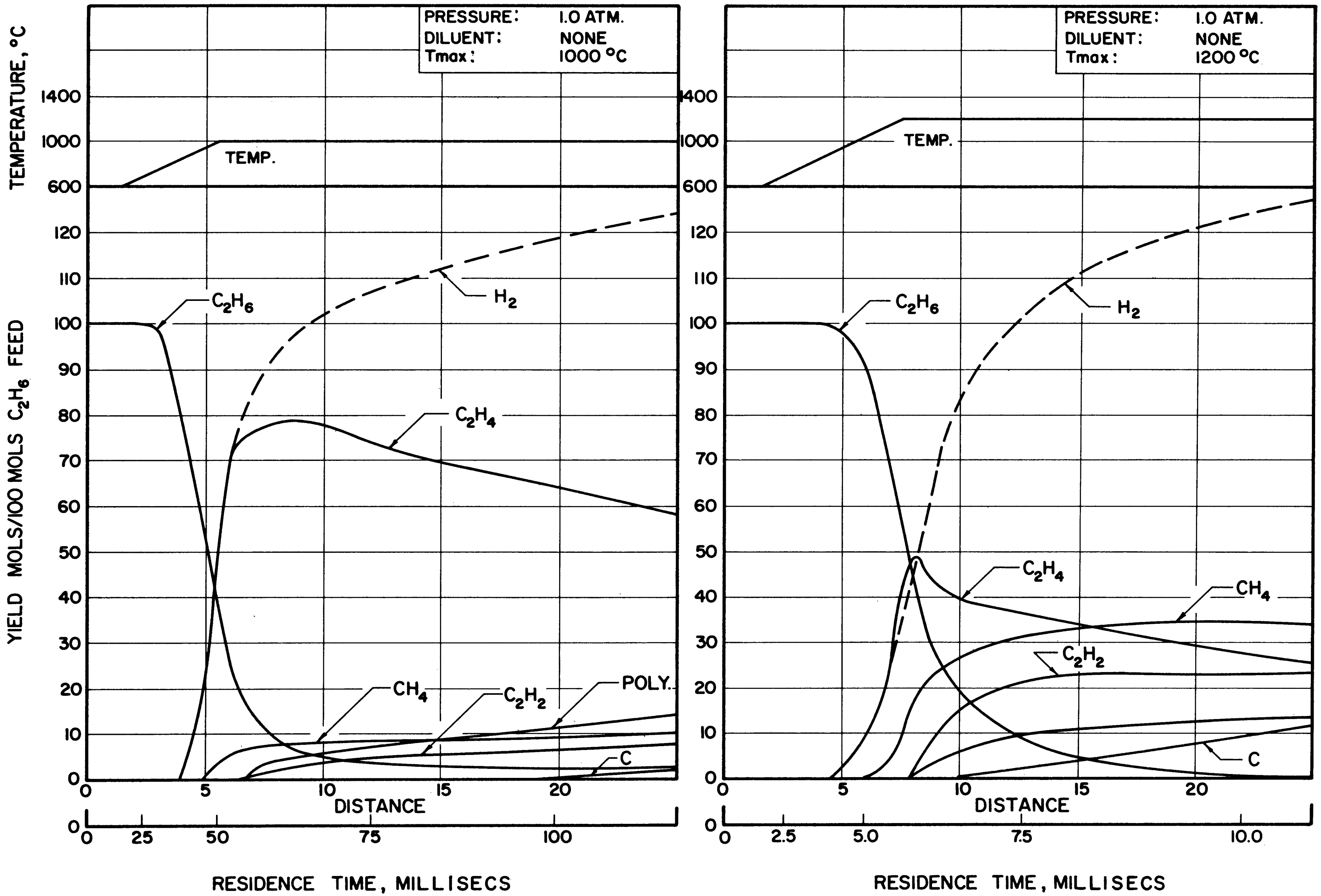

Figure 39. Computed Product Distributions versus Residence Time (1 atm, no diluent, 1000°C and 1200°C).

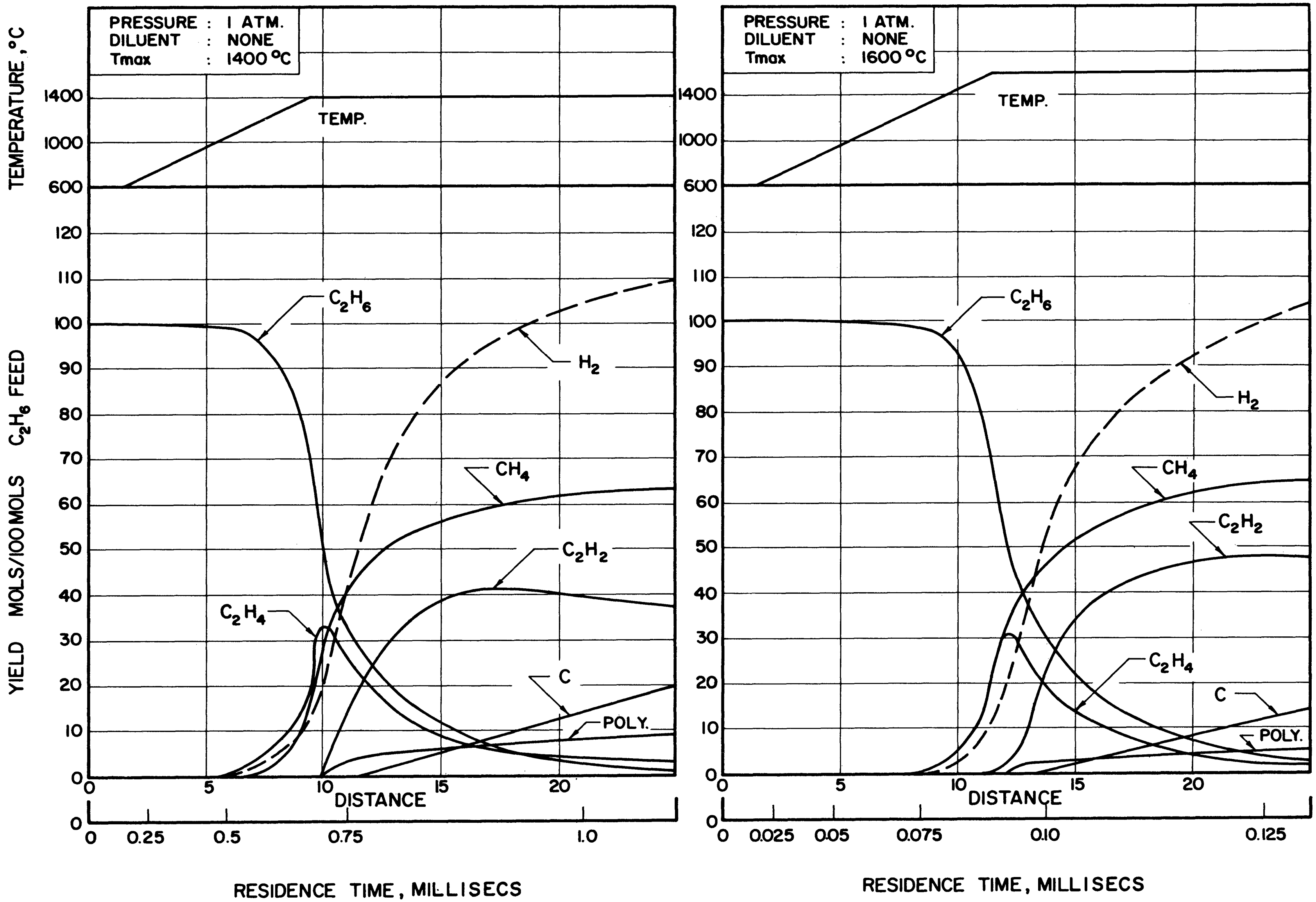

Figure 40. Computed Product Distributions versus Residence Time (1 atm, no diluent, 1400°C and 1600°C).

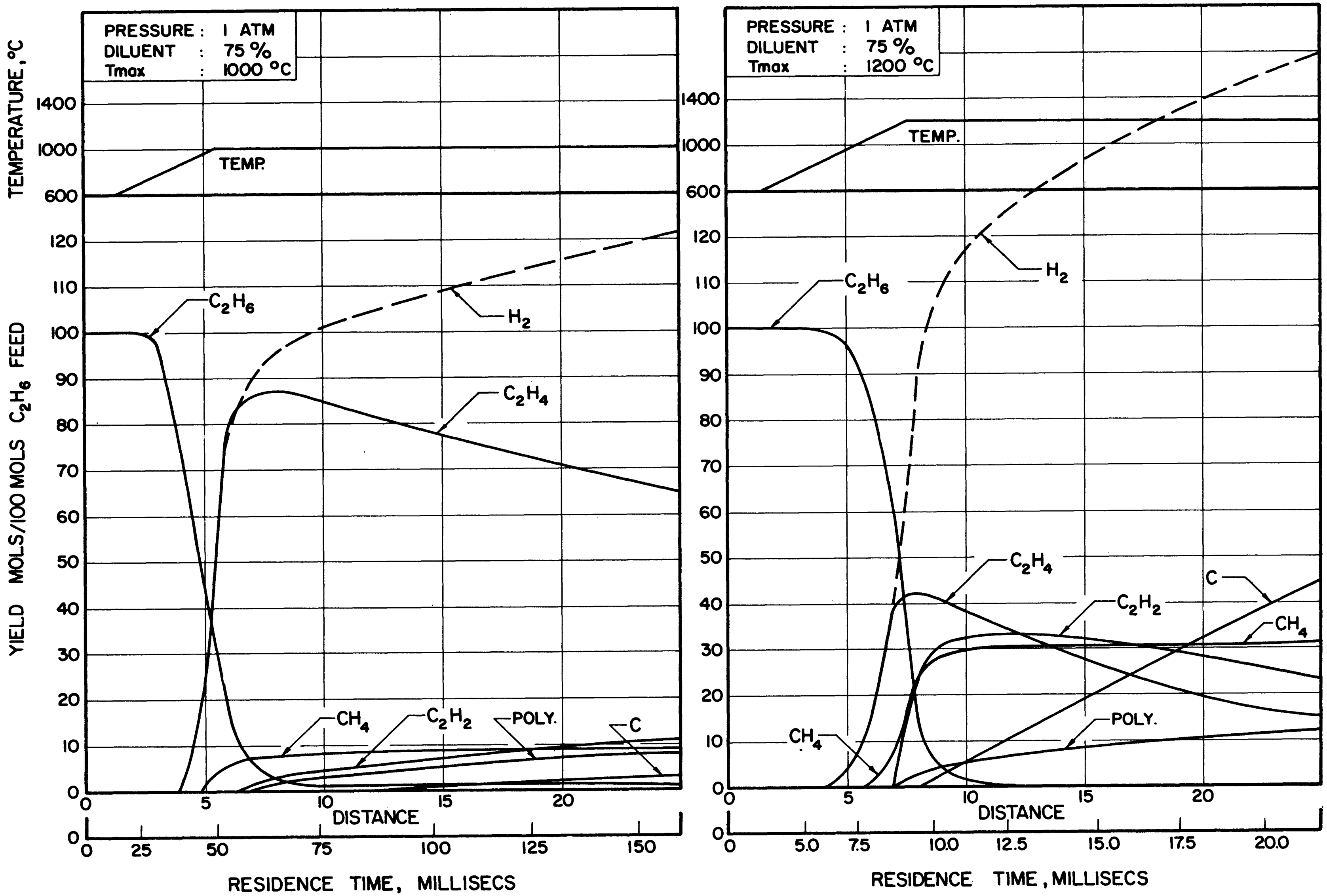

Figure 41. Computed Product Distributions versus Residence Time (1 atm, 75% diluent, 1000°C and 1200°C).

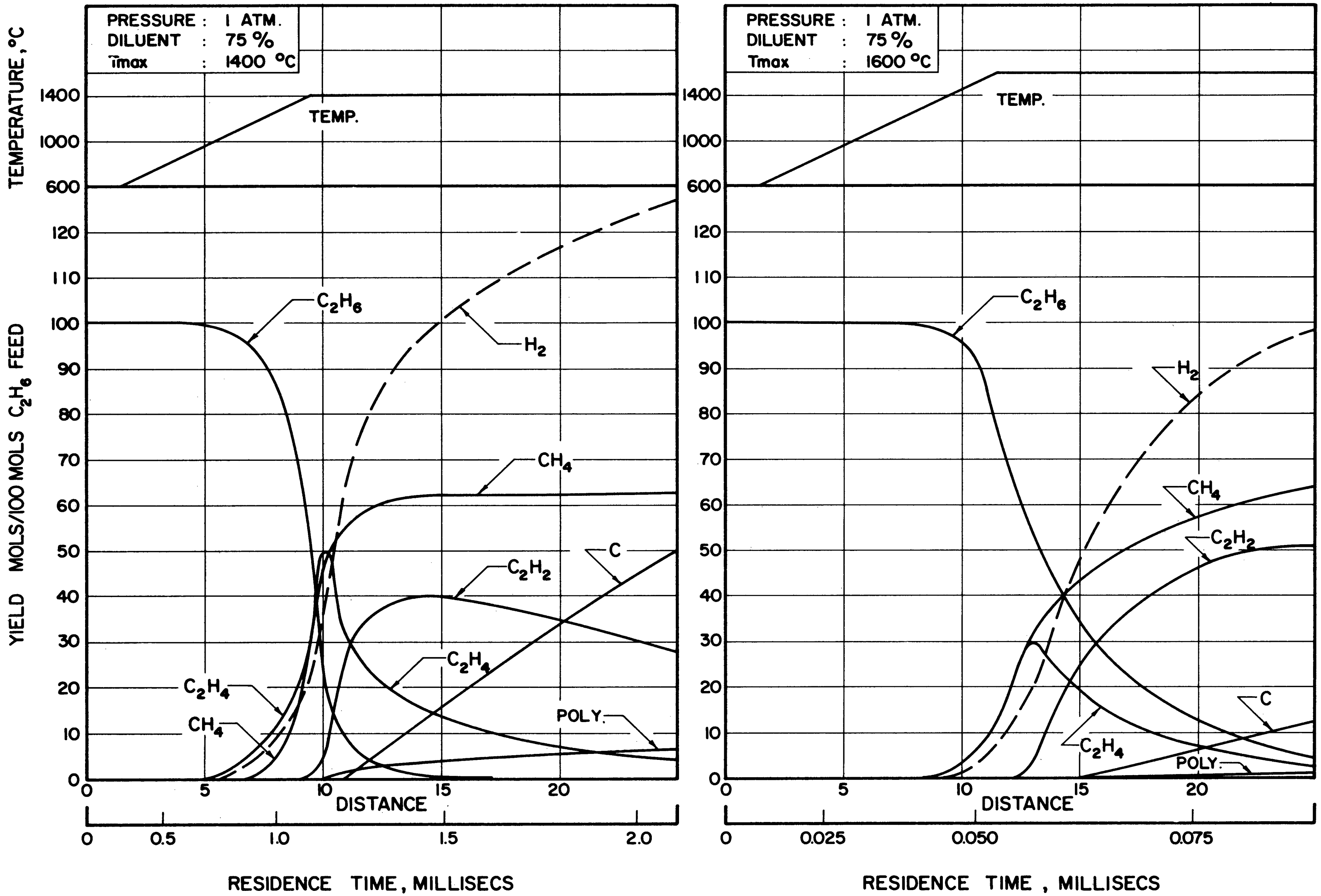

Figure 42. Computed Product Distributions versus Residence Time (1 atm, 75% diluent, 1400°C and 1600°C).

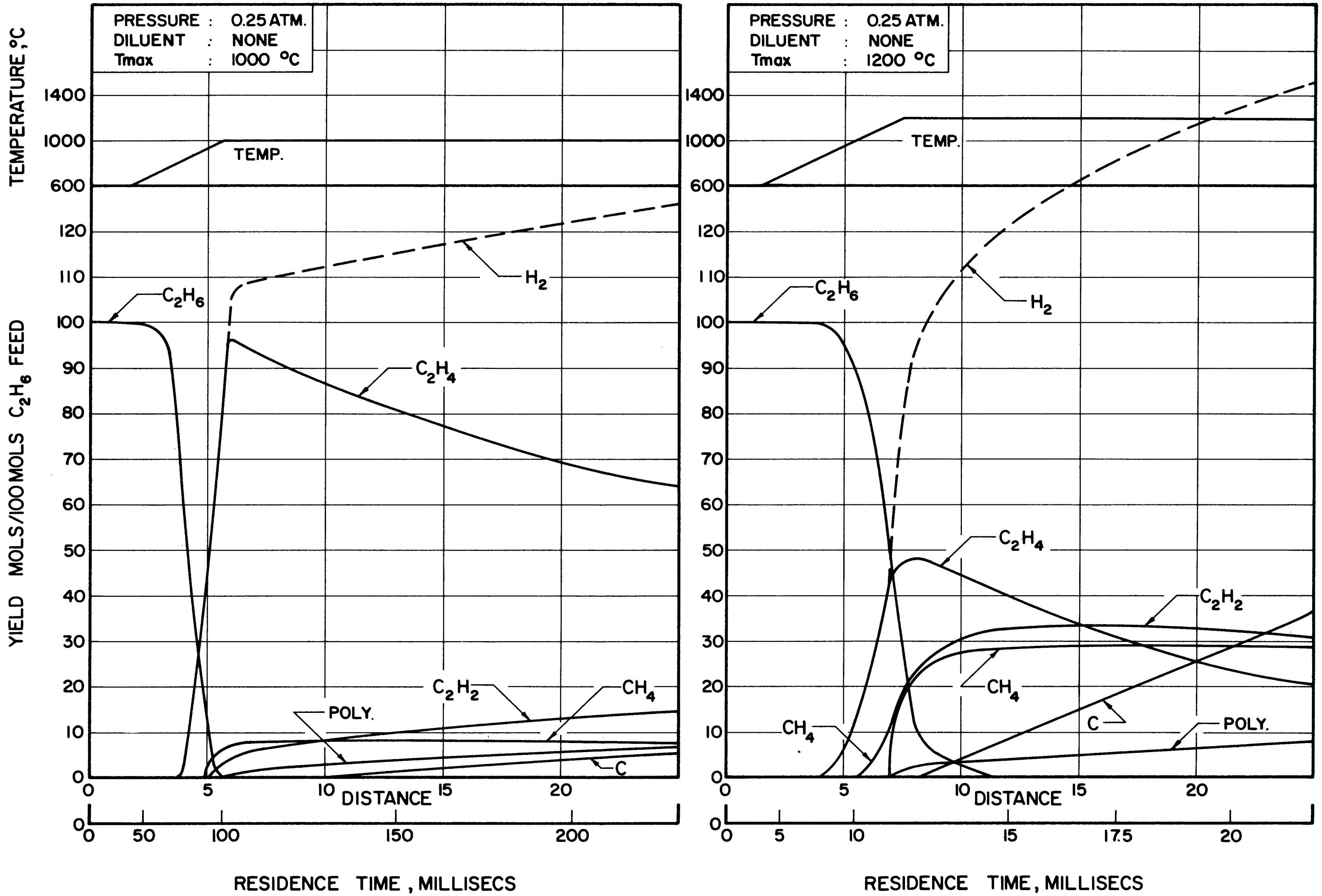

Figure 43. Computed Product Distributions versus Residence Time (0.25 atm, no diluent, 1000°C and 1200°C).

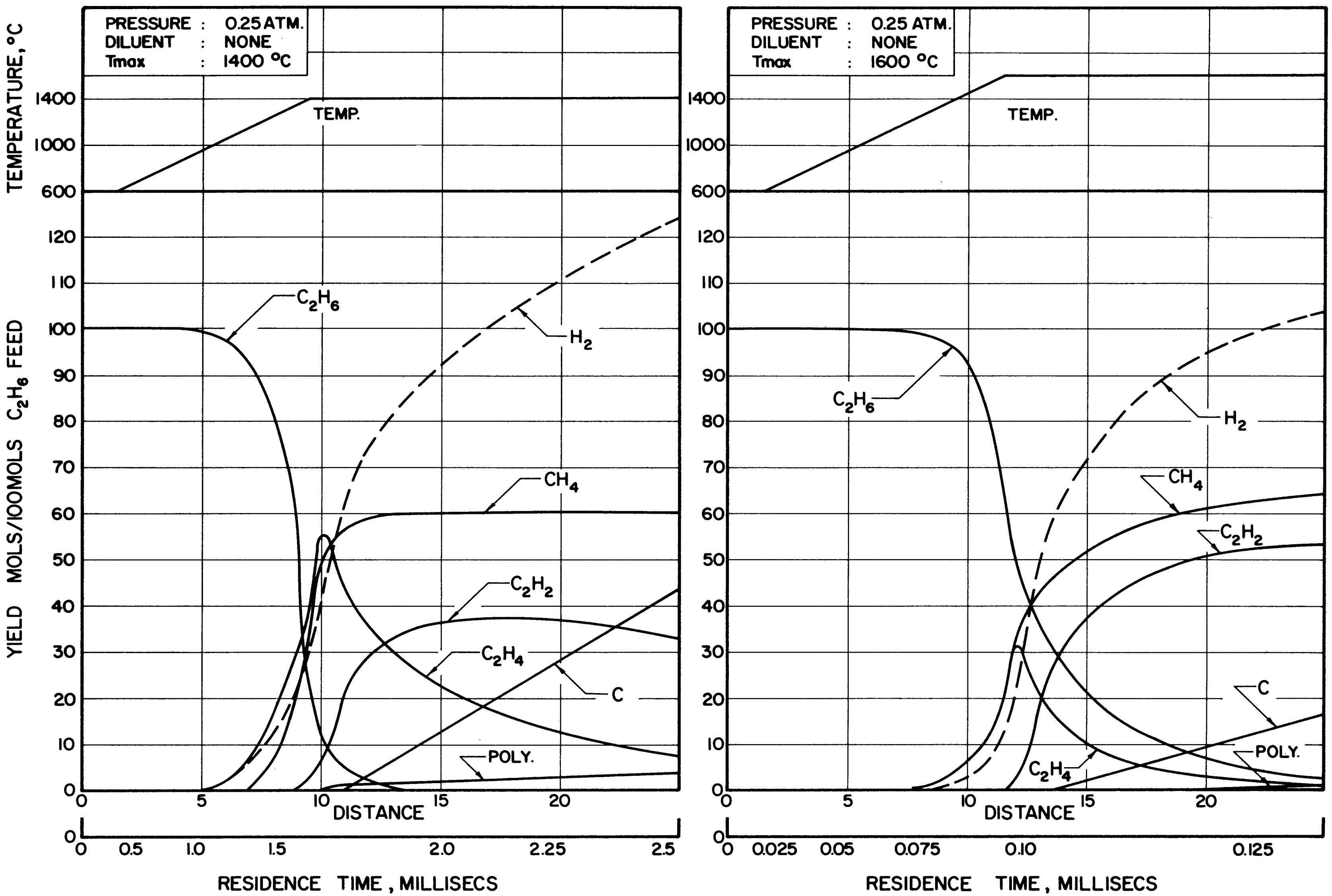

Figure 44. Computed Product Distributions versus Residence Time (0.25 atm, no diluent, 1400°C and 1600°C).

VII. CONCLUSIONS

A technique for carrying out a kinetic study in a non-isothermal field has been developed. The technique requires considerable mathematical labor (which is easily handled on a digital computer) but the need for an isothermal experiment is removed. The reactions studied in this work were fast, high temperature reactions for which the isothermal experiments can only be crudely approximated. Precise kinetic data were obtained and it is concluded that this technique will have wide general application in the field of fast high temperature kinetic studies.

The reaction studied in this work was the thermal decomposition of ethane to acetylene. The reaction proceeded through a series of consecutive steps from ethane to ethylene to acetylene to carbon. The kinetics of thermal decomposition of ethane, ethylene and acetylene were studied separately because of the complexity of the overall reaction.

The kinetic data for ethane decomposition was correlated with a model of two homogeneous parallel first order reactions to ethylene and methane. The rate constants for ethylene formation fell off considerably at higher temperatures and this was due to inhibition of the reaction by the secondary reaction products butadiene and propylene. The data of this work were found to be generally in agreement with previous workers.

The ethylene decomposition was correlated by a model of two homogeneous parallel reactions which were a first order formation of acetylene and a second order polymerization to butadiene (which subsequently reacted to vinylacetylene and benzene).

The acetylene decomposition was correlated by a model of two homogeneous parallel reactions which were a first order formation of carbon and a second order polymerization to vinylacetylene (with subsequent reaction to benzene).

The decomposition of ethane was found to be a chain reaction and it was concluded that the inhibition by the reaction products was due to shortening of the chain length. This is the only conclusion concerning mechanism that can be made as a result of this work. The decomposition of ethane was, however, shown to be consistent with the free radical chain mechanism ideas of Rice and Herzfeld. No conclusions could be made with regard to the mechanism of ethylene and acetylene decomposition.

The kinetic data on the individual steps were combined and an overall correlation developed. Some experiments were carried out in which all of the reactions were occurring and these product distributions were compared with calculated values using the overall correlation. Reasonable agreement was obtained so it is concluded that this correlation can be used to predict the product distribution for any desired reaction conditions.

A few calculations were carried out using this correlation over a wide range (part of the range represents an extrapolation) of the variables, temperature, pressure and residence time. The acetylene yield was found to increase with increase in temperature and decrease in pressure. The residence times were very small especially at the higher temperatures.

Future work of interest would be to investigate methane and propane as starting materials. It is thought that ethylene would be the intermediate preceding acetylene for these feed materials too so that a considerable part of this kinetic study would be applicable.

APPENDIX I

RAW EXPERIMENTAL DATA

TABLE II. Raw Data: Product Distribution Experiments

(All runs in reactor No. 2)

Run No.	80	81	83	84	86	87	88	89	126	115	78	127	Feed Gases		
Temp. °C (max)	816	816	816	816	996	996	996	996	996	1043	1052	1036			
Hydrocarbon	C_2H_6	C_2H_6	C_2H_6	C_2H_6	C_2H_4	C_2H_4	C_2H_4	C_2H_4	C_2H_4	C_2H_2	C_2H_2	C_2H_2	C_2H_6	C_2H_4	C_2H_2
Hydrocarbon Feed Rate Gm. ml/sec.	7.72 $\times10^{-5}$	2.42 $\times10^{-4}$	4.81 $\times10^{-4}$	1.18 $\times10^{-3}$	4.06 $\times10^{-5}$	1.60 $\times10^{-4}$	3.75 $\times10^{-4}$	1.07 $\times10^{-3}$	1.71 $\times10^{-3}$	8.35 $\times10^{-5}$	9.08 $\times10^{-5}$	6.08 $\times10^{-4}$			
N_2 Feed Rate Gm. ml/sec.	2.72 $\times10^{-4}$	7.30 $\times10^{-4}$	1.65 $\times10^{-3}$	3.31 $\times10^{-3}$	1.63 $\times10^{-4}$	5.14 $\times10^{-4}$	1.22 $\times10^{-3}$	3.12 $\times10^{-3}$	5.02 $\times10^{-3}$	2.81 $\times10^{-3}$	5.18 $\times10^{-3}$	6.65 $\times10^{-3}$			
Pressure, Atm.	0.992	0.993	0.999	1.011	0.992	0.993	0.999	1.011	1.030	1.000	1.037	1.037			
Product Distribution Mole%															
C_2H_6	13.82	21.35	21.2	25.3	0.192	0.196	0.155	0.133	0.058	-	-	0.029	96.8	-	-
C_2H_4	7.28	3.20	1.40	1.13	9.19	16.3	19.57	23.7	24.45	0.027	0.367	0.136	2.1	99.8	-
C_2H_2	-	-	-	-	1.78	1.57	1.05	0.269	0.080	2.50	8.02	6.97	-	-	97.9
CH_4	0.495	0.20	0.075	0.048	2.01	0.945	0.376	0.037	0.007	0.022	0.200	0.054	0.05	-	-
H_2	6.32	2.58	0.757	0.429	7.46	4.53	2.59	0.830	0.385	0.057	1.92	0.116	-	-	-
C_3H_8	0.086	0.041	0.020	0.028	0.049	0.046	0.087	0.055	0.053	-	-	0.026	0.08	-	-
C_3H_6	0.154	0.210	0.264	0.282	0.076	0.145	0.118	0.075	0.075	-	-	-	1.0	-	-
C_3H_4	-	-	-	-	0.049	0.095	0.078	0.035	-	0.029	0.043	0.091	-	-	-
C_4H_6	0.031	-	-	-	0.253	0.583	0.631	0.428	0.258	-	-	-	-	-	-
C_4H_4	-	-	-	-	0.194	0.296	0.232	0.057	0.018	0.064	0.554	0.286	-	-	-
C_4H_2	-	-	-	-	0.012	0.031	0.061	0.040	0.003	0.009	0.024	0.033	-	-	-
C_5H_6	-	-	-	-	0.071	0.133	0.086	0.015	0.006	0.006	-	0.024	-	-	-
C_6H_6	-	-	-	-	0.703	0.495	0.173	0.028	0.011	0.011	0.723	0.042	-	-	-
C	-	-	-	-	4.95	0.853	-	-	-	0.218	5.46	1.04	-	-	-
N_2	71.9	72.5	76.3	72.8	73.1	74.0	74.9	74.3	74.6	97.2	82.8	91.2	-	-	-
														0.2[1]	2.1[2]

1. C_4H_8
2. Acetone

TABLE III. Raw Data: Reaction Order Experiments

(All runs in reactor No. 2)

Run No.	49	50	51	52	53	54	55	56	57	58	115	114	113	112
Temp. °C (max)	874	874	874	874	875	1082	1082	1082	1082	1082	1043	1043	1043	1043
Hydrocarbon	C_2H_6	C_2H_6	C_2H_6	C_2H_6	C_2H_6	C_2H_4	C_2H_4	C_2H_4	C_2H_4	C_2H_4	C_2H_2	C_2H_2	C_2H_2	C_2H_2
Hydrocarbon Feed Rate Gm. ml/sec.	2.49 $\times10^{-4}$	4.46 $\times10^{-4}$	6.32 $\times10^{-4}$	1.02 $\times10^{-3}$	1.68 $\times10^{-3}$	2.28 $\times10^{-4}$	4.00 $\times10^{-4}$	6.10 $\times10^{-4}$	9.92 $\times10^{-4}$	1.59 $\times10^{-3}$	8.32 $\times10^{-5}$	1.42 $\times10^{-4}$	2.06 $\times10^{-4}$	3.89 $\times10^{-4}$
N_2 Feed Rate Gm. ml/sec.	4.52 $\times10^{-3}$	4.36 $\times10^{-3}$	4.11 $\times10^{-3}$	3.62 $\times10^{-3}$	3.02 $\times10^{-3}$	4.55 $\times10^{-3}$	4.41 $\times10^{-3}$	4.15 $\times10^{-3}$	3.72 $\times10^{-3}$	3.16 $\times10^{-3}$	2.80 $\times10^{-3}$	2.77 $\times10^{-3}$	2.68 $\times10^{-3}$	2.56 $\times10^{-3}$
Pressure, Atm.	0.998	0.998	0.998	0.998	0.998	1.001	1.001	1.001	1.001	1.001	1.000	1.000	1.000	1.000
Product Distribution Mole%														
C_2H_6	4.65	8.18	11.66	19.0	30.7	-	-	-	-	-	-	-	-	-
C_2H_4	0.494	0.938	1.33	2.21	3.45	4.14	7.00	10.36	16.02	24.55	0.027	0.032	0.030	0.068
C_2H_2	0.026	0.015	0.063	0.097	0.123	0.501	0.821	1.36	2.29	3.38	2.50	4.15	5.93	10.46
CH_4	0.029	0.049	0.073	0.132	0.227	0.028	0.069	0.136	0.351	0.743	0.022	0.033	0.044	0.078
H_2	0.384	0.701	1.08	1.80	2.89	0.509	0.985	1.71	3.25	5.46	0.057	0.093	0.147	0.292
C_3H_8	-	0.037	0.059	0.079	0.139	-	-	-	-	-	-	-	-	-
C_3H_6	0.038	0.077	0.111	0.182	0.304	-	-	-	-	-	-	-	-	-
C_3H_4	-	-	-	-	-	-	-	-	-	-	0.029	0.048	0.063	0.108
C_4H_6	-	-	-	-	-	0.051	0.122	0.255	0.480	0.852	-	-	-	-
C_4H_4	-	-	-	-	-	-	0.072	0.175	0.363	0.633	0.064	0.158	0.278	0.633
C_4H_2	-	-	-	-	-	-	-	-	-	-	0.009	0.015	0.031	0.064
C_5H_6	-	-	-	-	-	-	-	-	-	0.126	0.006	0.015	0.028	0.052
C_6H_6	-	-	-	-	-	-	0.018	0.049	0.150	0.311	0.011	0.018	0.052	0.207
C	-	-	-	-	-	-	-	-	-	-	0.218	0.382	0.516	0.986
N_2	94.3	90.0	85.6	76.2	62.15	94.8	90.9	86.0	77.0	64.0	97.2	95.5	93.3	88.0

TABLE IV.

Raw Data: Rate Constant Experiments

Run No.	18	19	21	22	42	43	44	45	46	118	96	97	98	128	129	130	131
Reactor No.	1	1	1	1	2	2	2	2	2	2	3	3	3	2	2	2	2
Temp. °C (max)	743	765	816	843	841	896	971	996	1055	782	843	901	1010	1032	1138	1225	1338
Hydrocarbon	C_2H_6	C_2H_6	C_2H_6	C_2H_6	C_2H_6	C_2H_6	C_2H_6	C_2H_6	C_2H_6	C_2H_6	C_2H_6	C_2H_6	C_2H_6	C_2H_6	C_2H_6	C_2H_6	C_2H_6
Hydrocarbon Feed Rate Gm. ml/sec.	3.80 x10^{-5}	9.20 x10^{-5}	8.35 x10^{-4}	8.74 x10^{-4}	1.16 x10^{-4}	1.85 x10^{-4}	4.24 x10^{-4}	6.10 x10^{-4}	6.31 x10^{-4}	1.41 x10^{-4}	4.72 x10^{-5}	1.024 x10^{-4}	2.22 x10^{-4}	8.50 x10^{-4}	8.65 x10^{-4}	8.32 x10^{-4}	4.84 x10^{-4}
N_2 Feed Rate Gm. ml/sec.	1.90 x10^{-4}	4.86 x10^{-4}	3.88 x10^{-3}	3.81 x10^{-3}	4.35 x10^{-4}	8.01 x10^{-4}	1.86 x10^{-3}	3.50 x10^{-3}	3.54 x10^{-3}	3.75 x10^{-4}	2.46 x10^{-4}	5.13 x10^{-4}	1.12 x10^{-4}	4.80 x10^{-3}	4.88 x10^{-3}	4.52 x10^{-3}	3.34 x10^{-3}
Pressure, Atm.	0.965	0.973	1.071	1.071	0.982	0.990	0.994	1.010	1.003	0.978	0.979	0.982	1.006	1.032	1.039	1.042	1.048
Product Distribution Mole %																	
C_2H_6	15.22	14.50	15.72	13.87	13.83	7.83	5.23	5.83	2.95	26.05	11.8	7.19	1.44	4.685	0.985	0.128	(1)
C_2H_4	1.08	1.15	1.75	3.85	5.71	8.76	10.45	7.33	8.96	0.850	3.51	7.64	10.32	7.74	8.25	5.65	
C_2H_2	-	-	-	-	0.040	0.136	0.344	0.246	0.799	-	-	0.066	0.921	0.484	1.96	4.22	
CH_4	0.048	0.097	0.085	0.210	0.317	0.723	0.725	0.691	1.17	0.047	0.236	0.633	1.666	0.970	1.94	2.47	
H_2	0.517	0.836	1.092	3.10	4.91	8.39	10.58	7.27	10.17	0.373	2.94	7.14	12.42	8.13	12.4	15.4	
C_3H_8	-	-	-	-	0.075	0.061	-	-	-	0.080	0.081	0.047	0.027	0.058	0.028	-	
C_3H_6	0.128	0.125	0.130	0.115	0.124	0.091	0.107	0.098	0.093	0.276	0.102	0.081	0.068	0.092	0.076	0.043	
C_3H_4	-	-	-	-	-	-	-	-	-	-	-	-	0.021	0.034	0.053	0.080	
C_4H_6	-	-	-	-	0.043	0.082	0.151	0.078	0.118	-	-	0.069	0.175	0.114	0.147	0.073	
C_4H_4	-	-	-	-	-	-	-	-	-	-	-	-	0.101	0.065	0.183	0.310	
C_4H_2	-	-	-	-	-	-	-	-	-	-	-	-	0.023	0.009	0.035	0.093	
C_5H_6	-	-	-	-	-	-	-	-	-	-	-	-	-	-	0.032	0.029	
C_6H_6	-	-	-	-	-	-	-	-	-	-	-	-	0.060	0.030	0.096	0.166	
C	-	-	-	-	-	-	-	-	-	-	-	-	-	-	-	-	
N_2	82.91	83.3	81.3	78.9	75.1	74.0	72.4	78.5	75.7	72.1	81.4	77.2	72.7	77.6	73.9	73.9	

Temp. °C at one inch intervals	18 Center	18 Wall	19 Center	19 Wall	21 Center	21 Wall	22 Center	22 Wall	42	43	44	45	46	118	96	97	98	128	129	130	131
	538	538	538	538	538	711	538	727	404	560	640	431	457	480	564	525	457	603	487	552	682
	657	632	643	621	632	776	638	788	606	704	718	592	545	603	688	684	652	735	656	726	904
	733	727	738	732	721	807	721	827	738	772	796	664	633	727	812	843	846	868	827	900	1016
	743	743	765	765	777	824	785	849	783	840	837	735	707	754	828	871	901	904	885	948	1082
	727	739	761	766	805	830	822	860	829	857	877	781	782	782	843	899	956	942	943	995	1116
	703	717	743	749	816	827	840	857	836	874	891	827	827	777	835	891	965	957	967	1018	1143
	677	689	721	732	812	818	843	851	833	870	904	849	871	771	827	895	973	970	991	1039	1169
	648	660	696	704	805	805	838	842	817	865	910	870	893	756	810	883	970	979	1010	1054	1188
	623	635	673	682	793	793	830	832	802	858	915	883	918	740	794	872	966	988	1029	1071	1219
	606	615	655	660	782	782	820	822	790	852	919	896	930	729	785	865	966	1000	1053	1102	1243
	593	603	642	649	771	770	811	812	779	851	922	909	942	717	776	857	966	1013	1079	1132	1266
	587	596	632	638	754	755	801	804	775	849	927	921	954	712	776	855	968	1021	1095	1155	1288
	582	592	622	627	738	741	791	793	771	852	932	932	966	707	773	854	969	1030	1112	1180	1307
	580	590	616	627	721	724	777	780	776	854	941	943	979	710	780	858	974	1030	1119	1191	1319
	577	590	610	621	701	710	762	768	780	865	950	956	992	713	785	862	979	1031	1127	1203	1327
	571	590	599	618	679	693	744	752	793	874	962	970	1006	720	799	872	989	1032	1132	1212	1335
	562	590	588	610	657	680	721	735	806	885	969	985	1021	728	814	882	999	1032	1138	1220	1338
	554	588	576	604	632	652	692	716	816	895	971	993	1038	731	819	885	1004	1017	1136	1222	1335
	545	582	560	593	604	621	655	691	835	896	971	995	1049	733	824	888	1010	996	1134	1225	1321
	-	566	-	-	-	593	616	659	841	893	964	996	1052	717	807	885	999	973	1123	1216	1304
	-	538	-	-	-	560	577	630	840	883	939	992	1055	700	791	857	988	949	1112	1205	1282
	-	-	-	-	-	-	-	593	830	854	888	971	1050	656	746	816	956	816	1093	1186	1232
	-	-	-	-	-	-	-	-	793	781	793	922	1030	614	703	775	924	682	1075	1167	1160
	-	-	-	-	-	-	-	-	711	593	621	757	979	429	554	506	716	-	924	993	1057
	-	-	-	-	-	-	-	-	449	-	538	631	782	-	-	-	395	-	774	819	827

(1) Reactor plugged with carbon during this run

TABLE IV. (Continued)

Run No.	24	67	68	47	48	99	100	101	110	111	112	116	117	102	103	104	82[2]	85[3]
Reactor No.	1	2	2	2	2	3	3	3	2	2	2	2	2	3	3	3	2	2
Temp. ^{o}C (max)	899	1046	1096	1132	1197	1024	1079	1130	937	990	1043	1099	1118	1049	1013	949	832	872
Hydrocarbon	C_2H_4	C_2H_4	C_2H_4	C_2H_4	C_2H_4	C_2H_4	C_2H_4	C_2H_4	C_2H_2	C_2H_2	C_2H_2	C_2H_2	C_2H_2	C_2H_2	C_2H_2	C_2H_2	C_2H_6	C_2H_6
Hydrocarbon Feed Rate Gm. ml/sec.	1.25 $\times10^{-4}$	5.65 $\times10^{-5}$	1.73 $\times10^{-4}$	5.34 $\times10^{-4}$	8.53 $\times10^{-4}$	2.77 $\times10^{-5}$	7.95 $\times10^{-5}$	2.74 $\times10^{-4}$	3.94 $\times10^{-5}$	1.44 $\times10^{-4}$	3.77 $\times10^{-4}$	8.75 $\times10^{-4}$	1.32 $\times10^{-3}$	2.06 $\times10^{-4}$	1.04 $\times10^{-4}$	8.17 $\times10^{-5}$	2.32 $\times10^{-4}$	5.12 $\times10^{-4}$
N_2 Feed Rate Gm. ml/sec.	4.05 $\times10^{-4}$	3.81 $\times10^{-4}$	1.14 $\times10^{-3}$	2.39 $\times10^{-3}$	3.63 $\times10^{-3}$	2.52 $\times10^{-4}$	6.59 $\times10^{-4}$	1.55 $\times10^{-3}$	3.84 $\times10^{-4}$	1.07 $\times10^{-3}$	2.48 $\times10^{-3}$	4.80 $\times10^{-3}$	6.98 $\times10^{-3}$	1.55 $\times10^{-3}$	6.48 $\times10^{-4}$	5.43 $\times10^{-4}$	7.11 $\times10^{-4}$	2.30 $\times10^{-3}$
Pressure, Atm.	0.973	0.975	0.985	1.009	1.020	0.986	0.995	1.024	0.980	0.985	1.000	1.025	1.067	1.019	0.995	0.992	0.993	1.008
Product Distribution Mole %																		
C_2H_6	-	-	-	0.147	0.165	0.030	-	-	0.061	-	-	-	-	-	-	-	21.9	16.35
C_2H_4	19.59	6.12	6.56	11.2	10.1	5.09	5.69	8.13	0.119	0.152	0.068	0.085	0.118	0.057	0.083	0.086	1.86	1.16
C_2H_2	0.562	2.65	3.20	3.15	4.45	1.64	2.44	3.27	6.61	8.70	10.4	12.3	12.7	9.31	10.0	10.0	-	0.035
CH_4	0.64	0.916	0.660	0.593	0.680	0.835	0.525	0.616	0.065	0.079	0.077	0.104	0.115	0.061	0.095	0.070	0.302	0.229
H_2	2.43	5.74	5.32	5.32	6.68	3.63	4.37	5.52	0.256	0.298	0.290	0.418	0.409	0.321	0.494	0.306	0.896	0.625
C_3H_8	-	-	-	-	-	0.027	-	-	-	-	-	-	-	-	-	-	0.075	0.074
C_3H_6	-	-	-	-	-	0.028	-	0.047	-	-	-	-	-	-	-	-	1.73	1.67
C_3H_4	-	0.066	0.070	0.106	0.113	0.021	0.035	0.064	0.064	0.081	0.107	0.149	0.173	0.085	0.079	0.109	-	-
C_4H_6	1.14	0.126	0.126	0.222	0.182	0.079	0.077	0.127	-	-	-	-	-	-	-	-	-	-
C_4H_4	-	0.273	0.282	0.401	0.405	0.146	0.220	0.347	0.496	0.624	0.627	0.669	0.612	0.538	0.742	0.726	-	-
C_4H_2	-	0.047	0.070	0.078	0.101	0.041	0.048	0.077	0.031	0.052	0.063	0.075	0.072	0.046	0.048	0.036	-	-
C_5H_6	-	-	-	-	-	-	-	0.044	0.042	0.059	0.051	0.049	0.056	0.043	0.056	0.055	-	-
C_6H_6	0.17	0.400	0.349	0.232	0.260	0.173	0.178	0.247	0.273	0.200	0.205	0.153	0.151	0.146	0.382	0.323	-	-
C	-	1.91	0.764	0.840	0.888	1.74	1.23	0.928	1.24	1.56	0.983	1.27	1.36	0.976	1.48	0.474	-	-
N_2	75.4	82.0	82.7	77.8	76.0	88.1	85.2	80.6	90.6	88.6	87.2	84.7	84.0	88.5	86.5	87.7	73.4	79.8
Temp. ^{o}C at one inch intervals	638	546	577	511	554	420	375	453	423	549	450	521	477	424	543	512	438	471
	777	721	782	639	684	720	651	671	777	691	615	616	590	603	657	632	577	608
	849	846	907	769	778	838	816	890	842	832	710	734	701	780	829	754	718	664
	880	973	1030	831	835	956	982	967	907	891	806	799	769	857	882	807	766	720
	893	1002	1059	893	893	984	1021	1043	921	950	860	863	835	935	938	860	816	743
	899	1032	1088	935	919	1013	1060	1071	937	970	916	898	864	971	963	888	829	767
	893	1040	1092	977	944	1019	1069	1100	937	988	947	932	893	1007	988	916	832	780
	881	1047	1096	999	970	1024	1077	1108	933	989	979	961	920	1021	997	927	822	793
	867	1043	1095	1021	999	1022	1075	1117	931	990	998	990	946	1035	1007	939	812	804
	850	1041	1094	1038	1027	1014	1073	1120	927	988	1017	1012	982	1042	1010	943	804	815
	832	1038	1092	1054	1055	1010	1071	1123	923	985	1027	1035	1019	1047	1013	949	796	823
	810	1035	1091	1069	1079	1007	1070	1124	921	984	1035	1054	1043	1048	1013	949	791	832
	782	1032	1064	1082	1103	1007	1070	1127	919	982	1040	1074	1068	1049	1013	947	785	842
	758	1030	1038	1093	1127	1008	1070	1127	918	980	1043	1081	1082	1047	1008	942	788	851
	730	1027	1058	1104	1143	1010	1071	1127	917	978	1043	1089	1096	1043	1004	938	790	859
	699	1024	1080	1116	1162	1011	1072	1128	916	975	1043	1093	1106	1042	996	928	799	868
	663	1020	1072	1127	1177	1016	1075	1130	915	972	1041	1099	1118	1041	989	918	807	870
	629	1015	1066	1132	1190	1021	1080	1125	910	959	1038	1088	1107	1029	969	891	812	872
	593	999	1041	1132	1193	1012	1071	1121	904	946	1017	1077	1099	1019	949	866	818	862
	552	983	1017	1124	1197	1004	1065	1098	873	910	995	1054	1080	982	904	812	806	851
	-	943	972	1117	1190	977	1038	1074	842	871	960	1032	1061	946	860	760	795	830
	-	903	928	1089	1173	947	1011	1030	788	818	926	990	1021	895	801	701	762	808
	-	836	735	1038	1130	888	957	985	734	765	987	947	981	843	743	641	730	756
	-	770	731	831	939	830	904	711	630	556	803	724	757	605	467	391	-	550
	-	680	-	-	778	466	560	438	526	349	549	-	-	367	-	-	-	-

(2) 1.78 x 10^{-5} gm. mol/sec. propylene added in feed
(3) 5.12 x 10^{-5} gm. mol/sec. propylene added in feed

TABLE V.

Raw Data: Inhibitor Experiments

Run No.	70	71	72	73	74	119	120	121	122
Temp. °C (max)	863	863	863	863	863	880	880	880	880
Hydrocarbon	C_2H_6	C_2H_6	C_2H_6	C_2H_6	C_2H_6	C_2H_6	C_2H_6	C_2H_6	C_2H_6
Hydrocarbon Feed Rate Gm. ml/sec.	5.50 $\times10^{-4}$	4.97 $\times10^{-4}$	5.07 $\times10^{-4}$	5.08 $\times10^{-4}$	5.16 $\times10^{-4}$	2.24 $\times10^{-4}$	2.23 $\times10^{-4}$	2.33 $\times10^{-4}$	2.26 $\times10^{-4}$
Inhibitor	C_3H_6	C_3H_6	C_3H_6	C_3H_6	C_3H_6	--	C_4H_6	C_4H_6	C_2H_4
Inhibitor Feed Rate Gm. ml/sec.	5.21 $\times10^{-8}$	4.59 $\times10^{-6}$	1.14 $\times10^{-5}$	3.28 $\times10^{-5}$	1.08 $\times10^{-4}$	--	7.02 $\times10^{-6}$	7.22 $\times10^{-5}$	1.87 $\times10^{-5}$
N_2 Feed Rate Gm. ml/sec.	4.17 $\times10^{-3}$	4.22 $\times10^{-3}$	4.21 $\times10^{-3}$	4.20 $\times10^{-3}$	4.15 $\times10^{-3}$	2.17 $\times10^{-3}$	2.16 $\times10^{-3}$	2.18 $\times10^{-3}$	2.18 $\times10^{-3}$
Pressure, Atm.	1.004	1.004	1.004	1.004	1.004	0.990	0.990	0.990	0.990
Product Distribution Mole %									
C_2H_6	10.29	9.52	9.89	10.13	10.52	7.34	7.88	8.44	7.55
C_2H_4	1.19	0.886	0.722	0.496	0.213	1.94	1.47	1.05	2.26
C_2H_2	-	-	-	-	-	-	-	-	-
CH_4	0.047	0.057	0.065	0.059	0.066	0.121	0.118	0.130	0.119
H_2	0.939	0.601	0.454	0.253	0.089	1.59	0.995	0.428	1.46
C_3H_8	0.039	0.041	0.038	0.026	0.055	0.036	0.035	0.041	0.037
C_3H_6	0.001	0.096	0.240	0.691	2.26	0.071	0.091	0.132	0.074
C_3H_4	-	-	-	-	-	-	-	-	-
C_4H_6	-	-	-	-	-	-	0.289	2.87	-
C_4H_4	-	-	-	-	-	-	-	-	-
C_4H_2	-	-	-	-	-	-	-	-	-
C_5H_6	-	-	-	-	-	-	-	-	-
C_6H_6	-	-	-	-	-	-	-	-	-
C	-	-	-	-	-	-	-	-	-
N_2	87.5	88.8	88.6	88.4	86.9	88.9	89.1	87.0	88.5

Run No.	123	124	125	90	91	92	93	94	95
Temp. °C (max)	880	880	880	1091	1091	1091	1091	1091	1127
Hydrocarbon	C_2H_6	C_2H_6	C_2H_6	C_2H_4	C_2H_4	C_2H_4	C_2H_4	C_2H_4	C_3H_6
Hydrocarbon Feed Rate Gm. ml/sec.	2.26 $\times10^{-4}$	2.25 $\times10^{-4}$	2.24 $\times10^{-4}$	1.07 $\times10^{-3}$	1.07 $\times10^{-3}$	1.07 $\times10^{-3}$	1.07 $\times10^{-3}$	1.07 $\times10^{-3}$	3.21 $\times10^{-4}$
Inhibitor	C_2H_2	H_2	--	--	C_3H_6	C_3H_6	C_3H_6	C_3H_6	--
Inhibitor Feed Rate Gm. ml/sec.	9.62 $\times10^{-6}$	1.87 $\times10^{-5}$	--	--	1.91 $\times10^{-5}$	7.18 $\times10^{-5}$	1.12 $\times10^{-4}$	2.25 $\times10^{-4}$	--
N_2 Feed Rate Gm. ml/sec.	2.18 $\times10^{-3}$	2.16 $\times10^{-3}$	2.18 $\times10^{-3}$	3.29 $\times10^{-3}$	3.26 $\times10^{-3}$	3.30 $\times10^{-3}$	3.29 $\times10^{-3}$	3.32 $\times10^{-3}$	3.20 $\times10^{-3}$
Pressure, Atm.	0.990	0.990	0.990	1.016	1.016	1.016	1.016	1.016	1.013
Product Distribution Mole %									
C_2H_6	7.49	7.38	7.55	0.211	0.140	0.105	0.118	0.120	0.140
C_2H_4	1.80	1.83	1.76	18.92	19.8	20.2	20.35	20.55	3.12
C_2H_2	0.391	-	-	1.64	1.95	1.34	1.34	1.33	1.59
CH_4	0.117	0.117	0.116	0.398	0.475	0.793	1.02	1.62	3.62
H_2	1.42	2.51	1.42	3.34	3.17	2.68	2.55	2.80	3.09
C_3H_8	0.038	0.040	0.031	0.034	0.050	0.047	0.079	0.072	-
C_3H_6	0.075	0.073	0.069	0.094	0.161	0.608	1.09	2.07	1.31
C_3H_4	-	-	-	0.092	0.102	0.196	0.290	0.433	0.748
C_4H_6	-	-	-	0.573	0.567	0.529	0.539	0.536	0.164
C_4H_4	-	-	-	0.311	0.292	0.246	0.228	0.232	0.208
C_4H_2	-	-	-	0.077	0.071	0.057	0.058	0.052	0.040
C_5H_6	-	-	-	0.058	0.071	0.090	0.106	0.151	0.116
C_6H_6	-	-	-	0.175	0.152	0.161	0.179	0.208	0.535
C	-	-	-	-	-	-	-	-	-
N_2	88.7	88.0	89.2	74.0	73.1	73.0	72.0	69.80	85.2

APPENDIX II

RESULTS CALCULATED FROM RAW DATA

TABLE VI. Results: Product Distribution Experiments

Hydrocarbon Feed C_2H_6

Run No.	Temp. °C (max)	Conv. %	Hydrocarbon Product Distribution Moles/100 moles of hyd. feed reacted			
			C_2H_4	CH_4	H_2	C_3H_8
80	816	33.2	96.5	7.06	92.0	1.25
81	816	11.3	96.3	7.35	94.9	1.51
82	816	4.35	96.8	6.70	78.7	2.08
83	816	2.29	97.0	6.05	72.3	4.73

Hydrocarbon Feed C_2H_4

Run No.	Temp. °C (max)	Conv. %	C_2H_2	CH_4	H_2	C_4H_6	C_4H_4
86	995	49.2	19.9	22.5	83.7	2.84	2.18
87	995	29.4	23.1	13.8	66.7	8.53	4.33
88	995	14.8	30.8	11.0	76.0	18.5	6.80
89	995	7.17	14.7	2.04	45.4	23.4	3.10
126	995	3.86	8.20	0.67	39.4	26.4	1.80

Run No.	C_6H_6	C	C_2H_6	C_3H_8	C_3H_6
86	7.90	55.5	2.16	0.54	0.86
87	7.24	12.6	2.86	0.68	2.12
88	5.07	-	4.55	2.56	3.47
89	1.55	-	7.27	3.02	4.09
126	1.11	-	5.97	5.43	7.72

Hydrocarbon Feed C_2H_2

Run No.	Temp. °C (max)	Conv. %	C_4H_4	C_6H_6	C	H_2	C_2H_4
78	1043	44.6	8.55	11.2	84.2	29.7	5.67
127	1043	19.6	16.8	2.42	61.0	6.8	8.0
115	1043	12.5	17.8	3.05	60.5	15.8	7.4

Run No.	CH_4	C_3H_4
78	3.10	1.13
127	6.0	5.45
115	3.12	7.60

TABLE VII. Results: Order of Reaction Experiments

Hydrocarbon Feed C_2H_6

Run No.	Temp. °C (max.)	Hydrocarbon Mole. Fr.[1]	Hydrocarbon Reaction Rate Gm. moles/sec. Disappearance	Formation	
			C_2H_6	C_2H_4	CH_4
49	874	0.0486	2.04×10^{-5}	1.98×10^{-5}	1.42×10^{-6}
50	874	0.0857	3.82×10^{-5}	3.69×10^{-5}	2.40×10^{-6}
51	874	0.122	5.55×10^{-5}	5.38×10^{-5}	3.52×10^{-6}
52	874	0.200	9.25×10^{-5}	8.78×10^{-5}	6.29×10^{-6}
53	874	0.322	1.44×10^{-4}	1.38×10^{-4}	1.15×10^{-5}

Hydrocarbon Feed C_2H_4

			C_2H_4	C_2H_2	Polymer[2]
54	1082	0.0444	2.93×10^{-5}	2.41×10^{-5}	5.57×10^{-6}
55	1082	0.0763	6.09×10^{-5}	4.00×10^{-5}	2.32×10^{-5}
56	1082	0.115	1.09×10^{-4}	6.61×10^{-5}	5.20×10^{-5}
57	1082	0.183	2.18×10^{-4}	1.14×10^{-4}	1.12×10^{-4}
58	1082	0.284	3.82×10^{-4}	1.68×10^{-4}	2.21×10^{-4}

Hydrocarbon Feed C_2H_2

			C_2H_2	C	Polymer[2]
112	1043	0.119	8.26×10^{-5}	2.88×10^{-5}	6.82×10^{-5}
113	1043	0.0656	3.50×10^{-5}	1.48×10^{-5}	2.76×10^{-5}
114	1043	0.0452	2.08×10^{-5}	1.11×10^{-5}	1.53×10^{-5}
115	1043	0.0270	1.04×10^{-5}	6.30×10^{-6}	7.26×10^{-6}

1. Arithmetic mean of inlet and outlet
2. C_4's, C_5's, C_6's, CH_4 (Expressed on C_2 basis)

TABLE VIII. Results: Rate Constant[1] Experiments

Pair of Runs	Activation Energy kcal/gm. mole	Pre-exp. Factor sec^{-1}	Temp. (max) °C	1/Temp. x 10^4 $°K^{-1}$	Rate Const. sec^{-1}
Disappearance of ethane[3], first order					
18 19	97.33	9.55×10^{19}	743 765	9.83 9.64	0.117 0.310
18 21	87.44	7.02×10^{17}	743 816	9.83 9.17	0.115 2.02
18 22	84.97	2.04×10^{17}	743 842	9.83 8.95	0.113 4.78
19 21	84.70	1.95×10^{17}	765 816	9.64 9.17	0.289 1.99
19 22	82.39	6.30×10^{16}	765 842	9.64 8.95	0.287 4.70
21 22	77.78	7.61×10^{15}	816 842	9.17 8.95	1.89 4.52
118 42	96.64	5.78×10^{19}	760 841	9.68 8.96	0.209 6.57
42 43	66.25	5.05×10^{13}	841 896	8.96 8.55	5.20 21.4
43 44	55.04	3.67×10^{11}	896 971	8.55 8.03	19.3 79.5
45 46	39.45	6.45×10^{8}	996 1055	7.88 7.52	104 212
128 129	36.42	1.77×10^{8}	1032 1138	7.65 7.08	143 406
82 85	65.94	1.33×10^{13}	832 872	9.05 8.72	1.21 3.52
96 97	70.54	3.22×10^{14}	843 901	8.95 8.51	5.17 23.8
97 98	56.70	7.57×10^{11}	901 1010	8.51 7.79	21.2 167
18[4] 19	103.8	2.18×10^{21}	745 765	9.82 9.64	0.120 0.312
21[4] 22	74.32	1.14×10^{15}	927 956	9.13 8.89	1.72 4.23
Disappearance of ethylene, first order					
24 67	64.94	5.42×10^{11}	899 1047	8.53 7.57	0.435 9.65
67 68	76.28	3.74×10^{13}	1047 1096	7.57 7.30	8.55 24.4
47 48	53.61	9.90×10^{9}	1132 1197	7.12 6.80	45.6 106
99 100	60.22	1.03×10^{11}	1024 1079	7.71 7.40	7.48 20.9
100 101	70.01	3.79×10^{14}	1079 1130	7.40 7.12	18.2 46.5
Disappearance of acetylene, first order					
110 111	59.08	1.56×10^{11}	937 990	8.26 7.91	3.40 9.54
112 116	57.78	7.66×10^{10}	1043 1099	7.60 7.29	19.9 48.1
112 117	68.47	4.87×10^{12}	1043 118	7.60 7.19	21.2 84.5
102 103	42.38	1.78×10^{8}	1049 1013	7.56 7.78	17.6 11.3
103 104	17.01	6.61×10^{3}	1013 949	7.78 8.18	8.59 6.07
Methane formation from ethane, first order					
18 21	91.54	1.41×10^{17}	743 816	9.83 9.17	0.00301 0.0606
19 22	69.18	4.26×10^{14}	765 842	9.64 8.95	0.0117 0.123
118 42	53.72	4.47×10^{9}	760 841	9.68 8.96	0.0193 0.132
43 44	47.95	6.28×10^{8}	896 971	8.55 8.03	0.703 2.44
45 46	53.66	7.52×10^{9}	996 1055	7.88 7.52	5.35 13.7
Polymerization of ethylene, second order[2]					
24 67	63.80	1.30×10^{14}	899 1047	8.53 7.57	145 2,560
67 68	75.50	6.66×10^{15}	1047 1096	7.57 7.30	2,150 6,000
47 48	50.85	1.01×10^{12}	1132 1197	7.12 6.80	12,500 28,200
Acetylene formation from ethylene, first order					
24 67	81.44	1.15×10^{14}	899 1047	8.53 7.57	0.0652 3.87
67 68	92.52	8.34×10^{15}	1047 1096	7.57 7.30	4.13 14.5
47 48	61.93	1.03×10^{11}	1132 1197	7.12 6.80	24.2 65.2
Carbon formation from acetylene, first order					
110 111	55.39	7.90×10^{9}	937 990	8.26 7.91	0.813 2.16
112 116	72.75	4.15×10^{12}	1043 1099	7.60 7.29	3.49 10.6
112 117	82.64	1.90×10^{14}	1043 1118	7.60 7.19	3.70 19.5
Acetylene polymerization, second order[2]					
110 111	45.20	4.05×10^{11}	937 990	8.26 7.91	2,810 6,180
112 116	35.64	9.83×10^{9}	1043 1099	7.60 7.29	11,970 20,650
112 117	46.67	7.35×10^{11}	1043 1118	7.60 7.19	13,300 34,100

1. Rate constant defined on C_2 basis
2. Rate constant units are liter gm. mol^{-1} sec^{-1}
3. Ethylene formation rate constant is .95 times ethane
4. Based on $T_c + 3/4(T_w - T_c)$, all other based on center T_c

TABLE IX. Results: Inhibitor Experiments

Run No.	Temp. (max) °C	Inhibitor	Mole Ratio Inhibitor to Feed	Rate of formation Gm. moles/sec.		
Ethane Feed				C_2H_4 x10^5	CH_4 x10^6	C_3H_8 x10^7
70	863	C_3H_6	0.0003	5.01	2.03	15.9
71	863	C_3H_6	0.0092	3.17	2.54	15.9
72	863	C_3H_6	0.0225	2.38	2.92	14.0
73	863	C_3H_6	0.0677	1.29	2.66	8.25
74	863	C_3H_6	0.209	0.434	2.92	21.6
119	880	None	0	4.26	2.96	8.78
120	880	C_4H_6	0.0312	3.09	2.86	8.52
121	880	C_4H_6	0.310	2.13	3.28	10.3
122	880	C_2H_4	0.0600	3.69	2.92	9.10
123	880	C_2H_2	0.0424	3.94	2.88	9.30
124	880	H_2	0.100	4.02	2.89	9.72
125	880	None	0	3.81	2.84	7.57
Ethylene Feed				C_2H_2 x10^5	C_4H_6 x10^5	
90	1091	None	0	7.30	2.55	
91	1091	C_3H_6	0.0179	8.70	2.52	
92	1091	C_3H_6	0.0672	6.05	2.38	
93	1091	C_3H_6	0.105	6.15	2.64	
94	1091	C_3H_6	0.211	6.35	2.48	

APPENDIX III

CALCULATION OF CORRECT MEAN TEMPERATURE FOR A LINEAR RADIAL TEMPERATURE DISTRIBUTION

Rewriting Equation (18)

$$A = \frac{\frac{F}{a}\left(\frac{P}{R}\right)^m \int_{x_i}^{x_o} \left[\frac{1 + x + N_D/F}{1 - x}\right]^m dx}{\int_0^L \frac{e^{-E/RT(\ell)}}{T(\ell)^m}\, d\ell} \qquad (18)$$

it can be seen that the only part of Equation (18) that is temperature dependent is the integral

$$\int_0^L \frac{e^{-E/RT(\ell)}}{T(\ell)^m}\, d\ell \qquad (29)$$

The objective now is to determine the correct value of temperature (T) to substitute into Equation (29) when a linear radial temperature gradient is assumed. This was accomplished by a numerical calculation with n taken to be unity. The reactor was divided into five equal area rings and the temperature at the mid point of each of the rings determined from the temperature gradient. The linear temperature gradient was thereby approximated by a series of steps. The values of $e^{-E/RT}/T$ were then evaluated for each of the steps and the arithmetic mean of the five values was taken as the correct solution. The value of T that corresponds to this mean value of $e^{-E/RT}/T$ was then the correct mean temperature. The numerical work is summarized below for a linear temperature distribution 1540°R at the center (T_C) and 1600°R at the wall (T_W).

Fractions of radius that give five equal area rings	0.446	0.632	0.775	0.895	1.0
Mid points of rings	0.223	0.539	0.703	0.835	0.947
Temps. at mid points °R	1553.4	1572.4	1582.2	1590	1596.7
Values of $e^{-E/RT}/T \times 10^{21}$	0.974	1.60	2.09	2.50	2.93

Therefore, the mean value of $e^{-E/RT}/T$ is 2.02×10^{-21} which corresponds to a mean temperature of about 0.7 of the difference between the wall (T_W) and center (T_C) temperatures. In view of the approximate nature of the calculation, a mean temperature of 3/4 of the difference is used,

$$\text{i.e.} \quad T\ \text{mean} = T_C + 3/4\,(T_W - T_C) \tag{30}$$

APPENDIX IV

SAMPLE CALCULATIONS

The pair of runs 47 and 48 (ethylene feed) are selected for this example solution. The kinetic model used for this calculation is a first order disappearance of ethylene. The experimental data for these two runs are:

	47	48
Run Number	47	48
Inlet conversion (x_i)	0	0
Outlet conversion (x_o)	0.360	0.434
Feed rate C_2H_4 gm.moles/sec(F)	5.34×10^{-4}	8.53×10^{-4}
Feed rate N_2 gm.moles/sec(N_D)	2.39×10^{-3}	3.63×10^{-4}
Mean pressure atm. (P)	1.009	1.020
Reactor Number	2	2

Temperature Profile °C($T(\ell)$), 1-inch intervals (read down columns)

Run 47			Run 48		
511	1021	1127	554	999	1177
639	1038	1132	684	1027	1190
769	1054	1132	778	1055	1193
831	1069	1124	835	1079	1197
893	1082	1117	893	1103	1190
935	1093	1089	919	1127	1173
979	1104	1038	944	1143	1130
999	1116	831	970	1162	939
					778

Rewriting Equation (18) from section IIF

$$A = \frac{\frac{F}{a}\left(\frac{R}{P}\right)^m \int_{x_i}^{x_o} \left[\frac{(1 + x + N_D/F)}{1-x}\right]^m dx}{\int_0^L \frac{e^{-E/RT(\ell)}}{T(\ell)^m}\, d\ell} \qquad (18)$$

Since the kinetic model in this case is a first order reaction n is 1. Trial values of E are assumed and values of A are computed from (18) using the data of run 47 and then the data of run 48. The calculations are carried out on a digital computer and the results are:

Assumed E values kcal/gm. mol.	ln A(A in 1/hr) Run #47	Run #48
27.78	21.684	22.054
38.89	25.795	26.016
44.44	27.841	27.981
50.10	29.882	29.938
55.55	31.918	31.888
61.11	33.952	33.834
66.67	35.982	35.776
72.22	38.010	37.715
77.78	40.035	39.651
83.33	42.058	41.584
88.89	44.079	43.515
111.11	52.149	51.224

The solution is the E value for which the A values are equal and it can be seen from the results above that this lies between the E values of 50.10 and 55.55. It was found that ln A is almost linear with respect to E so that linear interpolation is quite accurate, which gives the solution

$$E = 53.61 \text{ kcals/gm. mol.}$$

and $\ln A = 31.205$

i.e $A = 3.56 \times 10^{13} \text{ hr}^{-1}$ or $9.90 \times 10^{9} \text{ sec}^{-1}$.

The values of the rate constant are now determined from the Arrhenius equation using the maximum temperature for each of the runs,

	Run #47	Run #48
T max °C	1132	1197
T max °K	1405	1470
$A\ e^{-E/RT}\ sec^{-1}$	$9.90 \times 10^{9} \times e^{-\frac{53.61}{R \times 1405}}$	$9.90 \times 10^{9} \times e^{-\frac{53.61}{R \times 1470}}$
k sec^{-1}	45.6	106.5
1/T°K	7.12×10^{4}	6.80×10^{4}

These two values of the rate constant can be found on Figure 21.

APPENDIX V

MODIFICATION OF CALCULATIONS TO HANDLE PARALLEL REACTIONS

The equations developed in section II are of the form

$$A \rightarrow B + C$$

It was found, however, that the decompositions proceeded by two parallel steps of the form,

$$A \rightarrow B + C$$

$$A \rightarrow D$$

A, B and D are hydrocarbons and C represents hydrogen. The equations have to be modified so that the rate constants for the formation of B and D can be determined. Rewriting Equation (18),

$$A = \frac{\frac{F}{a}\left(\frac{R}{P}\right)^m \int_{x_i}^{x_o} \left[\frac{1 + x + N_D/F}{1 - x}\right]^m dx}{\int_0^L \frac{e^{-E/RT(\ell)}}{T(\ell)^m} d\ell} \tag{18}$$

it can be seen that the only part of (18) that has to be modified is the integral,

$$\int_{x_i}^{x_o} \left[\frac{1 + x + N_D/F}{1 - x}\right] dx \tag{31}$$

Let the total conversion of A be x, the conversion (x_B) of A to B be βx and the conversion (X_D) of A to D be δx. β and δ are constants and their sum is unity.

The $(1 + x + N_D/F)$ in Equation (31) represents the total number of moles divided by the feed rate F, so that for the two parallel reactions this becomes

$$1 - x + 2\beta x + \delta x + N_D/F \tag{32}$$

which is

$$1 + x(2\beta + \delta - 1) + N_D/F \tag{33}$$

The $(1 - x)$ in Equation (31) represents the mols of A left divided by the feed rate F and this remains unchanged.

Therefore, the integral (31) for the case of the two parallel reactions above becomes,

$$\int_{x_i}^{x_o} \left[\frac{1 + x(2\beta + \delta - 1) + N_D/F}{1 - x}\right]^m dx \tag{34}$$

This Equation (34) can now be written twice in terms of each of the parallel reactions since $x_B = \beta x$ and $x_D = \delta x$,

$$\int_{x_{B,i}}^{x_{B,o}} \left[\frac{1 + x_B\left(\frac{2\beta + \delta - 1}{\beta}\right) + N_D/F}{1 - \frac{x_B}{\beta}}\right]^m dx_B \tag{35}$$

$$\int_{x_{D,i}}^{x_{D,o}} \left[\frac{1 + x_D\left(\frac{2\beta + \delta - 1}{\delta}\right) + N_D/F}{1 - \frac{x_D}{\delta}}\right] dx_D \tag{36}$$

Equations (35) and (36) replace the upper integral in Equation (18). The new equations have the same form as the old ones, the only difference being the addition of some constant factors so that the method of solution proceeds as before.

APPENDIX VI

CALCULATIONS TO SHOW EFFECT OF REVERSE REACTION

Nitrogen dilution was used to reduce the reverse reaction effects of the reactions,

$$C_2H_6 \rightleftarrows C_2H_4 + H_2 \qquad (1)$$

$$C_2H_4 \rightleftarrows C_2H_2 + H_2 \qquad (2)$$

Some calculations were made and are summarized here to show that the effects of reverse reaction are negligible.

The rate equations considering the reverse reactions will be

$$C_2H_6 \text{ disappearance rate} = k_1 \left[C_{C_2H_6} - \frac{C_{C_2H_4} C_{H_2}}{K_{c,1}} \right] \qquad (37)$$

and

$$C_2H_4 \text{ disappearance rate} = k_2 \left[C_{C_2H_4} - \frac{C_{C_2H_2} C_{H_2}}{K_{c,2}} \right] \qquad (38)$$

where k_1, k_2 are rate constants, $K_{c,1}$, $K_{c,2}$ are equilibrium constants. The second terms in Equations (37) and (38) represent the reverse reaction effects. The first and second terms are calculated for a number of experimental runs using exit concentrations and the second term expressed as a percentage of the first term. Partial pressures which are proportional to the concentrations are used in the calculations summarized below.

Reaction $C_2H_6 \rightleftarrows C_2H_4 + H_2$

Run No.	T max °C	C_2H_6 press. atm	$\frac{C_2H_4 \times H_2}{K_{p,1}}$ atm.	Ratio %
18	743	0.152	0.000113	0.074
118	782	0.261	0.0000317	0.012
21	816	0.157	0.000119	0.076
44	971	0.0523	0.00103	1.97
46	1055	0.0295	0.000364	1.24
130	1225	0.0128	0.0000668	0.522

Reaction		$C_2H_4 \rightleftarrows C_2H_2 + H_2$		
Run No.	T max °C	C_2H_4 press. atm.	$\frac{C_2H_4 \times H_2}{K_{p,2}}$ atm.	Ratio %
24	899	0.196	0.00286	1.46
67	1046	0.0623	0.0037	5.94
68	1096	0.0661	0.0222	3.36
47	1132	0.1125	0.00139	1.23
48	1197	0.102	0.00125	1.23

It is seen that the reverse reaction term can be considered negligible, so that an irreversible reaction can be assumed.

APPENDIX VII

FLOW DIAGRAMS FOR COMPUTER PROGRAMS

(i) Solution for E and A values

The equation that is to be solved is Equation (18) below

$$A = \frac{\frac{F}{a}\left(\frac{R}{P}\right)^{n}\int_{x_i}^{x_o}\left[\frac{1+x+N_D/F}{1-x}\right]^{n}dx}{\int_{0}^{L}\frac{e^{-E/RT(\ell)}}{T(\ell)^{n}}\,d\ell} \qquad (18)$$

The method of solution is to obtain a set of A values for an assumed set of E values for each experimental run. A pair of runs are considered together to obtain unique solutions for E and A. The integrals in Equation (18) were evaluated numerically by Simpson's Rule. The upper integral was divided into 20 increments for the integration. The reactor length was divided into 25 increments and the temperature distribution was approximated by a series of small steps so that the temperature in each increment could be assumed constant. The reaction order n is known from a separate set of experiments so that it will have a numerical value at the time of calculation. The first step of the program evaluates the conversion integral, the second step the temperature integral and the final step the A value corresponding to the E value assumed. The next E value is selected and the calculation repeated. The flow diagram for this calculation follows.

Evaluation of upper integral

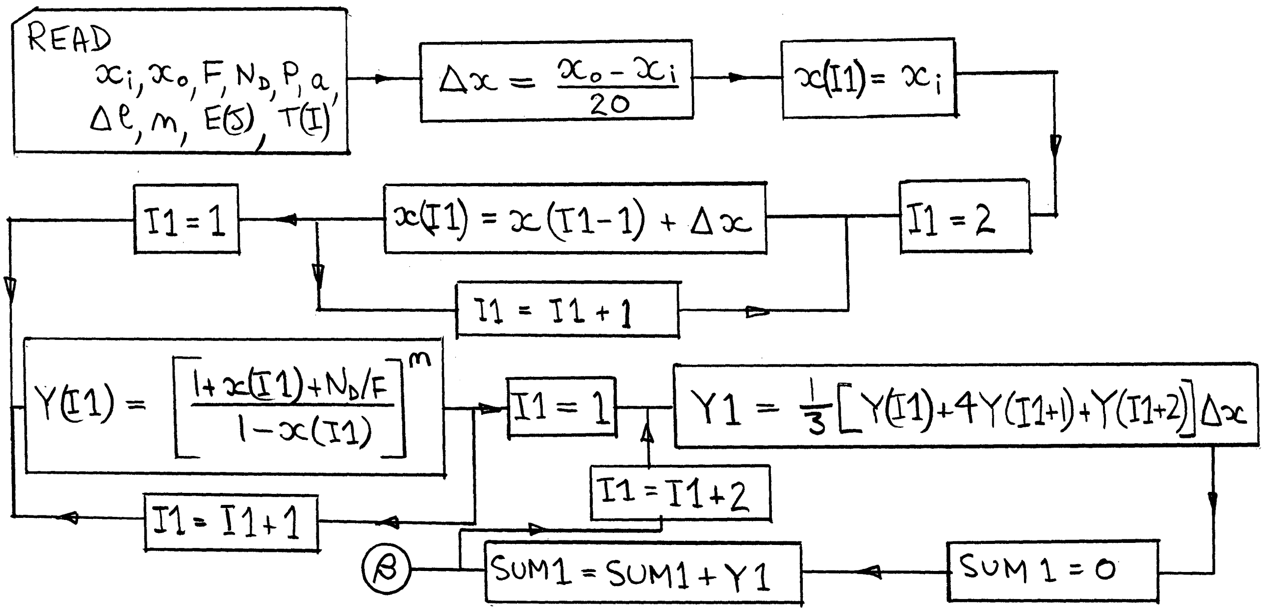

Evaluation of lower integral

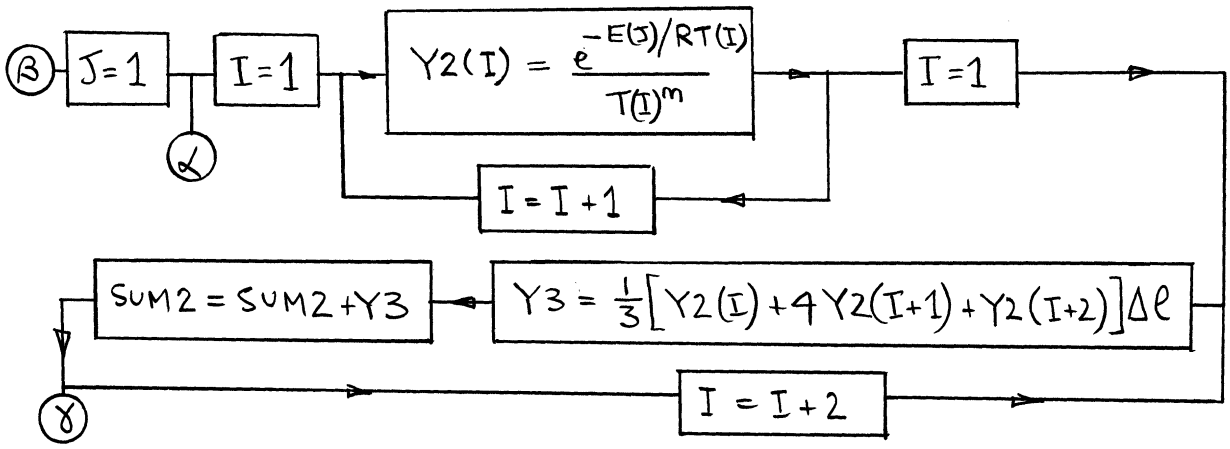

Calculation of A

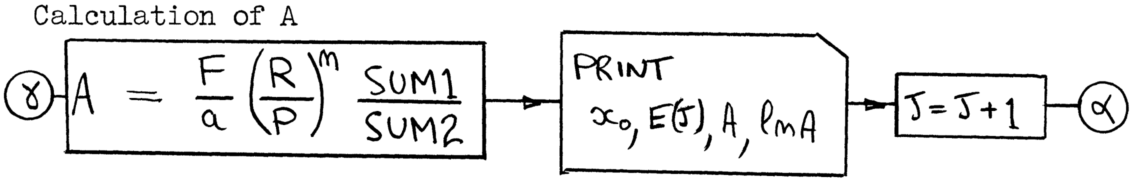

I, J are indexes

Y, SUM1, SUM2 are intermediate variables

(ii) Solution of Rate Equations for Product Distributions

The rate equations for the six reactions that appear in section VIB are:

$$\frac{dN_{C_2H_6}}{dV_R} = -k_1\left[C_{C_2H_6} - \frac{C_{C_2H_4}C_{H_2}}{K_{c,1}}\right] - k_2 C_{C_2H_6} \qquad (22)$$

$$\frac{dN_{C_2H_4}}{dV_R} = k_1\left[C_{C_2H_6} - \frac{C_{C_2H_4}C_{H_2}}{K_{c,1}}\right] - k_3\left[C_{C_2H_4} - \frac{C_{C_2H_2}C_{H_2}}{K_{c,3}}\right] - k_4\left[C_{C_2H_4}\right]^2 \qquad (23)$$

$$\frac{dN_{C_2H_2}}{dV_R} = k_3\left[C_{C_2H_4} - \frac{C_{C_2H_2}C_{H_2}}{K_{c,3}}\right] - k_5 C_{C_2H_2} - k_6\left[C_{C_2H_2}\right]^2 \qquad (24)$$

$$\frac{dN_{CH_4}}{dV_R} = 2k_2 C_{C_2H_6} \qquad (25)$$

$$\frac{dN_{C_4}}{dV_R} = \frac{1}{2}k_4\left[C_{C_2H_4}\right]^2 + \frac{1}{2}k_6\left[C_{C_2H_2}\right]^2 \qquad (26)$$

$$\frac{dN_{C}}{dV_R} = 2k_5 C_{C_2H_2} \qquad (27)$$

$$\frac{dN_{H_2}}{dV_R} = k_1\left[C_{C_2H_6} - \frac{C_{C_2H_4}C_{H_2}}{K_{c,1}}\right] - k_2 C_{C_2H_6} + k_5 C_{C_2H_2}$$

$$+ k_3\left[C_{C_2H_4} - \frac{C_{C_2H_2}C_{H_2}}{K_{c,3}}\right] + k_4\left[C_{C_2H_4}\right]^2 \qquad (28)$$

The rate constants (k) are represented by the Arrhenius equation

$$k = A e^{-E/RT} \tag{21}$$

The reactor is divided into 25 increments and the temperature profile is approximated by a number of small steps so that the temperature is constant in each increment. The rate dN/dV_R is approximated by $\Delta N/\Delta V_R$ and the ΔN in each increment is computed using the concentrations at the end of the previous increment. In this way the calculation proceeds throughout the reactor. The flow diagram for this calculation follows.

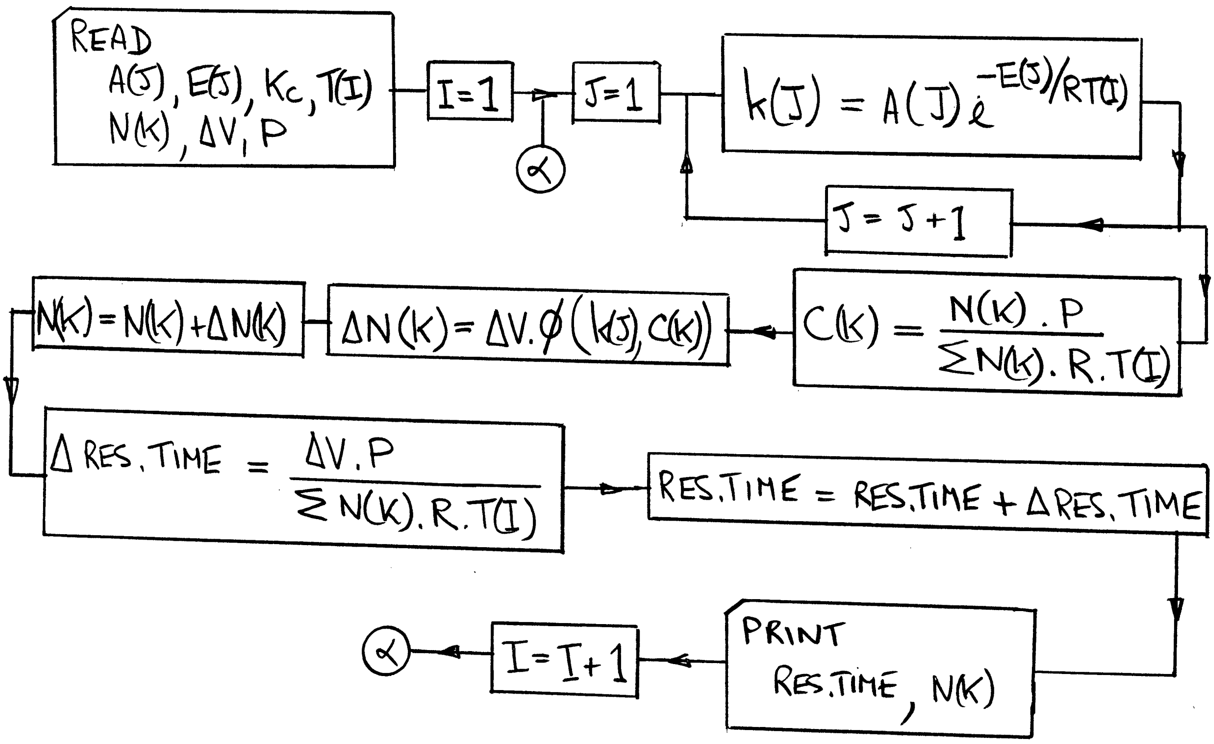

I, J, K are indexes

ϕ represents Equations (22) to (28)

APPENDIX VIII

TABLE X APPROXIMATE VALUES OF BOND ENERGIES

Bond energies in kcal

	C_2H_5 - H	CH_3 - CH_3
	98	83
Steacie[44]		
	CH_2CH - H	CHC - H
	104	121
	C - H	C - C
	92	77
Daniels[14]		
	C = C	C ≡ C
	122	200

BIBLIOGRAPHY

1. Akin, G. A., Reid, T. F. and Schrader, R. J. American Institute of Chemical Engineers Meeting, Chicago, Illinois, December 9-14, 1957.

2. A.P.I. Research Project #44, Selected Values of Physical and Thermodynamic Properties of Hydrocarbons and Related Compounds, Carnegie Press, 1953.

3. A.P.I. Research Project #44, Catalog of Mass Spectral Data, Carnegie Institute of Technology, 1959.

4. Aten, C. F. and Greene, E. F. Disc. Faraday Society, 22, 162, (1956).

5. Benson, S. W. The Foundations of Chemical Kinetics, McGraw-Hill Book Company Inc., New York, 1960.

6. Bixler, G. H. and Coberly, C. W. Ind. Eng. Chem. 45, 2596, (1953).

7. Bogart, M., Schiller, G. R. and Coberly, C. W. Petroleum Processing, 8, 377, (1953).

8. Bone, W. A. and Coward, H. F. J. Chem. Soc., 93, 1197, (1908).

9. Bone, W. A. and Coward, H. F. Proc. Chem. Soc. (London), 24, 167, (1908)

10. Brooks, B. T., Boord, C. E., Kurtz, S. S., Jr., and Schmerling, L. The Chemistry of Petroleum Hydrocarbons, Vol. II, Reinhold Publishing Company, New York, 1955.

11. Burk, R. E., Baldwin, B. G. and Whitacre, C. H. Ind. Eng. Chem., 29, 326, (1937).

12. Calderbank, P. H. and Hovnanian, V. P. Ind. Chemist, 33, 557 (1957).

13. Dahlgren, G. Jr., and Douglas, J. E. J. Am. Chem. Soc., 80, 5108, (1958).

14. Daniels, F. Ind. Eng. Chem., 35, 504 (1943).

15. Dinstes, A. I., Kvyatkovskii, D. A., Stepukhovich, A. D. and Frost, A. V. Zhur. Obsh. Khim., 7, 1754, (1937).

16. Eastwood, S. C. and Potas, A. E. Petroleum Engr., 19, 43, (1948).

17. Eltenton, G. C. J. Chem. Phys., 10, 403, (1942).

18. Eltenton, G. C. J. Chem. Phys., 15, 455, 465, 474, (1947).

19. Farnesworth, J. F., Manes, M., McGurl, G. V. and Bretz, G. M. Ind. Eng. Chem., 47, 1517, (1955).

20. Frey, F. E. and Smith, D. F. Ind. Eng. Chem., 23, 948, (1928).

21. Greene, E. F., Taylor, R. L. and Patterson, W. L. Jr., J. Phys. Chem., 62 238 (Feb. 1958).

22. Hague, E. N. and Wheeler, R. V. J. Am. Chem. Soc., 51, 378, (1929).

23. Hasche, R. L. Chem. and Met. Engr., 49, #7, 78, (1942).

24. Hepp, H. J., Spessard, F. P. and Randall, J. H. Ind. Eng. Chem., 41, 2531, (1949).

25. Hobbs, J. E. and Hinshelwood, C. N. Proc. Roy. Soc. (London), A167, 439, (1938).

26. Kinney, R. E. and Crowley, D. J. Ind. Eng. Chem., 46, 258, (1954).

27. Kuchler, L and Thiele, H. Z. Phys. Chem., B.42, 359, (1939).

28. Lee, E. H. and Oliver, G. D. Ind. Eng. Chem., 51, 1351, (1959).

29. Marek, L. F. and McCluer, W. R. Ind. Eng. Chem., 23, 878, (1931).

30. Miller, I. F. University of Michigan Industry Program, Report IP-392 October 1959 (Ph.D. Thesis, University of Michigan).

31. Molera, M. J. and Stubbs, F. J. J. Chem. Soc. 381, (1952).

32. Paul, R. E. and Marek, L. F. Ind. Eng. Chem., 26, 454, (1934).

33. Pease, R. N. J. Amer. Chem. Soc. 50, 1779, (1928).

34. Pease, R. N. J. Amer. Chem. Soc. 51, 3470, (1929).

35. Rice, F. O. and Herzfeld, K. F. J. Am. Chem. Soc., 56, 284, (1934).

36. Rice, F. O. and Dooley, M. D. J. Am. Chem. Soc., 55, 4245, (1933).

37. Sachsse, H. Z. Physik, Chem., B31, 87, (1935).

38. Schutt, H. C. Chem. Engr. Prog., 55, #1, 68, (1959).

39. Semenov, N. N. Some Problems in Chemical Kinetics and Reactivity, Vols. I and II. Princeton University Press, Princeton, 1959.

40. Sittig, M. Petroleum Processing, July, 1011 (1955).

41. Snow, R. H., Peck, R. E. and Von Fredersdorff, C. G. A.I.Ch.E. Journal, 5, 304 (1959).

42. Staveley, L. A. K. Proc. Roy. Soc. (London) A162, 557 (1937).

43. Steacie, E. W. R. and Shane, G. Can. J. Research, B18, 351 (1940).

44. Steacie, E. W. R. Atomic and Free Radical Reactions, Vols I and II, Second Edition, Reinhold Publishing Company, New York, 1954.

45. Storch, H. H. and Golden, P. L. Ind. Eng. Chem., 26, 56, (1934).

46. Taylor, H. A. and van Hook, A. J. Phys. Chem., 39, 811 (1935).

47. Tropsch, H., Parrish, C. G. and Egloff, G. Ind. Eng. Chem., 28, 581, (1936).

48. Tropsch, H. and Egloff, G. Ind. Eng. Chem., 27, 1063, (1935).

49. Zelinski, N. D. Ber., 57, 264 (1924).

NOMENCLATURE

A	Pre-exponential factor in Arrhenius equation (sec^{-1})*
a	Cross sectional reactor flow area (cm^2)
C	Concentration (gm. mole/liter)
E	Activation energy in Arrhenius equation (kcal/gm. mole)
F	Feed rate of hydrocarbon (gm. moles/sec)
$K_{p,\ c}$	Equilibrium constant pressure units, concentration units
k	Rate constant (sec^{-1})*
L	Total length of reactor (cm)
l	Arbitrary length along reactor (cm)
M	Mole fraction
N	Flow rate of any component (gm. moles/sec)
N_D	Flow rate of inert diluent (gm. moles/sec)
N_T	Total flow rate (gm. moles/sec)
P	Pressure (atmospheres)
R	Gas constant
T	Temperature (°K)
$T_{C,\ W}$	Reactor temperature at center, wall (°K)
V_R	Reactor volume (liters)
$x_{i,\ o}$	Conversion inlet, outlet
α, β, δ	Constants

* These units are for first order reaction. Units for second order reaction are liters gm. mol^{-1} sec^{-1}.